Section 8-B:

Fatigue, Creep-Fatigue, and Thermomechanical Fatigue Life Testing of Alloys

Gary R. Halford and Bradley A. Lerch
Glenn Research Center at Lewis Field
National Aeronautics and Space Administration
Cleveland, Ohio

and

Michael A. McGaw
McGaw Technology, Inc.
Lakewood, Ohio

OUTLINE

Section 8-B: Fatigue, Creep-Fatigue, and Thermomechanical Fatigue Testing of Alloys

I. INTRODUCTION TO FATIGUE CRACK INITIATION LIFE TESTING

The fatigue crack initiation resistance of an alloy is determined by conducting a series of tests over a range of values of stress amplitude or strain range. The observed number of cycles to failure is plotted against the stress amplitude or strain range to obtain a fatigue curve. The fatigue properties quoted for an alloy are typically the constants used in the equation(s) that describe the fatigue curve. Fatigue lives of interest may be as low as 10^2 or higher than 10^9 cycles. Because of the enormous scatter associated with fatigue, dozens of tests may be needed to confidently establish a fatigue curve, and the cost may run into several thousands of dollars. To further establish the effects on fatigue life of the test temperature, environment, alloy condition, mean stress effects, creep-fatigue effects, thermomechanical cycling, etc. requires an extraordinarily large and usually very costly test matrix. The total effort required to establish the fatigue resistance of an alloy should not be taken lightly.

Fatigue crack initiation tests are conducted on relatively small and presumed to be initially crack-free, samples of an alloy that are intended to be representative of the alloy's metallurgical and physical condition. Generally, samples are smooth and have uniformly polished surfaces within the test section. Some may have intentionally machined notches of well-controlled geometry, but the surface at the root of the notch is usually not polished. The purpose of polishing is to attain a reproducible surface finish. This is to eliminate surface finish as an uncontrolled variable. Representative test specimen geometries will be discussed later. Test specimens are cyclically loaded until macroscopically observable cracks initiate and eventually grow to failure. Normally, the fatigue failure life of a specimen is defined as the number of cycles to separation of the specimen into two pieces. Alternative definitions are becoming more common, particularly for low-cycle fatigue testing, wherein some prescribed indication of impending failure due to cracking is adopted. Specific criteria will be described later. As a rule, cracks that develop during testing are not measured nor are the test parameters

intentionally altered owing to the presence of cracking. The topic of fatigue crack propagation testing of alloys is discussed in **Sections 8-D, -E, & -H (?).**

Microscopic size fatigue cracks tend to nucleate quite early in cyclic life (in first 1 to 10%) in the high-strain, plasticity-dominated, low-cycle life regime. In this regime, cyclic plasticity is widespread throughout the specimen test section, and the range of plastic strain is used as a measure of the severity of fatigue "loading". On the other hand, cracks begin to appear quite late in cyclic life (90 to 99%) in the very low strain, elastically dominated, high-cyclic life regime. There is a gradual transition between these two extremes of behavior for intermediate strain ranges and cyclic lifetimes. In the high-cyclic life regime, the cyclic behavior at the macroscopic, phenomenological level is usually considered by design engineers to be linearly elastic and thermodynamically reversible. It is important to recognize, however, that the micro-mechanisms of fatigue crack nucleation and growth in metals and alloys are linked directly to the occurrence of reversed cyclic plasticity. Fatigue will not occur with out it. Even fatigue cracking that occurs in the range of a billion cycles to failure or more *must involve* reversed plasticity. It is also important to recognize that the fatigue process is a progressively degenerative one. For any given condition of cyclic loading that eventually leads to a fatigue failure, there is some, albeit minute, permanent change from one cycle to the next. While the macroscopic behavior may appear to be linear, reversible, elastic, etc., at the microstructural level, irreversible, non-linear, inelastic deformations occur in highly localized regions that accumulate until macroscopically observable cracking occurs.

Although the results of crack initiation tests conducted on small specimens do not precisely establish the fatigue life of a large part, such tests do provide useful information on the intrinsic fatigue crack initiation behavior of a metal or alloy. As a result, such data can be utilized to develop engineering design criteria to prevent initiation of fatigue cracks in structural components. The use of small-specimen fatigue test data are the basis of fatigue design codes for pressure vessels, piping components, nuclear reactors, turbine blades, wheels, and shafts, complex welded, riveted, or bolted structures, automotive and off-highway equipment, exotic aerospace components, and even soldered joints of lead-less electronic chips.

All alloys and metals in structural elements are susceptible to fatigue crack initiation if the structure is subjected to sufficiently large and numerous amplitudes of cyclic loading.

Following a brief description of the phenomena of crack initiation and early growth, this section examines specimen design and preparation, as well as the apparatus used in crack initiation testing. Variables that influence the resistance of alloys to fatigue crack initiation, such as the effect of mean and residual stress, stress concentrations, stress amplitude, and surface properties, are briefly reviewed. The initial portion of this section deals with fatigue testing of alloys in the regime wherein the isothermal temperature of testing is below the range wherein behavior is significantly influenced by time-dependent mechanisms such as creep, oxidation, and metallurgical transformations. The testing procedures, instrumentation, and hardware must be altered to accommodate Creep-Fatigue (C-F) Testing and Thermo-Mechanical Fatigue (TMF) Testing, and these items will be addressed as required throughout this section.

For information on the planning and design of fatigue test matrices and statistical analysis of the test results, see the article *"Fatigue Data Analysis"* in this Volume *{?}*.

II. PROCESS OF FATIGUE CRACK INITIATION AND EARLY GROWTH

Fatigue crack initiation and early growth requires cyclic inelastic deformation. For alloys and metals tested at sub-creep temperatures the non-linear inelastic behavior is invariably plasticity, i.e., the slip associated with dislocation motion along the most densely packed crystallographic planes aligned favorably with the maximum resolved shear stress. In low-cycle fatigue testing, the cyclic plasticity is widely spread throughout the gage portion of the specimen and is readily measured with commercially available strain measuring devices. In this regime the cyclic stresses will be near or above the conventional offset yield strength of the alloy. Cyclic strain hardening or softening typically also occurs. On the other hand, at very long cyclic lives cyclic plasticity is still present, although certainly not detectable with conventional strain measurement techniques. Reversed crystallographic slip is highly localized within a few of the most favorably oriented grains or near highly localized stress concentrations. Stress-strain response appears to be totally elastic in this life regime. Because

of the extreme localization at the smallest cyclic stresses and strains and hence longest lives, the tendency is for only one major crack to initiate and grow to failure in this regime. In the high strain regime, corresponding to low-cycle fatigue lives, there is a tendency for the material to develop multiple crack initiations and early growth followed by eventual link-up of independent cracks into a single fatal fatigue crack. The transition between low-cycle fatigue and high-cycle fatigue is essentially a gradual one with mechanisms varying more in degree than in kind. The region between low- and high-cycle fatigue is referred to as intermediate-cycle fatigue.

With few exceptions, such as rolling contact fatigue and influences of mechanical or metallurgical surface treatments, cracks initiate at a free surface. Usually the surface is the external surface of the specimen, although it could be an internal surface associated with a void or a de-bonded internal particle. Cyclic plasticity is less constrained at a free surface because of the fewer nearest neighbors and hence fewer atomic bonds available to inhibit dislocation motion. Dislocations also exit and disappear at free surfaces, leaving one atomic-sized step for each dislocation that exists on a particular slip plane. Typically, more than one slip plane is involved. Any given slip plane experiences non-reversed slip, i.e., the amount of slip in the slip direction of the plane during one direction of loading is not recovered in the opposite direction when the direction of loading is reversed. Rather, the overall deformation is recovered, but some of it may be on parallel slip planes. The active parallel slip planes are separated by numerous atomic distances and form what are known as a slip bands. Within a band the to-and-fro slip is not uniform, resulting in considerable disarray beneath the surface and outcroppings that are highly irregular. These are referred to as persistent slip bands, i.e. those deeper than several microns below the free surface. Persistent slip bands remain active throughout the bulk of the cyclic life.

As the number of applied fatigue cycles of cyclic plasticity increase, the severity of the irregularity increases until such time as the outcroppings form extrusion/intrusion pairs within the slip bands. Intrusions are the nuclei or formative stages of atomic-sized fatigue cracks known as Stage I cracks (defined as cracking along the crystallographic slip plane). The intrusion grows slowly with continued cycling. Once the depth of the intrusion is great enough, the surrounding material perceives it as a crack that exerts its own highly localized stress-strain

field. At this stage of the evolving fatigue process the nucleated crack's stress-strain field, which superimposes itself on the applied stress-strain field, becomes the dominant field. The cracking response changes accordingly and the global crack direction turns to become perpendicular to the maximum principal stress direction immediately in front of the crack. This signals the onset of Stage II fatigue cracking which generally prevails until fatigue failure occurs. Inspection of a fatigue fracture surface with the naked eye generally reveals primarily Stage II cracking as Stage I cracks are seldom greater than a grain size or two in depth. Cracks may also start at the location of surface irregularities due to grain boundaries, chemical attack, and casting or machining imperfections. Nevertheless, cyclic plasticity is always a necessary ingredient for the nucleation process.

Although the scenario described above is simplified, it provides phenomenological insight into the gradual, progressive nature of the fatigue process that are useful in understanding cyclic testing in the low-, intermediate-, and high-cycle fatigue regimes. There are no sharp demarcations between the three regions when described by the number of cycles to failure. In fact, the distinction is better founded in terms of the magnitude of the range of cyclic plastic strain than in terms of number of cycles, because of the overwhelming influence of the plasticity. As an example, high-ductility, low-strength metals such as copper behave in a low-cycle fatigue manner even at a 10^6 cycles to failure, because the cyclic strain range may be half plastic and half elastic even at this life level. By contrast, a low-ductility, high strength hardened ball-bearing steel exhibits high-cycle type fatigue behavior at cyclic lives of only 10^3 owing to the minuscule amount of plasticity that is overwhelmed by the large elastic component of cyclic strain.

III. FATIGUE TESTING MACHINES

Numerous types of testing machines have been developed for fatigue crack initiation testing. Fatigue testing machines covered in this Section deal with nominally uniaxial normal stress applications. Multiaxial fatigue loading, including torsional and contact fatigue (rolling

elements, gears, impact, etc.) are covered in other Sections. Most fatigue testing machines have been developed to a high degree and are marketed commercially to laboratories for conducting a wide variety of fatigue testing. Machines have been developed for various modes of loading which, in turn, dictate the configuration of the test specimen. Considerable variation of specimen geometry can be accommodated by each of the modes as discussed in the following paragraph.

A. Fatigue Loading Modes

Three basic modes of loading are used; a) direct axial loading, b) plane bending, and c) rotating beam. Specimens for direct axial stress machines may have a wide range of cross-sectional geometries (solid or hollow), and have a uniform gage length with axial cross-sections that are round, elliptical, square, rectangular, or thin sheet. Non-uniform cross-section specimens include sharp notches and low-stress concentration, hourglass-shaped specimens for diametral strain control. Bending specimens may have cross-sections of uniform width and thickness for 3- or 4-point loading, or tapered cross-sections (designed for constant stress along the length) for cantilevered plane bending or rotating beam testing. All bending specimens could be machined with stress concentrations in the form of notches. Examples of standardized fatigue test specimens will be presented later.

B. Classifications of Fatigue Testing Machines

In addition to the loading mode, fatigue-testing machines are further classified by their basic drive mechanism and by the test parameter to be controlled.

The basic drive system is most often electrical. An electric motor directly drives rotating beam testing machines. An eccentric cam attached to a drive motor deflects the cantilevered end of a plane bending fatigue specimen. Eccentric cams coupled with flexure-plate, parallel-motion pivoted lever arms can also drive axially loaded specimens in a direct stress machine. Direct stress machines can also be modified with fixturing to perform plane bending fatigue tests, either in 3-point or 4-point bending. The rotary motion of an eccentric on

an electric drive motor can be used to excite a linear oscillating spring-mass system at its resonance point to provide direct stress loading of a fatigue specimen. Electromagnetic excitation can be used to excite a mass or inertial system to load a specimen in direct stress or plane bending. Ultrasonic fatigue testing is possible at frequencies up to 20KHz using electromagnetic excitation of a specimen gripped at one end and excited at its natural frequency in the axial direction. Even piezoelectric devices have been used to create small high frequency displacement excitations for specialized fatigue testing. Electric motors also turn the pumps to pressurize the fluids used in modern servohydraulic testing machines. The greatest versatility comes with closed-loop, servohydraulic-testing systems that offer capability to control any of the primary fatigue variables provided that variable can be sensed electronically.

Test parameter control is usually fixed for the simplest and least costly fatigue machines. Rotating beam testing is generally done under constant bending moment control. Provided the maximum bending stress remains linearly elastic, the elastically calculated stress or strain is presumed to be controlled constant. However, should a small amount of inelasticity occur at the peak stress of the cycle, the maximum stress will drop due to stress redistribution. This action results in neither a constant pure stress or strain control, although the strain or displacement will tend to be controlled more consistently than the stress might be. For plane bending, if the loading is performed through a rotating eccentric, the control condition is closest to a constant displacement control. If the loading is via a bending fixture attached to a direct stress machine that is under load control, then the control mode for the bending specimen is constant bending moment. Servohydraulic direct stress machines can be operated in constant load, strain, or displacement control depending upon which variable's signal is being sensed and fed back into the servocontrolled loop. While the most versatile, such machines typically require higher initial, operating, and maintenance costs.

All fatigue-testing machines have a basic loading frame that resists the loads imposed on the test specimen. It also supports a number of other components, including the drive mechanism that transmits loading to the specimen through grips, load cells, extensometry, and other measurement devices. If heating, cooling, or environmental chambers are involved, they too have to be supported by the loading frame. Key attributes of the loading frame are to provide accessible space for installing and removing test specimens, and once installed, have

very high stiffness relative to the stiffness of the specimen. In other words, the testing machine should undergo as little elastic loading displacement as possible. Ideally, the bulk of the displacement should be absorbed by the specimen. The loading train within the testing machine should also have excellent alignment of the load line with the specimen to prevent premature specimen warpage or buckling under high loads. Typical load train components in a modern servohydraulic axial fatigue machine are shown in **Fig. 1 (a) and (b)**. Schematic diagrams of the load train components for other common fatigue testing machines are shown in **Fig. 2 (a) to (g)**.

A brief description of the various commercially available fatigue-testing machines is given below.

1. Axial (Direct-Stress) Fatigue Testing Machines

The direct-stress fatigue-testing machine subjects a test specimen to a uniform stress or strain through its cross section. For the same cross section, an axial fatigue-testing machine must be able to apply a greater force than a static bending machine to achieve the same stress. Axial machines are used to obtain fatigue data for most applications and offer the best method of establishing, by closed-loop control, a controlled strain range in the plastic strain regime (low-cycle fatigue).

i. Servohydraulic closed-loop systems offer optimum control, monitoring, and versatility. These can be obtained as component systems and can be upgraded as required. A hydraulically actuated cylinder typically is used to apply the load in axial fatigue testing. A servo-valve governs the flow of hydraulic fluid to the cylinder. The direction and rate of flow is dictated by the electronic control signal to the servo-valve through a feedback control loop. Because of the versatility the servohydraulic system provides in control modes (load, strain, displacement, related variables, or computed combinations of these variables such as plastic strain), the same machine can be used for both high-cycle fatigue and low-cycle (stress or strain-controlled) fatigue testing. A wide variety of grips, including self-aligning (typically tension-tension only) types, are available for these machines.

ii. Electromechanical systems have been developed for axial fatigue studies. The crank and lever machine of **Fig. 2(a)** is an example of one of the testing systems

using this drive mechanism. Forced vibration and resonant systems have also been used extensively. Older machine designs were open-loop systems, but newer machines have closed-loop features to continuously maintain loading levels. An older style forced-vibration, rotating eccentric mass machine with a direct-stress fixture is shown in **Fig. 2(e)** and a closed-loop resonant machine is sketched in **Fig. 2(f)**.

In crank and lever machines, a cyclic load is applied to one end of the test specimen through a deflection-calibrated lever that is driven by a variable-throw crank. The load is transmitted to the specimen through a flexure system, which provides straight-line motion to the specimen. The other end of the specimen is connected to the loading frame. Some machines have a hydraulic piston that is part of an electrohydraulically controlled load-maintaining system that senses specimen yielding. This system automatically restores the preset load through the hydraulic piston. Thus, the static and dynamic loads are applied to opposite ends of the specimen, making it possible to maintain a constant load on the specimen regardless of dimensional changes caused by specimen fatigue.

Electromagnetic or magnetostrictive excitation may be used for axial fatigue testing machine drive systems when low-load amplitudes and high-cycle fatigue lives are desired in short test durations. The ultrahigh cyclic frequency of operation of these types of machines (on the order of 10 to 25 KHz) enables testing to long fatigue lives ($>10^8$ cycles) within weeks. An example of one of these types of machines is illustrated in **Fig. 2 (g)**. A comprehensive review on all aspects of ultrasonic fatigue testing is given in **[1]**.

2. Bending Fatigue Machines

The most highly used type of fatigue machine has probably been the bending fatigue machine. These simple, inexpensive systems have allowed laboratories to conduct extensive test programs with a low investment in equipment. The most common general-purpose bending fatigue machines are cantilever beam plane bending (repeated flexure) and rotating beam.

i. Cantilever beam plane bending machines use flat test specimens that have a tapered width and uniform thickness. This configuration results in a sizable portion of the test specimen volume having a uniform bending stress. Substantially smaller loads are required than for axial fatigue of the same section size. In bending, the stress is highest at the

surface making this test mode advantageous for studying the effects of surface treatments or coatings.

Because of their large displacement, the cam or eccentric principles used in cantilever beam plane bending machines typically have a limited cyclic frequency compared to rotating beam types. Both deflection-controlled and load-controlled types are available and are in use today.

ii. Rotating beam machines are the earliest type of fatigue testing machine and they remain in occasional use today. The specimen has a round cross section and is subjected to dead-weight loading while swivel bearings permit rotation. A given point on the circular test section surface, during each rotation, is subjected to sinusoidal stress variation from tension on the top to compression on the bottom. It is not possible to run mean stress effects tests with this machine.

Typical rotating beam machine types are shown in **Fig. 2**. The R. R. Moore-type machines, **Fig. 2 (b)** typically operate at 167 Hz. In all bending-type tests, only the material near the surface is subjected to the maximum stress; therefore, in a small-diameter specimen, only a very small volume of material is under test. Thus, the fatigue strength and lives obtained from small rotating beam fatigue tests typically are invariably higher than those obtained from axial fatigue tests for specimens with the same cross-sectional area.

C. Regimes of Operation

The choice of the fatigue testing machine will depend strongly on the fatigue life regime to be investigated and upon the type of fatigue data desired.

1. High-Cycle Fatigue

At the high cycle fatigue (HCF) end of the fatigue spectrum (10^5 to 10^8 and higher), high frequency cycling is an absolute must. It requires nearly 12 days of cycling at 1000 Hz to reach 10^8 cycles to failure. Even ultrasonic fatigue testing at 20,000 Hz would require 14 hours to reach this life level. Fortunately, in the HCF regime, the cyclic plasticity is so minuscule that, specimen heating, while ever present, does not restrict testing. Rise-in-temperature measurements made during high frequency cycling have, however, been used successfully to

help identify high cycle fatigue endurance strengths [2]. On the macroscopic phenomenological level, specimen behavior is considered to be linearly elastic. Hence, load-controlled testing is entirely adequate, and in practical fact is virtually dictated. Any conventional fatigue extensometer would be of no added value to testing, even if means were found to keep it from being shaken off at higher frequencies.

In the high cycle fatigue regime, statistical variation in fatigue life is quite large (See the section on statistical aspects of fatigue data). This dictates multiple test results to provide a sufficient database to establish the fatigue resistance of the material. The exceptionally large amount of total testing time in turn requires multiple fatigue testing machines. Consequently, the cost per machine must be relatively low. The simpler fatigue testing machines based on constant loading or displacement in plane bending, rotating bending, and direct stress are used almost exclusively for evaluation of very high cycle fatigue resistance of materials. Ultrasonic fatigue testing is rarely used because the cyclic strain rates are much higher than found in service. This large difference in strain rate may result in different micro-mechanisms of straining and hence, fatigue crack initiation mechanisms.

2. Low-Cycle Fatigue

Conventional low-cycle fatigue (LCF) crack initiation data in the regime of 10 to 10^5 cycles to failure are best obtained under strain-cycling conditions, leaving little choice but to use an electrohydraulic direct stress fatigue machine with an extensometer and servo-strain control. The cyclic frequency need not be high. Even at 1 Hz, 10^5 cycles can be reached in just over a day. In fact, higher frequencies would not be desirable at lower life levels where cyclic plasticity could be significant. Energy dissipation due to rapid cyclic plasticity would cause considerable, and highly undesired, specimen heating[1] (assuming the specimen is not already being heated to an elevated test temperature).

Elevated-temperature fatigue testing, especially low-cycle isothermal creep-fatigue (ICF) and thermomechanical fatigue (TMF), invariably requires servo-controlled, strain-cycling capabilities to avoid undesirable creep or plasticity ratchetting strains. The maximum

cyclic rates during TMF cycling are typically quite low because of the relatively low rate at which temperatures of test samples can be changed in a controlled manner. Because of the relatively long testing time per cycle for ICF and TMF tests, and because of the high costs per test and high machine acquisition and maintenance costs, there have been few published investigations[2] of the statistical nature of ICF and TMF. High-temperature fatigue testing will be discussed in greater detail in following paragraphs.

IV. ANCILLARY EQUIPMENT & SPECIMENS

A fatigue-testing machine typically will have a number of components or accessories added to the basic loading frame. The most common are shown in **Fig. 3**. Ancillary equipment performs various functions such as load and strain detection, specimen gripping and alignment, and provides a controlled environment for the specimen. Load cells, grips and alignment devices, extensometry, environmental chambers, furnaces and other methods of heating are briefly discussed below.

A. Load Application, Measurement and Control

1. Hydraulic Cylinder

The forces and displacements in servohydraulic materials testing systems are produced by a hydraulic actuator, **Fig. 1(b)**. Many types of hydraulic actuators (cylinders) are in common use in industrial equipment, however, hydraulic cylinders used in materials testing machines are differentiated from others in the following ways: 1) they are fatigue rated, so that they may be reliably used in fatigue testing where the duty cycles will be substantial; 2) they

---

[1] If cyclically generated heat is not dissipated, the resultant thermal expansion of the specimen test section creates an "apparent" mechanical strain. Under servo-controlled cyclic straining, thermal expansion would be offset by enforced compression and hence compressive mean stress; destroying the original purpose of the test.
[2] Proprietary databases exist in some large corporations for certain critical materials applications.

feature specialized seal designs to enable high lateral stiffness to be obtained, which is important in maintaining alignment during testing.

2. Load Cell

The force-measuring device in a fatigue machine is called a load cell. It typically consists of resistance strain gages bonded to a linear elastic spring element, which carries the same load as the specimen. The gages make up an electrical resistance bridge circuit. Applied load creates a bridge out-of-balance that is linearly proportional to the load. Load cell design is sophisticated and has evolved over several decades. Load cells must be accurate to within 1 per cent of the applied load (ASTM Standard E4)[3] and insensitive to side loads. Load cells should be stiff and stable and have minimal amounts of hysteresis and nonlinearity. Commercially available load cells are insensitive to small thermal fluctuations. However, care must still be taken to ensure that the cell is thermally protected during testing at elevated temperature. In addition, the load cell and cabling should have shielding to prevent electronic noise, particularly as induced from specimen heating systems. Load cells are designed with overload protection, which prevents damage of the cell due to misuse and must be rated for fatigue testing.

The above description applies to load cells used in axial loading as well as some plane bending loading (3- and 4-point loading not discussed herein) wherein the bending loads are imposed by loading in an axial loading frame. Cantilever plane bending fatigue testing is done in smaller, simpler testing machines and the load cell used to measure the bending load may differ in detail. For plane cantilever bending using an eccentric drive mechanism, the bending load cell may be built into the grips. Some rotating bending test machines do not use a load cell, but rather rely on deadweight loading and knowledge of the lever arm distance to determine the applied bending moment. All force-measuring systems require periodic calibration to ensure accuracy. Methods of calibration and the intervals at which they are performed are specified in standards such as ASTM E4. An excellent review of load cell design can be found in **[4]**.

[3] Table 1 contains a listing of ASTM Standards [3] pertinent to all aspects of fatigue testing.

Most often, the forces and displacements imparted on a test specimen by a testing machine originate from a hydraulic cylinder, the ram displacement of which is controlled by a servo-valve, **Fig. 1(b)**.

3. Servo-valve

Servo-valves are electromechanical devices that provide a means of controlling the flow of (hydraulic) fluid supplied to a hydraulic cylinder. This is generally accomplished by an electrically actuated element connected to a spool (**Fig. 3(b)**), where the spool is machined in such a manner so as to permit fluid flow to occur in proportion to its position relative to fluid inlet and outlet ports. These devices generally have a transfer function expressed in terms of the current (in milliamperes) required to develop a specific rate of flow. The type of servo-valve described is by far the most common design in use with servohydraulic materials testing equipment, and provides acceptable frequency response for most fatigue testing applications. Another type of servo-valve used in materials testing applications uses a voice coil to actuate a pilot spool (**Fig. 3(c)**), which in turn ports fluid to a main stage spool, which in turn is used to port fluid to the actuator. This arrangement, in which the pilot spool position, obtained with a sensor (LVDT) is used in a control loop, provides very high frequency capability for materials testing. Servo-valve designs of this type are often used in carrying out high cycle fatigue studies, as fatigue lives in excess of 10^6 cycles can be economically produced.

{Attn.: MTS or Instron reviewers - Are there additional factors that may be important that have been overlooking here?}

B. Gripping Systems

Well-designed fixturing is required to transmit the applied load through the specimen to the load cell. The grip system must be versatile enough to allow easy installation of the specimen, but must not cause damage to the specimen test section during installation and testing. In addition, the grips must ensure good alignment and be able to withstand the environment associated with the test. The gripping system should have high lateral stiffness to

maintain good alignment (more about alignment can be found in a subsequent section). For uniaxial, tension-compression testing, the specimen and grips must be designed such that there is no backlash while passing through zero load.

Modern gripping systems usually consist of a block of high-stiffness metal (typically steel) which attaches to the load train. The body of the grip may be water-cooled to prevent overheating during tests at elevated temperatures. The grip body has some type of insert that aids in specimen installation and accommodates the geometry of the specimen grip ends **(Fig. 4)**. The inserts are typically made of a material with high hardness (such as tool steel) to minimize wear and distortion due to repeated clamping. For elevated temperature operations, a high temperature alloy is often chosen.

To properly grip the specimen, inserts are used in the grip body or directly on the pull rods. These are generally of the collet or wedge type. Some of the more common types of inserts are shown in **Fig. 5**. Collets can be used for flat and round specimens and are most often used for tension-compression testing. Wedge inserts are used for flat specimens, primarily tested in tension. Both collets and wedges generally operate in a grip such as the one shown in **Fig. 4**. The specimen is held in place via friction that is regulated by squeezing the sample within the inserts using hydraulic pressure. This system provides easy specimen installation and maintains excellent alignment. The griping surfaces of the insert often have a knurled surface or are treated with an abrasive coating to enhance the friction and allow higher axial loads to be applied without the specimen slipping in the grips. Grip surfaces that are too coarse can cause unwanted grip failures.

When testing at elevated temperatures, the grips must be able to maintain their operating capabilities. There are two basic methods for gripping at high temperatures. The first is to keep the grips out of the hot zone and water-cool them to prevent overheating. This is most effective with heating systems where only localized heating (in the gage section) occurs, such as induction, radiant heaters, and small furnaces. The drawback to cooed grips is that the grips act as a large heat sink, pulling the heat out of the specimen. This can make it difficult to achieve an acceptably low thermal gradient along the length of the specimen test section.

The second method is to employ hot grips. With this gripping system, the grips reside in or near the hot zone. This is commonly used with large muffle-type furnaces. Negligibly

low thermal gradients along the specimen test section are easily achieved with hot grips, as the grip temperature is similar to that of the test section. The grip material must be of a high temperature alloy, typically a nickel or cobalt-based alloy. Care must be taken to ensure that the specimen does not permanently affix itself to the grips. A high temperature lubricant such as $MoSi_2$ or $A1_20_3$ is typically used to prevent this from happening. Hot grips are generally replaced at a greater frequency than cooled grips due to long term deformation (creep) of the grips, and oxidation and microstructural instabilities that may weaken and distort the grip material.

Another type of fixture is commonly used for threaded samples. These fixtures consist of a block of material with internal threads to accommodate the specimen. To lock the specimen to the grips, jamb nuts are tightened to preload the specimen grip ends within the grips and eliminate backlash. Care must be taken to avoid applying a torque across the specimen test section during installation. This fixture has an advantage that very small specimens can be used, thus minimizing material mainly due to the relatively short grip section needed compared to wedge or collet grips. The disadvantage of such grips is that alignment can be poor and can vary from set-up to set-up for a given specimen as well as from specimen to specimen. Also, notch-sensitive materials may tend to break in the threads rather than the test section if the thread diameter is too small compared to the gage section diameter.

Grips for 3- and 4-point bending carried out in an axial loading frame often take the form of simple rollers that transmit normal forces to the surface of bending specimens, but negligible shear forces. Care is taken to maintain the orientation and location of the rollers and the specimen relative to the loading frame. Consideration should also be given to surface initiated cracking from the contact line of the rollers, although this is offset by the compressive Hertzian stresses imposed by the rollers. For bending in both directions, symmetric sets of rollers must be located on the opposite faces of the bend specimen and preloaded to prevent backlash. Three- and four-point bending fatigue tests are used often to test notched geometries or to grow cracks for subsequent fracture toughness testing.

Grips are considerably simpler and alignment, while still important, isn't as critical for cantilever plane bending using an eccentric drive as it is for axial loading. The larger, fixed end of the specimen is typically bolted to a rigid plate on the test frame. The flat plane of the

specimen must remain plane and be aligned with respect to the bending axis. Clamping forces must be high enough to prevent relative motion in the grips, but not so high as to introduce clamping stresses that would to the reduced width and thickness of the test section. Gripping of the cantilevered end of the specimen is relatively unimportant because of the low bending stresses present. However, the gripping and means of force transmittal must freely accommodate the forced displacement of the end of the specimen that traces the arc of a circle. The specimen must be free of loading along its longitudinal axis and free of all extraneous bending moments. Collet, or lathe, grips are commonly used for rotating beam specimens and must be designed so that fretting does not occur in the grip. Also, the grip design must prohibit seizure of the specimen thus allowing easy specimen removal without damage. Care must be taken that the tightening of the grips does not induce misalignment and hence unwanted stresses in the specimen test section.

C. Extensometry & Strain Measuring Devices

Since fatigue damage occurs as a result of plasticity, it is desirable to measure the deformation occurring within the gage section during a test. The deformation or displacements can be easily tracked using a number of devices. The most accurate methods involve measurement of the strain in the gage section of the specimen. Measurements over larger sections such as displacement between the crosshead (stroke) should not be used as they include displacement components from the load train as well as the deformation that occurs in the specimen. A number of studies have been conducted in which strain has been measured on specimen ridges outside the gage section **[Refs. 5,6]**, an approach that involves analysis of the deformation in the radius section to determine only the contribution to displacement coming from the gage section. The relative contributions are dependent upon the degree of plastic strain, thus a variable calibration is required.

Direct measurements on the gage section are more straightforward and can be performed with a number of devices such as strain gages, extensometers and optical devices. The key to any of these devices is that, in addition to taking accurate strain readings, the device cannot affect the fatigue life of the sample. In addition, these devices should not only be

able to record displacement, but also be stable enough to be used to close a feed-back loop in a strain-controlled mode. Resistance strain gages are very accurate and can be used to both measure strains in any direction and control strain during the test. They are best suited for nominally elastic straining tests. Sustained cyclic strains larger than about are inappropriate for use of resistance strain gages. Strain gages can be very small in size and, therefore, many can be applied to a standard test specimen and used to measure bending strains, Poisson's ratio, and strains in various axes. Commercially available gages provide resolutions and accuracies suitable for fatigue testing. Standard texts on strain gage usage, see for example [7], can guide the user in this area. The gages should be rated for cyclic use over the range of strains needed for the test. Care must be taken to ensure that specimen surface preparation for gage installation does not induce premature fatigue cracking of the specimen.

Resistance strain gages are used principally at room temperature. However, resistance strain gages are available that have limited use at temperatures as high as 800°C [8,9]. These gages are used where measuring strains in various directions on the specimen is desirable, or where easy access to the specimen by an extensometer is not possible (e.g., in a furnace). However, they are difficult to use, often suffer from long-term drift, and must be individually compensated for each temperature range. More information on these gages can be found in ASTM E1319.

The most common method of measuring strains in fatigue tests is through the use of a mechanical extensometer. Extensometers employ some method of contact with the specimen that relays the displacement via a lever system to an electronic sensing element. The sensor is generally a strain gage bridge, a capacitance transducer, or a Linear Variable Differential Transformer (LVDT). Generally, LVDTs are larger and heavier than the other two types.

Extensometers are rated according to their accuracy (ASTM E83). Like load cells, extensometers should have a linear response and have minimal hysteresis (ASTM E606). Extensometers require periodic calibration ([5] and ASTM E83) to ensure their accuracy.

1. Axial Extensometers

For tests at room temperature, clip-on extensometers are generally used, attaching to the specimen using breakaway features such as springs, sheet metal clamps, and other low pressure clamping arrangements. Metallic knife-edge probes provide a sharp point of contact

and are mechanically set to the exact gage length. Often, small strips of tape are adhered to the specimen to give the knife-edges something to 'bite into' without damaging the specimen.

When testing at elevated temperatures, the sensing element of the extensometer must be protected from the heat. Moving the sensor away from the heat source by the use of longer probes can accomplish this. However, metal probes are no longer suitable and are replaced with a ceramic material. The probes are rods with a suitable specimen contact geometry such as knife-edge, V-notch, or conical point, dependent on the specimen material and gage section geometry. The probes must not damage the surface of the specimen, must be unreactive with the specimen material, must remain in stationary contact with the specimen surface, and must not deform (particularly creep) during the test.

The extensometer probes are mechanically preloaded (typically using springs) to hold them in direct contact with the specimen surface. The force must be sufficient to prevent slippage of the probes, but not so high as to deform the specimen (particularly due to creep) or to otherwise influence specimen failure. Commercial extensometers are available with a wide range of contact forces. The extensometer is mounted to a fixture that may also act as a heat shield, further protecting the sensing element. The extensometer-sensing element is usually air or water-cooled to maintain temperature equilibrium during the test so that there is no temperature induced drift in the strain reading.

Where a large furnace is used (generally with hot grips), the sensing element must be moved even further from the specimen and long probes or rods must be used to transfer the specimen displacement out of the furnace to the sensing device. Systems of this type can be found in **[10-12]**.

Optical extensometers are also available. Most are based on lasers. Their major advantage is the zero mass of a laser beam that offers potentially high response to specimen straining. Another advantage, depending upon the type of laser detection employed, is elimination of direct attachment of an extensometer to the specimen. This is particularly important for brittle and notch-sensitive materials. Of course, an optical path must be available between the specimen and the laser/detector. This type of extensometer, however, can be expensive to purchase, set up, and maintain. While speckle-pattern and interferometric systems are available, their adaptation for closed-loop servo-strain control is quite difficult. For that

reason, only the optical target (flag) system will be discussed herein. This system uses a laser beam and detector array to scan the displacement of flags that define a gage length. Typically, the laser scans multiple times per second and averages the distance between two flags attached to the specimen. Unfortunately, current scanning rates are too low to achieve high-strain rate response. Another problem is that the flags have to be specially designed to maintain a sharp edge at temperature, must adhere to the specimen without inducing damage, and must remain on the specimen throughout the duration of the test. A good comparison of the capabilities of a laser/target extensometer with various other types of strain measuring devices can be found in **[13]**.

2. Diametral Extensometers

Diametral extensometers are used to measure the change in diameter of a specimen due to Poisson's contraction. They are used primarily with axially loaded, hourglass fatigue specimens and at large strain ranges where premature cyclic plastic buckling would rule out use of straight gage length specimens. Generally, the design is a hinge and transducer, with the extensometer mass being supported by wires or self-centering springs, such that very low contact forces are needed. This avoids some of the problems associated with use of axial extensometers. Diametral strain can be converted into axial strain using equations found in **[Refs. 11,14,15 (p. 67-86)]**. However, if the load is not constant (a result, for example of cyclic strain hardening or softening) during a constant diametral strain range controlled test then the longitudinal strain range will vary. However, computer-controlled testing could be used to compensate so as to maintain a constant total axial strain range. Another drawback to the diametral extensometer is that the change in diameter of the specimen during a fatigue test is very small and high resolution is required for the sensing device. However, this extensometer is typically used for large strain ranges and sensitivity therefore isn't critical. Only a small volume of material experiences the full loads and strains during the test, which limits the size of microstructural features that can be effectively sampled. A number of diametral extensometer designs and additional information on them can be found in **[14]**. Diametral extensometers were used extensively prior to the development of current generation of axial extensometers.

D. Heating Systems

When fatigue testing is conducted at elevated temperatures, any method, which can heat the specimen to the desired temperature and be adaptable to the existing test equipment might be used. The key to choosing the appropriate heating method depends primarily on ease of use and the ability to obtain the desired temperatures and thermal gradients. According to ASTM E606, the thermal gradient within the gage section shall be within 2 C° or 1 per cent of the test temperature, whichever is larger. Also, the nominal temperature should not vary during the test by more than ± 2 C°. These requirements are not overly restrictive, but do require some consideration and effort to achieve. There are various heating methods that can easily attain these limits and have proven themselves for use with fatigue testing and these are discussed in this section. Test results not meeting ASTM standards should be so indicated and the deviation quantified.

One of the most versatile methods of heating and probably the most widely used for low cycle fatigue of metallic materials is direct induction heating. Induction heaters generate either audio or radio frequency electromagnetic fields to induce eddy currents in the near surface of a test specimen. The current is passed from the induction generator into water-cooled, copper tubing wrapped into coils, which surround the specimen. These coils can be made to fit any size or shape of specimen, which makes this system of heating highly versatile. The tubing is normally covered with a high temperature insulating material to prevent accidental shorting between coils. There is generally no limitation on the maximum temperature that can be obtained using induction heating, provided that the induction generator has sufficient capacity and adequate cooling is available for the working coils. For the majority of test specimens and materials, a 5 kW induction heater will suffice. These types of heaters have very low thermal mass and are ideal for rapid thermal cycling such as would be needed for thermomechanical fatigue (TMF) testing. The major disadvantage of induction heating is the difficulty in establishing the required thermal gradient. Localized heating can readily occur with temperatures varying by as much as 20 C° over short distances (0.25"). Manipulating the position and proximity of the induction coils can bring these gradients into compliance with

requirements. Unfortunately, this process is more art than science. At least one method has been developed ([16, Fig. 6]) which separates the coil into three independent segments. Each segment can be moved while the specimen is at temperature thereby greatly reducing the time required to establish an acceptable thermal gradient.

Another disadvantage to direct induction heating is that temperature measurement requires thermocouples to be bonded to the specimen (i.e., welded). If there is poor contact between the specimen and the thermocouple, the thermocouple will be independently heated by the induction field and give erroneous readings. Unfortunately, welding thermocouples onto the gage of the sample may initiate premature cracking. There are at least three ways to work around the thermocouple attachment problem: 1) Weld the control thermocouple to a place other than the gage section such as the grip. The temperature relation between the gage section and the grip would have to be determined with a calibration specimen and shown to be constant from one specimen to the next. 2) Use a non-contacting temperature measurement device (e.g., optical pyrometer). 3) Use susceptor heating. In this method, a susceptor material, usually SiC, graphite or metal is placed within the induction coil. The induction field heats the susceptor, which, in turn, radiates heat to the specimen. This method is commonly used for materials that are poor electrical conductors. Even though a susceptor is used, some amount of coupling between the induction field and the specimen may still occur. Also, a susceptor has a larger thermal mass and the temperature of the specimen cannot be changed as quickly as by direct induction. Therefore this type of heating may have limited use for TMF testing.

Another type of heating, quartz-lamp radiant heating, works particularly well with flat specimens (but has also been used successfully with cylindrical specimens). With this method radiant energy is focused onto the specimen by means of a parabolic reflector. Since the lamps are designed for a specific focal length which ensures a certain area of constant temperature, they are not readily adaptable to specimens and test setups other than for what they were originally designed. The lamps have very fast heating rates and are suited for moderately rapid thermal cycling. Care must be taken to ensure that the specimen is not shadowed by instrumentation.

Radiant heating using wire resistance coils in a hollow furnace is also a common heating method. Muffle furnaces, either split or in one piece, can be used, but these are

typically large. Smaller furnaces can be constructed out of banks of individual heating elements or of continuous windings of Nichrome wire for specific applications. Both furnace types can be manufactured in single- or multi-zone configurations. These furnaces provide uniform and constant temperatures with very low thermal gradients and are ideally suited for long term exposures. Since the area within the furnace is essentially at the same temperature, thermocouples need not be in intimate contact with the specimen. This permits the use of wrap-around and probe-type thermocouples. However, the furnaces are generally large which increases the distance between the load platens resulting in a less stiff load train. Also, access to the specimen with instrumentation is difficult and must be considered before the furnace is constructed in order to include a sufficient number of properly sized ports. Finally, the very large thermal mass of these systems makes them poorly suited for rapid thermal cycling. A highly specialized radiant heating system consists of a silicon carbide heating element that is inserted inside a tubular specimen and radiates heat to the inside surface of the specimen. Thermal gradients throughout the wall and along the length are disadvantages, but this is offset by entirely freeing up the external surface outer diameter of the specimen for any extensometry or other measurement paraphernalia **[15, p 67-86]**.

Direct resistance heating is another specialty heating technique that has been used to advantage for elevated temperature fatigue tests including TMF **[17-19]**. The specimen itself becomes the heating element. Although a metallic specimen possesses a low electrical resistance, passing a very high current (on the order of a kiloampere) directly through the specimen will produce heat within the specimen that is proportional to the product of the current times the voltage drop across the length of the specimen. Extraordinarily high rates of heating are attainable. Transverse temperature gradients are inherently small compared to other heating techniques because the heat is generated uniformly within the material. Heat transfer isn't necessary to heat the interior, as heat is being generated uniformly throughout the volume of a uniform test section at the same rate as at the surface. Actually, the center of the specimen may be ever so slightly hotter than the surface because of radiation losses and the slightly higher heat flow rate of surface material Extensive water-cooling is necessary to prevent oxidation and contact resistance of all high-current connections, including those of the specimen to its grips. Water-cooling assists rapid specimen cooling when TMF tests are

conducted. Disadvantages of direct resistance heating include safety concerns regarding large currents and the potential for inadvertent short circuit arcs that could produce instant molten metal and severe burns. Large currents also introduce control difficulties and high magnetic fields causing interference with sensitive electronic control equipment indigenous to modern fatigue testing systems.

With all heating methods, temperature is commonly controlled using commercially available, solid state temperature controllers. These controllers can be purchased with resolutions far superior to what is needed for fatigue testing. PID (Proportional, Integral, and Derivative) control settings can be adjusted to maintain the control temperature to within 0.1 C° of the desired temperature. These controllers can be operated manually or programmed to follow a signal generator output. Hence, temperature cycling can be phased with mechanical strain cycling during a thermomechanical fatigue test.

To minimize temperature variations during testing due to air currents in the laboratory, it is recommended that an enclosure be installed around the zone of the specimen. Another important concern for all methods of specimen heating is unwanted electronic interference created by the temperature controllers. Unless an off-the-shelf engineered testing system is purchased, care is required to shield or filter troublesome signals.

E. Environmental Chambers

When environments other than still laboratory air are desired, an environmental chamber (**Fig. 7**) must be used. Examples include vacuum or inert gases (argon, helium) to eliminate effects of oxidation at high temperatures; high pressure; high-temperature gases such as oxygen or hydrogen to simulate liquid rocket engine environments; radiation from radioactive sources for the study of nuclear reactor components; cryogenic environments for the study of alloys used in super cold applications, or even corrosive environments that can degrade a material's fatigue properties. Each environment poses its own set of concerns for the protection of grips, extensometry, and load cells. If, for example, a vacuum or pressurized chamber is required, any parasitic loads transmitted through the structural components required

to maintain the environment (seals, baffles, bellows, etc) must be eliminated from the load cell signal.

Careful attention must be given to gaining access to the specimen and grips for installation and removal of specimens and the attachment and support of extensometry. Viewing ports are also highly desirable. For sealed systems, insulated electrical feed-through connectors are required for transducer signals (strain, pressure, temperature, etc.).

F. Representation of Material and Specimen Configurations

A specimen is a representative sample of an alloy and is used to determine and compare the material's basic fatigue characteristics. In addition to this primary use, specimens can be designed to study the effects on fatigue resistance of several important factors. These can be categorized as:

- Geometric features such as stress concentrations including intentional notches, holes, fillet radii, and attachment configurations, unintentional voids or flaws, and damage due to handling or service use.
- Bulk properties such as those influenced by degree and orientation of cold working, temperature of testing, thermal exposure, heat treatment, and radiation.
- Surface related effects including mechanical surface finish, shot peening, burnishing, laser shock treatment, residual stresses, environmental interactions, fretting, galling, and coatings.
- Loading related factors such as mean stress, multiaxiality, cumulative damage, temperature of testing, thermal cycling, and creep-fatigue interaction that might occur at low testing frequency and hold times.

Nomenclature for a typical fatigue specimen is given in **Fig. 8.** A test specimen has three sections: the test section, a transition zone, and the two grip ends. The test section is where the quoted stresses, strains, temperature, environment, etc. are measured or controlled and where fatigue cracking and failure is designed to occur. The majority of the specimen deformation occurs in this section. The grip ends are designed to transfer load from the test machine grips to the test section and may be identical at either end, particularly for axial fatigue tests. The transition from the grip ends to the test area is designed with large, smoothly

blended radii to minimize stress concentration in the transition, which could otherwise initiate undesired fatigue cracking.

The design and type of specimen used depends on the fatigue testing machine and the objective of the fatigue study. The test section in the specimen is reduced in cross section to increase the stresses and strains there and hence avoid failure in the transition region and in the grip ends. The test section should be proportioned to properly test the material, accounting for adequate sampling of specific microstructural features (e.g., defects, grain size, etc.), yet still be small enough that the load capacity of the load frame is not exceeded.

The location from which a test specimen is taken from the initial product form is important because the manner in which a material is processed influences the uniformity of microstructure along the length of the product as well as through its thickness. For example, the properties of metal cut from castings are influenced by the rate of cooling and by shrinkage stresses at changes in section. Generally, specimens taken from the surface of castings are stronger. Many ASTM standards, such as E8 and B557, provide guidance in the selection of test specimen orientation relative to the rolling direction of plate or the major forming axes of other types of products and in the selection of test specimen location relative to the surface of the product.

Orientation is also important to standardize test results relative to the directionality of properties that often develops in the microstructure of materials during processing. Some causes of directionality include the fibering of inclusions in steels, the formation of crystallographic textures in most metals and alloys and preferred growth directions in directionally solidified and single-crystal materials.

G. Specimen Machining and Surface Preparation

Because fatigue crack initiation typically is surface dependent, proper machining and surface preparation of test specimens is critical. Unless care is taken, scatter caused by variable surface conditions will overwhelm the inherent scatter of the material being studied.

Because a primary aim of fatigue testing is comparison of materials, uniform preparation procedures must be established. Machining operations must not alter the surface

structure of the metal; thus, heat generation, heavy cutting, and severe grinding are prohibited. Final machining should be parallel to the direction of applied stress. Transition fillets must be blended into the test area without steps or undercutting. Surface polishing using metallographic techniques is preferred for smooth specimens, where machining marks are removed by a sequence of grinding steps. Example procedures for machining of specimens are given in ASTM E466 and [20].

The final polishing is not a buffing operation, but a cutting operation that uses lapping compounds or aluminum oxide powder in a liquid medium to remove grinding scratches. For flat sheet or plate specimens, edges should be slightly rounded and ground to eliminate nicks, dents, cuts and sharp edges, which can lead to premature crack initiation. The relationship between surface characteristics and fatigue properties is discussed later in this article.

Test specimens received from a machine shop are expected to meet size specifications provided to the shop. To ensure dimensional accuracy, however, each test specimen should be measured prior to testing. Gage length, fillet radius, and cross-sectional dimensions are easily measured. Cylindrical test specimens should be measured for concentricity. Maintaining acceptable concentricity is extremely important in minimizing unintended bending stresses. In general, flat specimens are difficult to manufacture without twisting or bending; especially if they are taken from rolled products. The potential warpage of thin specimens along with their inadequate section modulus lead to ready elastic buckling under compressive loads. Therefore, these types of specimens are usually only tested in tension. Lateral anti-buckling guides can be used to prevent buckling of compressively loaded thin flat specimens [21]. However, the buckling guides introduce other problems (surface contact and small amounts of rubbing action at points of contact) which can affect the fatigue properties.

The product form from which the specimen is taken often influences the geometry of a test specimen. Obviously, only flat specimens can be obtained from sheet products. Test specimens taken from thick plates or bar stock may be either round or flat. Occasionally, sub-scale specimens must be employed if the product form is too small for standard specimen dimensions.

1. Cylindrical Specimens

Three types of specimens with circular cross sections are commonly used:

- Specimens with tangentially blending fillets between the test section and the grip ends, **Figs. 9 (a) and 9 (b)**.
- Specimens with a continuous radius between the grip ends with the minimum diameter at the center, **Figs. 9 (b), 9 (d),** and **10 (a)**. These are referred to as hourglass specimens and are commonly used when strain ranges are larger than 2%.
- Specimens for use in cantilever beam loading with tapered diameters proportioned to produce nominally constant stress along the test section.

The design of the grip ends depends on the machine design and the gripping devices used. Round specimens for axial fatigue machines using grip inserts like those shown in **Fig. 5** may be threaded, button-head, or smooth-shank types. For rotating beam machines, short, tapered grip ends with internal threads are used, and the specimen is pulled into the grip by a draw bar. A long, smooth shank end is used on machines with lathe-type collets.

2. Flat Sheet and Plate Specimens

Generally, flat specimens for either axial or bending fatigue tests are reduced in width in the test section, but may have small thickness reductions as well. The most commonly used types include:

- Specimens with tangentially blending fillets between the test section and the grip ends, **Fig. 10 (c)**. This specimen has a straight gage section and is used in both axial and bending fatigue.
- Specimens with a continuous radius between the grip ends giving a flat hour glass design, **Fig. 10 (d)**. These are also used in both axial and bending fatigue tests.
- Specimens for use in cantilever reverse bending tests with tapered widths, **Fig. 9 (c)**. Flat specimens generally are clamped in flat wedge-type grips, or may be held with a stiff bolted clamp/joint friction grip for reversed axial loading. Pin loading can be used when only tensile loads are encountered. When pin loading is utilized, the holes drilled in the grip end must be designed to avoid shear or bearing failures at the holes, tensile failure between the holes at maximum load, and fatigue cracking at the holes in the grip end. In axial fatigue testing of flat sheet specimens, the test length and cross-section must be designed to prevent premature buckling of the specimen.

H. Alignment Considerations

One of the keys to achieving accurate fatigue data include ensuring applied loading is aligned with the specimen axis. This is particularly important in axially loaded specimens. Poor and non-reproducible alignment produces bending strains that reduce the fatigue life and increase the scatter in the data. In fact, it has been calculated that the largest contributing factor to scatter in LCF data is due to bending **[22]**. Bending strains arise when there is a misalignment somewhere in the load train. The axiality and concentricity of the actuator, grips, test specimen, and load cell should be verified and corrected if there is a problem. Coarse adjustments can be made by removing the preload and loosening the load train. These components can then be shifted and/or shimmed to gain proper alignment. Once the load train has been re-tightened, the small bending strains, *which always exist*, must be measured and minimized. This is typically done by using a strain-gaged, trial test specimen, which allows bending strains to be calculated as a function of position along the test specimen, using the same material and test set-up as will be used in the actual test program. This process can be somewhat involved and there are many articles that describe it in detail (**[Refs. 23-26]** and ASTM El012).

During axial loading, the bending strains should be kept below a specified amount as described in various fatigue testing standards. For example, ASTM E606 recommends that the maximum bending strain should not exceed 5 per cent of the minimum axial strain range used during the test. If the bending strains exceed these amounts, then the test rig must be further aligned. In past years, this was done by a trial-and-error method similar to the coarse adjustment procedure described above. This process could take days of effort to achieve moderate bending results. Recently, a new device has been developed (**Fig. 11**), which fits into one end of the load train (**Fig. 3**) and allows adjustment of both angular and concentric components of bending while the load train is under preload. This reduces the time needed for achieving proper alignment to within a few hours.

The amount of bending strain in the specimen is affected by gripping methods and specimen design. Better alignment can be achieved using collet, wedge and button-head grips.

Threaded specimens generally give poorer alignment with equally poor reproducibility. Likewise, wear and oxidation of the grips can lead to poor alignment.

I. Graphic Recorders

In addition to software-based, digital recording methods, analog recording devices are also commonly employed for materials testing applications. Strip-chart recorders, enabling time-based paper chart records of various control and response variables are used. Generally, the strip chart record is used to provide a means to diagnose why a test went off-line, if it does so prior to failure, and to record the gross response variable behavior (e.g., load response) at the point of incipient failure under strain control conditions. Most pen-based strip chart recorders are useful for lower frequency testing applications (e.g., $<$1Hz), as their limited frequency response precludes use to higher frequencies. XY recorders are also commonly employed to record material stress-strain (load-displacement) response, or hysteresis loop response in fatigue tests. XY and strip chart recorders often feature a selection of pre-set gain ranges (e.g., .1V, 1V, 10V or 1V, 2V, 5V, 10V) for use in plotting signals from the test system. For materials testing applications, it is most desirable that the preset gain controls offer ranges that approximately double the previous setting's value with each subsequent setting (e.g., 1V, 2V, 5V, 10V). Analog recorders of these type are often used in conjunction with digital controllers and associated software, due to the additional flexibility offered.

V. ELECTRONIC TEST CONTROLS

Electronic test controls (controllers) are used to adjust and maintain the desired control parameter(s) for a given fatigue test. Controllers also provide test termination capabilities for many criteria: failure, load drop off, deflection or extension limit excellence, etc. Modern fatigue testing is generally performed using closed-loop servocontrollers, wherein the controlled parameter is continually sensed and compared to the desired command, and the

result of this comparison, the error signal, is used to drive the actuator (which may be hydraulic or electromechanical in nature). Sensors for measuring the relevant mechanical quantities (e.g., load cells, extensometers, etc., as discussed elsewhere in this article) provide the feedback, and the control mode of the test is defined by the sensor being used for feedback control. Control is typically effected through a Proportional-Integral-Derivative (PID) strategy wherein the error signal is amplified by gain terms that can be time-independent (Proportional Gain), as well as time-dependent (Integral and Derivative gain). A typical closed-loop control system is shown in **Fig. 12**.

A functional fatigue-testing machine requires the ability to flexibly define test needs with regard to command waveform generation and data acquisition. A variety of technologies are available to accomplish closed loop control of materials testing systems, in performing standard materials tests, and for the development of custom testing applications. This section discusses these technologies and particularly focuses on the software tool state of the art for materials testing.

A. Load Frames: Analog and Digital Controls

Analog controllers are the most commonly used test controllers in fatigue testing laboratories today. Analog controllers have been brought to a high level of refinement, and the latest examples exhibit relatively low noise and reasonably wide frequency bandwidth. Analog controllers typically provide numerous inputs and outputs that can be used to flexibly adapt to nearly any testing requirement. In addition, materials testing applications software that is designed for analog controllers can be used broadly on many different controller models. The disadvantages of analog controls include: many models do not provide the ability to switch control modes while the test system is energized (under hydraulic pressure), and, calibration of the sensors and the test controller is typically done through trim pot adjustments, a process that can be time-consuming.

Digital controllers have been available for the past several years, and the usability of these controllers continues to improve with each new generation. The fundamental difference between an analog controller and a digital controller centers on the summing junction, **Fig. 12**.

A digital controller closes the control loop using a microprocessor, instead of continuous-signal analog amplifiers. In a digital controller, the loop closure rate (the rate at which the microprocessor must update the control loop) is directly related to the maximum test frequency performance (e.g., bandwidth) that can be attained. The loop closure rates required for servohydraulic systems demand very high performance digital systems. The factors driving the development of digital controls include: control modeswitching is simpler, as the loop is digital, and many of the problems relating to offset error in analog systems are not present in their digital counterparts. In addition, from a manufacturer's viewpoint, the cost of digital technology continues to drop (for a given level of performance), and the manufacturing of digitally based products is inherently simpler, owing to fewer required circuit trim adjustments. The chief disadvantages of digital controllers are that changes to the controller organization cannot be done except through software modification of the controller, effectively isolating the user from making any change and, digital controllers generally require software graphical user interfaces. Most digital controller operator interfaces can be labyrinthine to navigate and use, complicating their use and increasing the probability of user mistakes.

B. Comparison: Analog and Digital controllers

Both analog and digital controls technologies are available for use in performing materials tests, and it is not possible to make, definitive statements regarding the superiority of either technology for materials testing needs. The decision as to which controller technology to use may be more prosaic as well: life cycle costs, training costs, etc. must all be carefully considered before a choice is rendered. Because analog controllers provide a nearly universal interface for admitting external program command signals, as well as provide high level conditioned transducer signals for data acquisition, they are easily interfaced to computers for test control purposes. The software created can be generally applied to testing needs regardless of the specific manufacture's model of the analog servocontroller. Digital controllers, on the other hand, feature software that is based on the 'command set' for the specific controller. Thus, materials testing needs that cannot be realized from off-the-shelf software must be custom-developed and any such software is uniquely tied to that specific digital controller

model. Finally, analog controllers have a demonstrated longevity, whereas the digital controller will likely have a much shorter obsolescence, owing to the rapid evolution of digital components.

C. Furnace Controls

The control of furnaces used in materials testing is largely accomplished using closed-loop temperature controls. Because thermal processes are inherently slowly varying (therefore the control loop update rate requirements are relatively modest), and because the costs of microprocessor technology continue to drop, nearly all temperature controllers available today are digitally based. Care must be exercised when selecting a given temperature controller to ensure that it is compatible with the control input requirements of the heating system that is being used. If thermomechanical tests are contemplated, or other non-isothermal temperature requirements are being contemplated, the temperature controller must have facilities for varying the temperature setpoint, either by means of an external command signal, or via a controller command set. Of the two, facilities for accepting an external command signal are preferred, as this provides the greatest flexibility and simplicity in the test apparatus.

D. Test Program Development

Software systems for performing materials tests have been in use for approximately 25 years [27]. During this period, computer technology has changed dramatically, but, ironically, testing needs have not. Scientists and engineers have a continuing need for flexible and powerful tools to design and conduct materials tests, be they standard tests or unique experiments representative of research and development efforts. Software systems developed to satisfy testing needs have typically been developed along three lines: single application software created uniquely to meet a specific testing requirement (e.g., ASTM E-606 Low Cycle Fatigue, etc.), general purpose testing software designed to provide a flexible set of tools that can be used to implement a broad spectrum of testing requirements, and lastly, custom-written test application software.

E. Single Purpose Software

Software for performing standardized tests is widely available from several vendors, operating for both analog and digital servocontrollers. Materials testing engineers charged with conducting standardized materials tests are strongly encouraged to review commercially available offerings before considering custom application software development. Most specific test requirements (for example, high-cycle fatigue, low-cycle fatigue, fatigue crack growth, etc.) are well represented by commercially available application software. While the cost of commercial materials testing software is significant, custom application development is non-trivial and time consuming.

G. General Purpose Software

Several examples of general purpose testing software are readily available from a variety of vendors. Generally, these applications operate on a PC interfaced (in varying degrees of complexity) to a servocontroller, either digital **[Refs. 28-30]**, or analog and/or digital **[Refs. 31-35]**. These tools permit the construction of reasonably complicated test sequences, and provide for data acquisition needs. Some systems provide the ability to build test sequences that are limit programmed (for example, a load-controlled, strain-limited waveform), can offer mutli-mode test control (e.g., dynamically switching control modes during the test), and can provide the ability to perform calculated control of either or both the control variable, as well as the significant waveform parameters (e.g., amplitude, rate, frequency, etc.), **Fig. 13**. Examples of the testing applications that can be accomplished with this class of testing software include thermomechanical fatigue (TMF), biaxial and multiaxial fatigue, creep-fatigue, bithermal fatigue, etc. These general purpose systems have grown in sophistication to the point where one must make careful consideration of one's testing needs before embarking on a custom application programming project; often, the general purpose system can provide the quicker solution, and at a much more attractive cost.

G. Custom Application Software

When testing requirements are very specific and unique, the materials test engineer must often develop their own materials testing application software. The approach taken can vary widely depending on the nature of the test controller and the needs of the application.

H. Data Acquisition Requirements

Regardless of the approach taken with respect to testing software, certain data acquisition requirements must be met with regard to the amount of data collected, the rate of collection, and the overall accuracy of the data collected. Fatigue tests involving the use of sinusoidal waveforms (commonly used for high cycle fatigue testing), for example, typically require a data collection rate of fifty (50) points per cycle to enable the cycle to be accurately rendered. A triangular waveform is most often used for low cycle fatigue testing. Accurately rendering a hysteresis loop in this case requires a data collection rate of up to four hundred (400) points per cycle. When selecting or evaluating data acquisition capabilities for fatigue testing, consideration must also be given to the specific properties of the A/D system: important characteristics include resolution, accuracy and noise level. Another important characteristic concerns how the A/D system handles multi-channel signal input. Typically, two approaches are taken: the first, and most common, approach is to simply multiplex the input signals to the A/D system. A concern here is the potential for channel-to-channel data skew: each channel scanned is obtained at a different time than the others. Depending on the conversion rate of the A/D system, and the testing frequency being employed, the channel skew can be significant. A second approach for handling multi-channel inputs is to use a simultaneous sample and hold amplifier for each channel. In this approach, all channels are sampled and held at the same time, and are then multiplexed to the A/D for conversion. Yet other data acquisition systems employ individual A/D converters for each input channel. The reader is referred to ASTM E-1856 for a more detailed discussion of this topic.

I. Data Analysis

The software available for data analysis largely mirrors that available for testing applications: the standardized test applications generally have built-in data analysis and reporting capabilities, optimized to report test results in standardized formats. However, test data obtained from general purpose testing software, and especially data obtained from custom application programs, must generally be imported into a data analysis program. The most common data analysis programs are the scientific data analysis and plotting applications widely available from many vendors. Another popular method is to import test data into spreadsheet programs. Many of the scientific analysis packages (as well as the spreadsheet programs) provide the ability to develop reasonably sophisticated analysis algorithms ('macros' in spreadsheets, for example), thus providing a convenient and powerful means of data analysis and presentation.

VI. BASELINE ISOTHERMAL FATIGUE TESTING

It is important to understand the underlying purposes of the testing to be performed. This will aid in selecting a fatigue testing machine and specimen design. Normally, a baseline condition is established from which effects on fatigue life of a wide variety of variables might be assessed. Laboratory ambient conditions of room temperature, atmospheric pressure and humidity are a commonly accepted condition for baseline testing, but other choices of, say, temperature may be more appropriate. Baseline testing is usually performed with the numerous fatigue life-influencing variables held constant at what would be considered "default" conditions. For example, completely reversed loading (zero mean stress) may be used, or perhaps zero to maximum loading is preferred owing to the nominal zero-to-max loadings expected in service. Note that rotating beam machines are incapable of mechanically imposing mean stresses. If mean stress assessment is contemplated for testing beyond the baseline, a different type fatigue machine is required.

The acquired baseline database may have value in serving any of several diverse purposes:

0 - Ranking fatigue resistance of alloys

0 - Micro-mechanistic studies

0 - Guiding development of fatigue life prediction models

0 - Statistical documentation

0 - Establishing fatigue design curves

0 - Failure analysis

A. Testing Regime

Of additional importance is the fatigue life regime of interest -- low-cycle or high-cycle fatigue. As discussed earlier, the amount of time available for testing along with the number of companion machines and their cyclic frequency capability will dictate which type machine is best suited. For fatigue lives far beyond 10^5, a high frequency of testing is a necessity. However at lives well below 10^5, high frequency is a liability, not an asset. With the exception of very high cyclic lives, servohydraulic, direct-stress, testing machines offer the greatest possible versatility in testing machines today. Specially designed, and hence costly, commercially available servohydraulic machines can achieve 1000 Hz.

B. Calibration and Standard Test Procedures

Once equipped with an appropriate fatigue testing machine and a specimen design, it is important to follow applicable ASTM (and ISO?) Standards for testing. The major items covered by ASTM Standards include calibration of load cells, extensometers, other sensors, read-out equipment and recorders for data storage, etc., alignment of loading axis of testing machine with grips and with the test specimen, specimen design including alignment of test section with grip ends, surface finish, and material quality control from specimen to specimen, purity of loading command signals, etc. **Table 1** lists the currently applicable ASTM Standards for baseline, and associated, fatigue testing.

Adhering to testing standards is particularly important in fatigue testing due to the inherently high degree of scatter in fatigue resistance. In creating the standards, efforts were put forth to ensure uniformity of specimen geometry, surface finish, loading alignment and gripping, temperature and humidity (for alloys sensitive to moisture level), and uniformity in all aspects of the testing machine frame and loading train, its ancillary equipment, controllers, recorders, data storage, and data manipulation.

C. Generating Fatigue Crack Initiation Data

The loading mode, life regime, test temperature and environmental conditions, mean stress, surface finish, heat treatment condition, etc. dictate the testing machine and ancillary equipment required. Once these are in place and calibrated, and the representative test specimens have been prepared, a baseline fatigue-testing program can be conducted. If the program involves several variables, it would be wise to first perform a "Design of Experiments (DoE)" study to maximize the information to be obtained while minimizing the number of tests and attendant costs. A Section of this handbook is devoted to such an approach. In any event, it should be noted that the cost of specimen preparation is usually not the dominant cost in a fatigue-testing program. It is wise to ensure a sufficient excess of specimens is made to more than adequately cover the initial number required in the program. Having specimens left over from a baseline study is often found to be beneficial, particularly if additional factors are to be studied and if scatter in fatigue lives has been great enough to warrant additional tests to better establish the statistical results. It is generally not possible to duplicate the specimen consistency at a much later date, so it is better to have extra than not enough specimens to begin a test program.

It is advisable to estimate the expected fatigue life of any test prior to starting to avoid excessively long or short test times. Past testing experience with similar materials is valuable in making life estimates. Empirical equations have been published for estimating fatigue resistance based upon conventional tensile test data for the material, temperature, and environment of interest. The equations of Manson **[36]** and Morrow **[37]** have proven invaluable in this regard[a]. See **equation (1)** to follow.

[a] In fact, the Method of Universal Slopes (MUS) [36] has been used to by-pass having to conduct fatigue tests. With appropriate factors of safety, the MUS has been used in the establishment of low-cycle fatigue design curves for many of the alloys used in the United State's Space Shuttle Main Engines [38]. The fatigue resistance of a large number of alloys in a variety of heat-treated conditions over a range of temperatures and aggressive environments has been established in this manner.

If a broad range of testing times are to be involved, it is also advisable to conduct the shortest time tests firsts, then take advantage of these results to govern the loading levels applied for the longest life tests. One should avoid running tests that must be discontinued because considerably less information is gained from such "run-outs".

Sufficient tests should be run to failure over the range of variables studied to permit a statistical assessment of the results. This is particularly true for the baseline results from which other fatigue test results are to be compared.

The extent to which the test data are recorded *during testing* depends on the end use of the fatigue data. In high-cycle fatigue, most alloys behave nominally elastically, and there is little reason to monitor test parameters during the test, as there will be little if any change to observe until fatigue failure is imminent. However, in strain-controlled low-cycle fatigue with observable amounts of plasticity, significant changes might occur that warrant recording, i.e., cyclic strain hardening or softening, relaxation of mean stress, and even cyclic stress-strain response changes due to crack nucleation. It is quite important to be able to monitor these changes during testing. For example, the hysteresis loop at "half-life" is usually chosen to be the representative loop of the entire fatigue test. This loop provides the values of the stress amplitude, stress range, mean stress, total strain range, inelastic (plastic) strain range, and the elastic strain range that are tabulated along with the number of cycles to failure. Since the number of cycles to failure isn't known until after the test has passed the "half-life" point, it is necessary to monitor and record this information either continuously or at intervals close enough to be able to interpolate to the half-life condition once the test has failed.

Baseline fatigue data are generally tabulated and plotted. Schematic fatigue curves [39] are shown in **Fig. 14 (a)** for strong, tough, and ductile alloys. The corresponding stress-strain hysteresis loops are depicted in **Fig. 14 (b)**. This figure illustrates the common observation that the number of cycles to failure for a 1.0% total strain range is approximately 1000 cycles, regardless of the strength or ductility level of an alloy when there is a trade-off between strength and ductility due to different alloy processing. Presuming an equation form, fatigue data can be analyzed using least squares curve-fitting analyses. The most common equation form for low-cycle fatigue and for lives to about 10^6 cycles is:

$$\Delta\varepsilon_{total} = \Delta\varepsilon_{elastic} + \Delta\varepsilon_{plastic} = B\,(N_f)^b + C\,(N_f)^c \qquad (1)$$

where,

$\Delta\varepsilon_{total}$ = Total mechanical strain range at half-life

$\Delta\varepsilon_{elastic}$ = Elastic strain range (= $\Delta\sigma/E$) at half-life

$\Delta\varepsilon_{plastic}$ = Plastic (inelastic) strain range at half-life

N_f = Number of cycles to failure (see following paragraphs)

b = Slope of elastic strain range life line on log-log coordinates

B = Intercept of elastic strain range life line at $N_f = 1$

c = Slope of plastic strain range life line on log-log coordinates

C = Intercept of plastic strain range life line at $N_f = 1$

$\Delta\sigma$ = Stress range at half-life

E = Modulus of elasticity

The Method of Universal Slopes that is used to estimate fatigue curves has the same form as equation (1). The values of the "universalized slopes" are given by:

b = -0.12

c = -0.60

The corresponding values of the intercepts are determined from conventional tensile test results for the alloy at the temperature and environmental conditions of interest:

B = $3.5\sigma_{ult}/E$, and σ_{ult} = ultimate tensile strength

C = $D^{0.6}$

D = ln[(100)/(100-%RA)] = true ductility (also true fracture strain)

%RA = Reduction of Area in tensile test

Morrow's formulation is similar and has seen widespread use in the automotive and off-highway equipment industries. It takes the following specific form:

$$(\Delta\varepsilon_{total}/2) = (\Delta\varepsilon_{elastic}/2) + (\Delta\varepsilon_{plastic}/2) = (\sigma'_f/E)\,(2N_f)^b + \varepsilon'_f\,(2N_f)^c \qquad (2)$$

where,

$\Delta\varepsilon_{total}/2$ = Total mechanical strain amplitude at half-life

$\Delta\varepsilon_{elastic}/2$ = Elastic strain amplitude (= $\Delta\sigma/2E$) at half-life

$\Delta\varepsilon_{plastic}/2$ = Plastic (inelastic) strain amplitude at half-life

$2N_f$ = Number of reversals to failure (= 2X number of cycles to failure

b = Slope of elastic strain amplitude life line on log-log coordinates

σ'_f/E = Intercept of elastic strain amplitude life line at $2N_f = 1$

c = Slope of plastic strain amplitude life line on log-log coordinates

ε'_f = Intercept of plastic strain amplitude life line at $2N_f = 1$

$\Delta\sigma/2$ = Stress amplitude at half-life

E = Modulus of elasticity

Morrow's fatigue life equation in its predictive form assumes the slopes and intercepts can be approximated from tensile test properties by:

b = n/(5 + n), where n is the strain hardening exponent (the cyclic strain hardening exponent, n' may give better predictions. Note, n' = b/c)

c = 1/(5 + n)

σ'_f/E = σ_f/E, where σ_f = true fracture stress (fracture load divided by fracture area)

ε'_f = ε_f = true fracture strain = true ductility (D)

The slopes and intercepts from the above equations are referred to as the basic fatigue properties. **Reference [40]** contains an extensive listing of these fatigue properties, along with

corresponding tensile properties, for a wide variety of steels, stainless steels, nickel-base superalloys, titanium alloys, aluminum alloys, weldments, and castings. How the fatigue properties might be affected by factors that influence fatigue behavior will be discussed in VII.

In the high-cycle fatigue regime, i.e., beyond approximately 10^6 cycles to failure, the log-log slopes of the fatigue curves tend to become shallower than at lower life levels. For certain steels and selected body-centered cubic (bcc) alloys, a fatigue or endurance limit "infinite" life for cyclic stresses below the limit may be observed in laboratory fatigue test results. Such limits may be erased by interspersed low-cycle fatigue loadings that can break up the dislocation pinning by small interstitial atoms in the bcc structure. Under these circumstances, the fatigue curve will continue to drop in strength level below the original fatigue limit. Slopes of the fatigue curve in the very high cycle fatigue regime may drop to -0.04 or less. Manson **[41]** has reported ultra high cycle fatigue life extrapolation procedures.

D. Criteria for Defining Fatigue Life

The first and most common definition of fatigue life for alloy testing is the number of cycles of loading required for complete fracture of the specimen into two pieces. This definition is unequivocal. It is easy to identify this terminal event in most fatigue tests[4]. At fracture, the specimen grips are free to move apart, allowing a mechanically activated switch to be tripped that stops the cyclic drive mechanism and the cycle counter. Electrical continuity of the specimen is also broken permitting direct electrical switching of circuits controlling the machine. Complete specimen separation is typically an acceptable measure of the crack initiation fatigue life for high-cycle fatigue wherein the fatigue crack nucleation portion dominates the total life (perhaps 90 to 99 %). However, since the separation life does include a portion of cyclic crack growth, this quoted life is somewhat larger than the number of cycles to physically initiate a crack. As the fatigue loading levels increase and the cyclic lifetime decreases into the low-cycle fatigue regime, less and less of the life is spent nucleating a crack and more and more life is spent growing the crack(s) to the critical length for sudden fracture

[4] During strain controlled tests at low strain amplitudes, cracking may reduce the stress level sufficiently that the specimen never separates. In this case, some other definition of failure must be used.

into two pieces. To accurately define the cyclic crack initiation life, particularly in low-cycle fatigue, one ideally would measure the actual crack size (depth and length) as cycling progressed. When a predetermined crack size was reached, the number of cycles to "failure" would be noted and testing stopped. Unfortunately, this is highly impractical for most testing because it can't be implemented on an automated basis for the large numbers of fatigue tests conducted annually.

The only practical definitions available are those based on measurements that are readily available from the test instrumentation. This is usually in the form of changes in specimen elastic or plastic "stiffness" as determined from stress-strain or load-deflection measurements. As a specimen develops a fatigue crack under completely reversed strain control, its growth causes the load carrying response of the specimen to decrease. Different degrees of drop in the cyclic load range for a fixed strain range have been used to define crack initiation failure for low-cycle fatigue testing. The most commonly used have been the very first indications of an impending drop in the load range (i. e., impending cracking) and a 5 percent drop in the load range. Obviously other percentage drops (10, 20, and 50) could be defined and used. Unfortunately, it may be difficult to distinguish between load range drop due to cracking and load range drop due to cyclic strain softening of initially work hardened materials. Even cyclic strain hardening could confound the measurement by offsetting the drop due to cracking.

A logical way to separate the effects on load response of cyclic strain hardening or softening from cracking is to track the ratio of the peak tensile load to the peak compressive load **[42]**. If only hardening or softening occurs, the load range will change, but the tensile/compressive load ratio will be affected very little. As fatigue cracking progresses, the decrease in the tensile load amplitude exceeds that of the decrease of the compressive load amplitude. This is observable in **Fig. 15 (a)** from a load versus time trace for a low-cycle, completely reversed, strain-controlled test **[43]**. As cracking occurs, the change of the load ratio is almost twice as much as the change in the load range, thus making it a more sensitive as well as a more physically-based measure of cracking. The load response would also be observable in a stress-strain hysteresis loop. In compression, the crack faces close and carry

load. This results in a cusp on the hysteresis loop near the compressive peak. In tension, the peak load is carried only by the smaller, un-cracked area.

To apply these criteria for defining fatigue crack initiation life the load ratio must be measured during the pre-crack nucleation period. Note that the load ratio during this interval may not equal 1.00. It has been observed to vary from as low as 0.9 to about 1.05 depending upon material. The ratio, however, is nominally independent of the amount of cyclic hardening or softening that occurs, and hence a greater duration of cyclic loading can be used to establish the average value of the ratio before cracking commences. A graphic quantitative example is given by **Fig. 15 (b)** based on the data from **Fig.15 (a)**. Both load ratio and load range are plotted versus applied cycles. The load ratio is relatively constant at 0.96 for the first half of the test, but by about 100 cycles, it begins to drop steadily. At about 200 cycles the ratio suddenly and inexplicably rises. This rise signals the end of useful information from the test. Even though the specimen is still in one piece, the computed stresses and strains are no longer representative of what is going on in the gage length of the specimen. At this point, the dominant crack has grown to a large fraction the specimen diameter and the extensometer is subjected to large amounts of bending in addition to axial deformation. The specimen may not have failed completely, but the test has. The corresponding load range is also shown. After considerable initial hardening of 25%, a half-life ('stabilized') value of 2800 lb. is reached. This is followed by an accelerating drop until complete fracture of the specimen occurs at greater than 214 cycles. For the particular test data shown, the load ratio and the load range follow approximately parallel behavior. For this example, a 5% drop in load range and load ratio corresponds to the same number of cycles ($\approx$ 138 cycles). Similarly, a 10% drop in both gives about 158 cycles. In this case, either the load range or the load ratio drop criteria would give acceptable definitions of fatigue crack initiation life. This is not expected to be the general case for the following reasons.

For a cyclically stable material with very little strain hardening within a hysteresis loop, a 5% load range drop would correspond to approximately a 10% drop in the load ratio if the only reason for load drop was the presence of a crack. This in turn would imply a 10 percent loss in specimen cross-sectional area if there were no concentration of stress surrounding the crack tip. However, since there is a concentration of stress in front of the crack, higher

stresses are encountered there, thus increasing the tensile load carrying capacity. Hence, a 10 percent loss of area would actually correspond to less than a 10 percent loss of load ratio. Load ratios in the neighborhood of 5 to 8 percent have been noted.

With modern automated data recording and reduction, it is possible to determine the fatigue life by all of the above definitions, including complete fracture into two pieces. In this way, any definition of fatigue crack initiation life can be selected for the purposes at hand. **References [42 and 43]** contain tabulated fatigue crack initiation lives for several engineering alloys for the four criteria such as discussed above, i.e.,

N_o First indication of impending cracking

N_5 Five percent drop in load range from stabilized range
(or at half-life value if stabilization does not occur)

N_i Ten percent drop in ratio of tensile to compressive load from stabilized range
(or at half-life if stabilization does not occur)

N_f Complete separation of specimen

Similar criteria based on the same concepts could be established for completely reversed, load-controlled tests. Instead of a decrease in load response due to cracking, an increase in strain or deflection response would be measured to define fatigue crack initiation.

Care should be exercised in applying the above criteria when multiple cracks initiate parallel to one another. Many shallow cracks will have the same integrated effect on specimen gage length compliance as one deeper crack. In addition, the exact location of the crack(s) relative to the contact points (defining the gage length) of the extensometer can have an appreciable influence on the apparent (measured) compliance. For example, should cracking initiate outside the gage section, the extensometer would not detect a change in compliance. Should cracking initiate within the gage section, the load path would not necessarily remain along the centerline of the specimen and bending would occur. This, in turn, can cause the extensometer to register different output depending upon the plane of bending relative to orientation of the extensometer. These confounding influences also affect the load range drop criteria for crack initiation.

E. Information to be Documented for Baseline Fatigue Tests

Guidelines are presented for what baseline fatigue test information should be documented. **Tables 2 and 3**, respectively, provide comprehensive listings of pertinent pre-test and in-test/post-test information to be considered for inclusion. In preparing **Table 3**, it was assumed that closed-loop; servo-strain-controlled axial fatigue testing was the mode of operation. If other modes of testing are used, the guidelines may have to be altered accordingly. Obviously, the information gleaned from a fatigue test in progress will depend on the extent of instrumentation available, the type of testing machine, and the mode of testing.

F. Example Crack Initiation Fatigue Life Curves

Fatigue curves are displayed in a variety of forms, although fatigue life is generally plotted on a logarithmic scale. The fatigue loading parameter is usually stress or strain. Stress is most commonly plotted as stress amplitude, stress range, or maximum stress, and the scale may be arithmetic or logarithmic. Examples were given in **Fig. 16**. These are referred to as S-N curves, and an indication of the mean stress ratio should always be given. When strain is the fatigue loading parameter, the total (elastic plus plastic), plastic, or the elastic strain ranges may be plotted. These are usually plotted on logarithmic scales as shown in **Fig. 17** and are referred to as strain-life curves. Unless the fatigue strain cycling ratio is given, it is understood the curves represent completely reversed loading. The plastic strain versus life curve is known as the Manson-Coffin (or Coffin-Manson) low-cycle fatigue curve. The elastic strain range versus life curve has come to be known as the Basquin curve **[44]**. The total strain range versus life representation of fatigue data has its origins in the late 1950's and early 1960's. Coffin **[45]** originally represented the elastic strain range versus life component of the total strain range versus life curve as a horizontal line with a strain range value equal to twice the 0.2% offset yield strength divided by the elastic modulus. Langer **[46]** used the same basic idea, but replaced the yield strength with the endurance limit strength. He went on to multiply the total strain amplitude by the modulus of elasticity to compute the pseudo-stress amplitude. The

resultant fatigue (S-N) curve could then be used in direct conjunction with elastic stress analyses. This representation was adopted by the ASME Code, Section III for Boiler and Pressure Vessel components.

Manson [47] and Morrow [37] carried the fatigue curve representation a step further by recognizing that the elastic strain range versus life curve had a negative slope such as first observed by Basquin a half century earlier.

Out of the total strain range versus life representation of fatigue resistance comes an important observation and useful concept (see, for example, [41]). At some point along the fatigue curve, the elastic strain range and the plastic strain range will be equal. This point defines what is known as the transition fatigue life, $N_{f,trans}$ and the corresponding transition total strain range, $\Delta\varepsilon_{total,trans} = 2\Delta\varepsilon_{plastic} = 2\Delta\varepsilon_{elastic}$. Below the transition fatigue life, the behavior is clearly low-cycle fatigue as the plastic strain range dominates over the elastic strain range. Low cycle fatigue actually continues to higher lives beyond the transition life. High-cycle fatigue behavior, in which the elastic strain range overwhelmingly dominates over the plastic strain range, doesn't begin until at least one order of magnitude in life beyond the transition life.

VII. TESTING FOR EFFECTS OF VARIABLES ON FATIGUE RESISTANCE

The fatigue resistance of an alloy is sensitive to a large number of variables. There are too many variables to investigate them all. To do so would require an enormous test matrix, a large number of fatigue testing machines, and a huge budget. Fortunately, similar behavior trends are observed by various classes of alloys. This allows engineers to experimentally document the behavior of many of the more commonly encountered variables using only a limited number of tests. As a prime example, several different models can describe the effects of mean stress on fatigue life. All predict lowered fatigue resistance to tensile mean stress and enhanced life with compressive mean stress. Another example is the correlation between tensile test properties and baseline fatigue resistance as given by equations (1) and (2), i.e., an

increase in an alloy's ductility generally enhances low-cycle fatigue life whereas increases in tensile strength produce greater high-cycle fatigue resistance. These correlations have proven quite valuable. If more accurate assessments of the effects of variables on fatigue are required, they can be determined experimentally. This section discusses the more commonly investigated variables.

The variables affecting fatigue can be categorized into four types: bulk, surface, geometric, and active loading related factors. Common examples of each type are listed in **Table 4**. Synergistic interactions may occur among these influences. For example, the loading related factor of high-temperature testing in air would induce the surface related factor of oxidation. Seldom are surface related effects of this nature beneficial to fatigue resistance.

Bulk and surface related property effects could be further classified as pre-existing or concurrent. Geometric effects are generally pre-existing with respect to laboratory specimen fatigue testing. Examples of pre-existing bulk effects are cold working introduced during the forming process and metallurgical heat treatment of the alloy. Either could significantly alter the strength of an alloy and hence alter its fatigue resistance. Concurrent effects can include time-dependent creep, oxidation, or solid state metallurgical changes, all resulting from exposure of the alloy to high temperature during operational use or specimen testing. Effects on fatigue resistance of pre-existing factors can be dealt with by simply considering the alloy as a new material to be evaluated.

Concurrent influences, however, require additional consideration to ensure testing adequately reflects the influences encountered in service. For example, high-temperature service may involve more than an order of magnitude greater exposure time than can be afforded during fatigue testing. Consequently, the testing program must be designed to provide data that can be extrapolated with confidence into the time regime of practical interest. This is a particularly vexing problem in the area of high-temperature fatigue, creep-fatigue, and thermomechanical fatigue (TMF) testing of alloys.

Invariably, engineering models of fatigue behavior are created to allow confident interpolation and extrapolation, particularly for structural applications. Models are calibrated to reflect the influences of a multitude of variables. Many models have been proposed over the past century. Those of greatest value for engineering design are the ones that are relatively

simple, logical, and clearly reflect a cause-and-effect relationship. They are the easiest to remember and use. Those models that reflect a high degree of mechanistic fidelity are naturally of greatest benefit to the material science and failure analysis community. If such models can also be expressed in tractable terms, they will also be used by engineers for designing in structural durability of machine components. Understanding the root causes of fatigue permits engineers to better guard against this insidious failure mode.

A. Pre-Existing Variables

Because of the similarities of testing for pre-existing bulk or surface related effects on fatigue resistance, they will be lumped together for discussion. Guidelines for information to be documented from fatigue tests of pre-existing variables are contained in Tables 2 and 3.

1. Bulk Property and Surface Related Effects

Material with pre-existing effects can be evaluated by conducting fatigue tests using the same techniques and procedures as for baseline fatigue testing. The affected material is considered as a new material, but one for which some background knowledge exists. It is not uncommon to see a series of fatigue curves for the same alloy composition wherein each curve reflects differing degrees of cold working, heat treatment, or surface finish. The fatigue results are typically used to select an optimum fabrication method or to indicate material conditions to be avoided. In general, fewer fatigue tests are required, *provided* the baseline results are well behaved and well defined. However, if there were more scatter in the property-affected results, more tests would be required to adequately define the new fatigue curve.

2. Geometric Effects

The most commonly investigated geometric effects are those of notches and the degree of the theoretical stress concentration (K_t) they impose. Invariable, the fatigue resistance decreases with higher stress concentration factors. The extent of fatigue strength loss for a given fatigue life, however, is never as great as might be suggested by the value of the stress concentration factor. Furthermore, the effectiveness of the stress concentration factor decreases

as the root radius decreases and the overall size of the notch decreases. There are several reasons for this behavior that are adequately explained in most text books covering fatigue. As discussed earlier it is of great importance to fatigue testing that uniformity of the notched specimens be maintained to reduce confounding scatter issues. Particular care is required to achieve this goal when dealing with very small notch root radii.

The testing of notched specimens in the high-strain, low-cycle fatigue regime may introduce yielding at the root of the notch. If the cyclic loads are great enough, the yielding will occur on each cycle, despite the fact that the overall specimen appears to behave nearly elastically. The cyclic strain range at the notch root will be larger than indicated by the theoretical stress concentration factor, and the cyclic stress range will be smaller. Analytic approaches are available to describe the stress-strain behavior at the notch root in terms of the applied loading and the materials cyclic stress-strain curve. See for example, applications **[48,49]** of Neuber's **[50]** and Glinka's **[51]** notch analysis approaches. Also of great importance to the fatigue testing of notched specimens is the cyclic relaxation of initial mean stresses at the notch root. For example, for zero to maximum load-controlled cycling, the local notch root stress can relax from an initial zero to maximum condition on the first cycle to a completely reversed condition as cycling progresses. Such changes in the local stress-strain response have a profound influence on the fatigue life of notched specimens. As the cyclic loading level is decreased and longer lives are achieved, there is less and less chance for relaxation of the initial cycle mean stress. Consequently, the resultant fatigue curve will exhibit a very low mean stress effect in the low-cycle regime, but will exhibit the full effect of mean stress in the high-cycle regime. Without performing a local stress-strain analysis at the root of the notch, it is nearly impossible to ascertain whether or not a mean stress will relax, and to what extent. The issue of mean stress relaxation becomes critically important in performing cumulative fatigue damage experiments with notched specimens.

Other specimen geometric effects include thin sections and sharp edges. Both can result in fatigue life reductions due to the fact that there is far less constraint to the motion of dislocations because of the high ratio of surface area to volume. This effect is accentuated at high temperatures wherein creep can occur more readily by grain boundary sliding. Reducing a section thickness to only one or two grain diameters can greatly reduce the normal constraint

offered by surrounding grains, thus enhancing creep deformation and increasing the degree of creep-fatigue interaction. When performing fatigue, creep-fatigue, and thermomechanical fatigue tests of thin sections one should caution against having too few grains through the thickness.

Yet another pre-existing geometric aspect is the so-called size effect. The smaller is the volume and related surface area of the fatigue affected zone of a test specimen, the less probability of encountering a microscopic flaw leading to early crack initiation. Large specimens with relatively large volumes and high surface areas will invariable exhibit lower fatigue lives than small specimens with relatively small volumes of highly stressed material. While this effect is not an overwhelming one, it should be considered when selecting a particular fatigue specimen for a testing program. In general, the highly stressed volume should be as large as can be tolerated, because many practical machine components have much larger highly stressed volumes than can be accommodated in a corresponding fatigue test specimen.

B. Concurrent Variables

Concurrent changes of the variables affecting the fatigue resistance are obviously more complex to evaluate. The fatigue resistance being measured is a moving target and quantitatively depends upon how much change has accrued over the period of testing. Concurrent changes are due to bulk and surface related factors as well as active load related effects due to mechanical loading and temperature changes during testing. Obviously, the information to be documented for fatigue tests involving concurrent variables is more extensive than shown in Tables 2 and 3.

1. Bulk Property and Surface Related Effects

Keep in mind that the laboratory fatigue results are being measured to help assess the structural durability of hardware with specific missions of exposure, loading, temperature, time, etc. Mission loadings often have total durations lasting into years of exposure that can not be affordably duplicated in laboratory tests. The laboratory coupon results must therefore

capture the concurrent influences in such a way that they can be generalized and then brought to bear on specific applications. To do so usually requires a physically based model or equation that can relate the laboratory conditions to the mission loading and exposure conditions. An analogy can be made to time-temperature parameters that relate higher temperature, shorter time laboratory stress-rupture results to longer time, lower temperature mission loading exposure. Available time-temperature parameters are generally consistent with the concepts of activation energy for thermally governed time-dependent creep processes. If models are not available for a smooth transition between laboratory and service conditions, extreme or bounding approaches may be necessary.

As an example, suppose the concurrent degradation in service is fretting. Alloy coupons could be prepared with surfaces that have been independently fretted to varying degrees. Subjecting these coupons to subsequent fatigue tests will demonstrate the effects of fretting as though it was a pre-existing influence. Testing in this step-wise sequence imposes all of the fretting damage at the beginning of the test and it could be expected to cause the maximum damage and hence a lower bound fatigue life. This testing philosophy assumes no concurrent synergy between accumulation of fretting damage and accumulation of fatigue damage. Similar evaluations are possible for effects of nuclear radiation on bulk properties (causing, for example, increased strength and decreased ductility), or oxidation on surface-related effects (decreasing surface resistance to cracking). One should not discount the option of testing with a few multiple steps. As an example, one could:

- Apply static oxidation to a specimen in a furnace for a time interval
- Follow by rapid fatigue cycling for a predetermined block of cycles
- Remove specimen from fatigue machine
- Re-insert into furnace for an additional time interval
- Reinstall in fatigue machine for an additional block of cycles
- Repeat process until specimen fails due to oxidation accelerated fatigue

While this procedure is manpower intensive, total testing time in a fatigue machine could be greatly reduced while developing data that are far more missions relevant.

2. Active Loading Related Effects

A number of active loading variables also fall into the category of concurrent variables. Prime examples of active loading variables are applied mean stresses, multiaxial stress-strain

states, cumulative fatigue damage (non-constant) loadings, and temperature-related effects such as creep-fatigue, and thermomechanical fatigue (TMF). The later two are of such significance and require so many changes to conventional fatigue testing procedures they merit separate discussion.

i. Mean stresses

Perhaps the most commonly considered variable for fatigue testing is the mean stress. Mean stress effects on fatigue were recognize by Gerber **[52]** as early as the 1870's, and have been a source of concern since. One of the most recent thorough reviews of the subject is given by Conway and Sjodahl **[53]**.

A typical mean stress evaluation test would be conducted under load control of axial or plane bending in the nominally elastic high-cycle fatigue regime. Under plane bending, one surface has a tensile mean stress whereas the opposite surface has a compressive mean stress of equal magnitude. It is not possible to run independent tensile or compressive mean stress bending fatigue tests. Since tensile mean stresses are typically more damaging than compressive mean stresses, the bending specimen would always initiate fatigue cracks from the tensile mean stress surface. The plane bending fatigue test is inappropriate for studying mean stress effects in the lower cycle to failure regime. Once small amounts of inelasticity occur at the outer surfaces, stress relaxation and redistribution occurs and the local mean stresses are no longer directly proportional to the imposed mean loads. In fact, the load amplitude and mean will not change as a result of the local changes in stress, and the test engineer will be unaware of any changes to the stresses. Note that it is not possible to conduct mean stress studies under rotating bending fatigue.

To avoid the problems of bending, axial loading is the recommended mode of testing for mean stress effects. **Figure 18** schematically illustrates the decrease in alternating stress fatigue resistance as the tensile mean stress increases. Frequently, the fatigue curve is displayed in terms of the maximum applied stress in the cycle. **Figure 19** shows typical results of the effect of the R stress ratio (= algebraic minimum/algebraic maximum) on the axial fatigue resistance of 2024-T3 aluminum alloy at room temperature over the life range of 10^4 to 10^7 cycles to failure **[53, p. 21]**. Care should be taken when mean stresses are applied under

load control at very high maximum tensile or compressive stresses. Too high a stress can cause yielding and hence cyclic ratchetting in the direction of the mean stress. If in tension, this can lead to eventual excessive tensile strain and subsequent tensile necking (as in a tensile test) and failure long before fatigue cracks have an opportunity to form and grow. Unless an extensometer is employed, small, but damaging, amounts of ratchetting may escape detection.

Mean loading effects in the low-cycle fatigue regime are best dealt with under strain control. The strain control mode rules out ratchetting, although initial mean stresses imposed by mean straining do have an opportunity to cyclically relax. When imposed strain ranges are large enough that the inelastic strain range is on the order of a tenth of the total or elastic strain range, there is a high probability that any initial mean stress will cyclically relax to zero, i.e., become completely reversed, even though the straining is not completely reversed **[54]**. In the high-strain, low-cycle fatigue regime, there is little, if any, effect of mean strain on fatigue life for ductile alloys. However, as the strain range is decreased and the life increases, a nominally elastic condition is reached. Then, a tensile mean strain will be accompanied by a directly proportional tensile mean stress, and the fatigue life will decrease compared to a completely reversed strain cycle. The end result is shown schematically in **Fig. 20**. Typical data of this nature have been reported for a high-temperature gas turbine engine alloy in **[55]**.

ii. Multiaxiality

Investigation of multiaxial stress and strain states on fatigue resistance is a perennial issue because the cyclic stress-strain state at critical locations in machinery components is rarely uniaxial. However, the vast majority of fatigue tests are performed using uniaxial loading. The issues involved are so extensive, the subject has merited a separate section in this Handbook (see Section _____), and will not be discussed further in this Section.

iii. Cumulative fatigue damage

Commonly employed cumulative fatigue damage tests involve random, or non-steady, loading wherein both the amplitude and mean value of the loading varies continuously, **Fig. 21(a)**. Such tests are attempts to simulate, in the laboratory, the detailed loadings encountered in service. The sequence of loading is commonly referred to as spectrum loading. Also

common are simplified, i.e., compressed, loading patterns that have been shown analytically to account for the equivalent amount of fatigue damage as existed in the more complex spectrum loading. These compressed loading patterns capture the basic profile of loading. An illustrative schematic example is shown in **Fig. 21(b)**. In this instance, the simplified loading pattern is arrived out by an equivalent rainflow cycle counting technique **[56]**. Obviously, reducing the number of loading levels permits simplification of testing. Because a loading pattern may repeat itself, the fatigue loading can be applied in the form of repetitive blocks. Terrestrial-based vehicles, aerospace airframes, and civil engineering structures such as bridges typically experience random loadings during their fatigue crack initiation lifetimes. Greater details on how to approach complex cumulative fatigue damage assessment and testing can be found in **[57]**

In the extreme are cumulative fatigue damage tests that involve only two loading levels, one in the low-cycle fatigue LCF) regime, the other in the high-cycle fatigue (HCF) regime. Using this highly simplified testing pattern, it has typically been observed that LCF cycling (to a fraction of the expected life) followed by HCF cycling to failure reduces overall life and the reverse loading order increases overall life. This is referred to commonly as the classical loading order effect **[58, 59]**, and is illustrated in **Fig. 22**. This effect is not captured by linear damage assessment. Consequently, non-linear cumulative fatigue damage models have proliferated **[59]** since Miner's linear damage rule was published in 1945 **[60]**. The accuracy and viability of any cumulative fatigue damage rule hinges upon the assumption that the physical mechanism of damage does not change as loading levels are changed. Clearly, understanding the damage mechanisms is an important and necessary step in the development of accurate models.

Cumulative fatigue damage testing may also involve more than just loading level variations. Changes in the type of loading (thermomechanical and isothermal **[61]**, axial and torsion **[62]**, fatigue and creep-fatigue **[63]**, etc.) during testing may also be of importance.

iv. Temperature-related effects

Temperature-related effects such as creep-fatigue, and thermomechanical fatigue (TMF) are of such significance and require so many changes to conventional fatigue testing procedures they merit separate discussion in the following sections.

VIII. CREEP-FATIGUE INTERACTION

A. Background

Creep-fatigue interaction testing and modeling have been intense activities since the late 1950's. Interest was spawned by the introduction and seemingly premature failures of components in structural equipment operating at elevated temperatures. Examples are: aeronautical gas turbine engines; steam turbines; nuclear reactors and pressure vessel and piping components for electric power generation and chemical processing plants; casting and forging dies; railroad wheels subjected to brake-shoe application, automotive cylinder heads, exhaust valves, manifolds, and exhaust piping systems; and reusable rocket engines to name a few. In many cases, the elevated temperature of operation is reasonably constant (isothermal) over a period of time while components are under load and can suffer creep or stress relaxation processes that hasten crack initiation and early growth. The modes of cracking have frequently exhibited creep-like fractures intermixed with cycle-dependent fatigue type cracking. Hence the descriptive name, creep-fatigue interaction.

Extensive reviews of creep-fatigue interaction were prepared in the early 1980's **[64-66]**. Over the intervening decades, over 100 models or their variations have been proposed to describe creep-fatigue interaction **[67,68]**. As many as a dozen of the models have survived and been applied to practical situations. The three most widely used are the Time- and Cycle-Fraction Rule of the ASME Code Case N-47-23 **[69]**, Strainrange Partitioning (SRP) **[70]** and its Total Strain Version **[71]**, and Continuous Damage Mechanics **[72]**.

B. Creep-Fatigue Testing

The fatigue machines and associated equipment normally used for creep-fatigue experiments are essentially the same as those used for baseline fatigue tests. Current practice calls for axial loading of a uniform gage length specimen mounted in a closed loop servo-controlled fatigue-testing machine with provisions for heating the sample to elevated temperatures. Closed-loop, strain-controlled testing is most commonly used, and if not, strain limit control is imposed to prevent creep ratchetting. The major difference between creep-fatigue and baseline isothermal fatigue testing is in the time per cycle. To introduce creep into the cycle, the frequency is reduced by cycling at a lower strain rate or by introducing a hold period at some selected point within each cycle. Most commonly, a hold period is inserted at the peak strains in a cycle, i.e., maximum or minimum algebraic strains, or at both peaks.

Creep-fatigue interaction testing is conducted at a high enough isothermal temperature that thermally activated, diffusion-controlled creep deformation mechanisms can operate under stress as a function of both time and temperature. As a rough rule of thumb, the transition temperature for creep is on the order of half the absolute melting temperature of an alloy. In earlier years, creep-fatigue testing was conducted to simply ascertain the extent of the damaging effect of creep on cyclic (fatigue) life. Today, tests are still run for that purpose, but more often than not creep-fatigue testing is designed also to evaluate and calibrate the constants in a viable creep-fatigue life prediction model.

The addition of creep to a cycle of normal fatigue loading will invariably reduce the cyclic life, although the clock time to failure may remain constant or actually increase. Conversely, the superposition of fatigue cycling and conventional monotonic creep will also alter the rate of creeping and the time to rupture. Because of the importance placed on knowing the values of stress and time-dependent deformation, it is generally regarded that creep-fatigue testing be done with axially loaded specimens equipped with extensometry. While some interspersed creep-fatigue testing, i.e., repeated blocks of brief periods of creep followed by brief periods of fatiguing, has been reported **[63]**, the most common tests involve repeating cycles of straining with hold periods imposed in tension or compression alone or in combination. The hold periods may be under constant strain or constant stress. If under

constant stress, strain limits are generally imposed to preclude ratchetting. Alternatively, creep could be introduced by controlled slow straining rates in tension, compression, or both.

Figure 23 illustrates the various isothermal hysteresis loops that are commonly encountered in fatigue and creep-fatigue testing. Cycles (a), (e), (f), and (g) were used to generated the data shown in **Fig. 24** for AISI type 304 stainless steel **[68]**. Here the inelastic strainrange is plotted against cycles to failure on log-log coordinates. As can be seen, significant cyclic life losses (a factor of 10 or more) are possible with strain hold periods of just 30 minutes per cycle in tension only. Hold periods of up to 180 minutes per cycle do not necessarily further reduce the cyclic life, implying a saturation condition beyond a certain hold period for strain hold (stress relaxation) type creep-fatigue cycles. Those cycles that are balanced in nature, i.e., the tensile and compressive halves experience the same strain rates or hold times, will not exhibit an algebraic mean stress, whereas the unbalanced cycles will. The mean stress is tensile if the hold period or slow straining rate is in compression, and vice versa. Evidence suggests that these mean stresses do not exhibit the classical mean stress effect on cyclic life in the high-strain range, low-cycle fatigue regime **[55]**, and hence can be ignored. Similar creep-fatigue cycling results for AISI type 304 stainless steel and Incoloy 800 have been reported by in **[73]**. These results were analyzed **[74]** by both the Time- and Cycle-Fraction rule and the method of Strainrange Partitioning based on information provided in **[73]**.

Comparison of the two creep-fatigue life prediction models is given in **Fig. 25**. In this instance, the Time- and Cycle-Fraction rule, which utilizes a stress-based approach to assessing creep damage does not do an acceptable job of predicting the laboratory results. Cyclic lives can be over-predicted by as much as a factor 5 and under predicted by a factor of 20, thus creating a band of uncertainty in predicted life of two orders of magnitude. The method of Strainrange Partitioning is a strain-based approach and assigns creep damage according the magnitudes of the creep strains encountered in a cycle. The figure indicates a strain-based approach is superior in this case.

A viable creep-fatigue model is of great importance in being able to design equipment to operate for long periods of time at elevated temperature. Services lifetimes are typically much greater than the longest affordable creep-fatigue testing lifetimes of laboratory

specimens. What a viable model has to offer is increased confidence in the extrapolations to longer times to failure than were used in the model calibration. A physically based model is expected to hold greater promise than simple empirical extrapolation of non-correlated laboratory data. Because laboratory creep-fatigue measurements are the basic ingredients of the foundation for assessing extrapolated long-time structural durability, it is imperative that accurate measurements and control of the testing variables be maintained. The problem is a much more stringent one than for lower-temperature, fatigue-life extrapolation because of the influence of time and temperature. Creep is sensitive to temperature in a highly nonlinear, exponential dependency and to stress and time of exposure in nonlinear power law dependencies. The temperature and time dependencies also include the effects of interaction with the environment. Typically, oxygen is the surrounding environment and surface oxidation can greatly influence the susceptibility of exposed surfaces to premature crack initiation and early growth. Most creep-fatigue models are calibrated and used without the benefit of separating the effects of oxidation from the creep effects. A listing of models with the potential for accounting specifically for oxidation or other environmental interaction effects is found in [68].

Creep-fatigue test results are generally more extensive than simpler fatigue results. **Table 5** lists, among other items to be discussed, the additional information that should typically be reported for each creep-fatigue test conducted.

IX. THERMOMECHANICAL FATIGUE (TMF)

A. Background

Thermal fatigue is a structural failure mode in many high-temperature components. Thermal fatigue loading is induced by temperature gradients during transient heating or cooling from one high temperature of operation to another. Thermal fatigue loading can also occur when heating and cooling are present simultaneously and thermal gradients are maintained during steady state operation. Internally air-cooled high-temperature turbine blades are examples. Thermal gradients produce differential expansion as the hottest material wants to

expand more than the cooler, but is constrained from doing so by the cooler and stronger material. The constraint is perceived by the hottest material as a compressive thermal strain that is no different in its affect on the material than would be a mechanically induced strain of equal magnitude. Similarly, the coldest material is forced by the hottest to expand more than normal. The thermally induced strain in the colder material is tensile. Conditions of strain compatibility will be maintained. The corresponding thermal stresses result directly from the thermal strains according to the current stress-strain relation and the necessity to obey the laws of equilibrium. The integrated sum of the internal stresses into forces must always equal zero. Because of the gradients of the primary variables, it is impossible to measure the thermal fatigue properties of a material in the same way that isothermal fatigue or creep-fatigue properties are measured, i. e., in terms of holding certain variables constant while the response of the others are measured. To overcome this basic difficulty, thermomechanical fatigue (TMF) tests have been devised.

B. TMF Testing

The testing machine and specimen set up for TMF testing are essentially the same as used for creep-fatigue testing or baseline high-temperature isothermal fatigue testing. The major distinction is that the temperature of the specimen, instead of remaining constant, must be programmed to vary in a precisely defined manner. Furthermore, the cycling rate must at times be rather high, requiring the ability to heat and cool the test specimen as rapidly as possible without creating undue thermal gradients. This requirement virtually rules out the use of conventional clamshell radiation furnaces because of their large thermal inertia. Most commonly, induction heating is used. This is because of the reasonably high rates of heating possible, and because the temperature gradient along the specimen gage length can be controlled better with a three-zone induction heating coil arrangement such as shown in **Fig. 6.** Induction coils are also more conducive for use of extensometers. Direct resistance heating, although not commonly used, has the capability of heating a sample so rapidly, that it could be melted in a matter of seconds. Heating is usually not the limiting factor in governing the cycling rate. Rather, cooling is. Forced air-cooling has been used successfully. Jets of air are

impinged on the specimen surface along the gage length and around the circumference. Excessive cooling induces thermal gradients, and hence unwanted thermal stress and strains. A balance must be achieved between cooling (as well as heating) rate and the extent of undesired thermally induced stresses and strains. Thermal cycling rates as fast as 3 min per cycle are employed on a routine basis. A test run to 12,000 cycles requires 36,000 minutes or 600 hours. This is without consideration of a hold period at the peak temperature. A testing program involving dozens of specimens could thus become extremely expensive and time consuming. Cycling rates as high 20 sec. per cycle have been achieved through diligence. However, the thermal gradients are quite high and control of the temperature and strain is poor, although reproducible. To help speed up TMF testing frequency, a common approach is to raise the minimum temperature in the laboratory TMF cycle. This can considerably reduce the time to cool since cooling follows an exponential decay curve. Removing the last portion of that curve can significantly decrease the cooling time per cycle. However, the range of temperature is reduced in the process, and the measured TMF characteristics are removed further from what occurs in most applications. For most industrial equipment, the minimum temperature in a thermal fatigue cycle is ambient, and is considerably below the minimum temperature usually selected for TMF testing. Normally, the testing conditions of temperature range, minimum temperature, and cycling rate are arrived at by compromise. Regardless of the minimum temperature selected for testing, there remains the desire to shorten the time per cycle and this leads to higher thermal gradients throughout the test specimen.

Of course, one of the purposes of TMF testing is to intentionally keep thermal gradients negligibly small while the overall temperature of the test volume of the specimen is raised and lowered cyclically. Simultaneously, the magnitude of the uniformly distributed strains (stresses) in the specimen is controlled independently of the temperature change, although a fixed phasing is usually maintained between them. As a consequence, the test specimen could be programmed to experience cyclic thermal and mechanical strains just as the material might at a critical point undergoing thermal fatigue in a structural element. In this way, a material's resistance to thermal fatigue can be experimentally evaluated for a range of phasings and amplitudes of strain (stress) and temperature. **Figure 26** illustrates a series of basic TMF strain cycles for the most rudimentary of TMF situations in which mechanical strain and temperature

vary in lock step with one another. A triangular waveform is used for the example cycles although sinusoidal is also in vogue. When the same waveform is used for both strain and temperature, their time phase shift can be described by a single parameter, the phase angle. In-phase cycling (0° phase shift) is defined as having the maximum algebraic strain occur at the same instant as the maximum temperature and the minimum algebraic strain occur at the minimum temperature. Out-of-phase TMF cycling (180° phase shift) is just the reverse of in-phase. A phase angle of 90° or 270° corresponds to a diamond (sometimes referred to as baseball) shaped pattern of mechanical strain versus temperature. The resultant stress-strain hysteresis loop for a diamond cycle will appear as unusual since the maximum and minimum temperatures do not occur at the maximum or minimum mechanical strain. These and other basic cycles (bithermal) to be introduced later serve as excellent uniform types of cycles for characterizing the TMF fatigue resistance of materials.

Rarely, however are the simple cycles discussed above encountered exactly in service. Since TMF fatigue life is generally wave shape dependent, means are required to generalize laboratory characterizations so they may be applied to any unique thermal fatigue cycle encountered in service. This is usually accomplished with a life prediction model. Again, physically based models will have the greatest potential for proper interpolation and extrapolation of results generated. There are spectra of TMF tests of any given type of cycle that could be conducted in a laboratory: phasings could cover the range from in-phase to out-of-phase and all points between, as well as for TMF cycles that aren't describable by quoting a simple measure of phasing; temperature ranges could be very narrow or very wide; the maximum and minimum temperatures could also cover a broad range, as could the mechanical strain range. The frequency or other measure of the cycling rate and hold periods is yet another critical variable to be investigated if one is to document the broad range of the thermal fatigue resistance of a material. A complete test matrix that could capture all of the pertinent variables is too large to be practical. Judicious selection of the variables and their combinations and ranges is usually required based upon the potential application of the results. The American Society for Testing and Materials (ASTM) Committee E08 on Fatigue is currently crafting a standard for basic TMF fatigue testing [75] involving simple waveforms (triangular, sinusoidal, etc.) of phased strain and temperature cycling. Once approved and published, the

standard will be a valuable document to consult before conducting TMF tests. **Table 5** lists in-test and post-test information that should be documented for each TMF test conducted.

As discussed in the reviews of **Refs. [76,77]**, the thermal fatigue resistance of a material is not necessarily derivable from isothermal fatigue resistance, and is frequently lower than isothermal fatigue resistance. This is generally observed, despite comparisons being made to isothermal fatigue resistance measured at the maximum TMF test temperature (i. e., usually thought to be the lowest isothermal fatigue resistance within the span of the TMF temperature range). The basis for comparison of isothermal and TMF fatigue resistance of a material is also important. For example, the TMF resistance may be poorer if the inelastic strain range is used as the basis of comparison, but could be better if the total strain range is used. This apparent dichotomy is a direct result of the differences in the cyclic stress-strain behavior between isothermal and TMF cycling. Comparisons of isothermal and TMF fatigue resistance to inelastic strain for two example alloys **[78, 79]** are shown in **Figs. 27 - 28.**

C. TMF Life Modeling

Because of the large number of variables and the inherent problem of not being able to afford to test for all possible combinations of variables, alternate approaches are desirable. One attractive approach is to adopt a TMF life prediction method. By calibrating the constants in equations representing the model, the means are available to calculate behavior under other conditions by interpolation and extrapolation. A variety of TMF life prediction models are discussed in **Refs. [68,74,77]**. Amongst the more frequently used models are the ASME's Time- and Cycle-Fraction Rule **[69]**, the Continuum Damage Model of ONERA (the French Space Agency) **[72]**, the University of Illinois' Creep-Fatigue-Oxidation Model **[80, 81]**, and the NASA Glenn (formerly Lewis) Method of Strainrange Partitioning (SRP) **[82]**.

The SRP approach for creep-fatigue and TMF life prediction takes advantage of bithermal fatigue testing **[83]**. As the name implies, bithermal cycling is conducted using two isothermal temperatures within each cycle. The high isothermal temperature represents the maximum temperature of a more complex TMF cycle, while the low isothermal temperature represents the minimum. The impetus for developing bithermal testing was to permit direct

measurement of both thermal expansion strain and mechanical strain without them being intermixed. Visual observation of a bithermal hysteresis loop unequivocally identifies these two types of strain. During conventional TMF cycling, thermal and mechanical strains are applied simultaneously and can only be separated by calculation. During bithermal cycling, mechanical straining (and stress) is applied only during the two isothermal halves, and not when the temperature is being changed. The stress on the specimen is controlled at zero during any change in temperature, thus providing a clear separation of thermal expansion and mechanical strains. A schematic bithermal hysteresis loop is shown in **Fig. 29**. An out-of-phase cycle is shown. All tensile mechanical straining is done at the low temperature and compressive mechanical straining at the high temperature. The loading sequence in traversing a cycle is noted in the inset table in the figure. The tensile loading from point A to B and unloading from B to C is done at the cold temperature where the elastic modulus is E_{cold}. It is presumed the temperature is low enough and the straining rate is high enough that time-dependent creep is precluded and only plasticity occurs. Hence, the tensile inelastic (plastic) strain is AC and the corresponding elastic strain is CB′, i.e., stress at B divided by E_{cold}. At point C the load is held at zero and the specimen temperature raised to the hottest temperature where the elastic modulus is E_{hot}. The specimen expands freely from C to D, a direct measure of the thermal expansion strain over the temperature range. Once thermal stability has been attained, the specimen is strained rapidly into compression until a predetermined stress is reached at point E. The inelastic strain DE″ is time-independent plastic strain. Under the stress at E, compressive creep occurs until the strain limit at point F is reached and the specimen is rapidly unloaded to point G. The amount of compressive creep strain is EF, and the compressive inelastic strain is DG = DE″ + EF (or E″G). The corresponding compressive elastic strain is the creep stress (along EF) divided by E_{hot}. Cooling from point G to point A completes the bithermal loop. The thermal contraction GA should be equal to the expansion CD. It is simple to interpret directly from the hysteresis loop of **Fig. 26** the magnitudes of the elastic strains, the inelastic strains, the total strains, and the thermal expansion strains. It is much more difficult to determine these parameters from a continuously varying TMF hysteresis loop. The elastic strain range for the bithermal loop is the sum of the absolute values of the tensile and compressive elastic strains. The corresponding inelastic strain range is the

width of the hysteresis loop at zero stress. There are two measures of this strain range, AC or DG. Theoretically, they must be equal; otherwise, cyclic ratchetting takes place. However, the fixed strain limits prevent ratchetting. Since every experimental measurement has some scatter, it is recommended that AC and DG be averaged to determine the value of the inelastic strain range. The total strainrange of the bithermal loop is the sum of the elastic and inelastic strain ranges. The loop also reveals the partitioning of the inelastic strains into its creep and plasticity components for use in the Strainrange Partitioning method for life prediction. An in-phase bithermal hysteresis loop would look just like the out-of-phase loop, except that the loop would be mirror imaged about the strain axis. Thermal fatigue cycles experienced in service rarely have high enough temperatures in both the tensile and compressive halves to suffer creep strains in both directions. Even the 90° or 270° diamond type cycles tend to experience creep strains predominately in tension or compression only. If, however, the total strain range is very large, all TMF cycles will experience reversed creep. Such cycles rarely, if ever, occur in service situations and are an artifact of TMF testing in the laboratory. By contrast, bithermal tests, for any magnitude of strainrange, can be devised that do not experience reversed creep.

Commercially available software is available to conduct bithermal tests on a routine basis using computer control.

Laboratory TMF testing is comparatively expensive. Obtaining data from tests of more than a couple of weeks duration (≈ 10,000 cycles) is prohibitively expensive. Accelerated TMF testing is generally not feasible. Hence, application of TMF life prediction methods to long-life structures requires considerable extrapolation of laboratory results. Three primary variables in the laboratory results must be extrapolated, cycles to failure, time to failure, and the mechanical component of the total strainrange. Because of the complexity of TMF cycling, it is essential to capitalize on calibrated models for both the failure and the flow (cyclic stress-strain) behavior. Failure behavior can only be calibrated with the longest life data available, but the flow behavior can be calibrated without carrying tests to the point of failure. Affordable yet realistically long hold times per cycle and small mechanical strain ranges can be applied for just a few cycles to capture the desired flow behavior under anticipated service conditions. Measured flow behavior can then be used to calibrate sophisticated cyclic viscoplastic models (see for example **[77, 84]**), or simpler empirical relations **[82]**. The latter

"Page missing from available version"

recently for the development of life prediction modeling for long-life automotive exhaust systems [85]. Since cyclic response behavior is so highly dependent upon the two major variables of time and temperature, it is imperative that modeling play a vital role in describing practical thermal fatigue cycles, and hence in extending the direct usefulness of failure data generated at shorter and more affordable lifetimes.

X. HELPFUL GUIDELINES FOR FATIGUE TESTING

Both novice and experienced fatigue test engineers should find the following operational guidelines of value. It should also be pointed out that there are a considerable number of commercial fatigue testing laboratories located through out the world. These laboratories may be equipped to perform certain tests more economically and timely than could be done in a smaller, less-equipped laboratory.

A. Overall Laboratory Operation, Safety and Training

- Operation of modern fatigue testing laboratories has become sophisticated. Hardware and software are complex and require considerable training for safe, accurate, and reliable operation.
- Carelessness is intolerable as serious, maiming accidents can occur in split seconds with fast-responding, high-pressure hydraulic equipment. Noise from hydraulic pumps, valves, and vibrating lines must be attenuated to prevent hearing damage to operators. High-temperature testing also poses a potential burn hazard. Shields, guards, and hazard warning signs are helpful in preventing accidents to laboratory visitors. OSHA and related safety regulations and procedures should be observed.
- Cleanliness of hydraulic fluid is crucial and systematic replacement of micron-level filters should be scheduled. Room air cleanliness is also important for reliable operation of all computers and electronic equipment.

• Calibration of all measuring devices, electronics, and computer software should be checked on a regular basis and a frequency of calibration policy established. See ASTM and ISO9000 Standards for maintaining quality systems.

• Basic and advanced training courses for use of testing machines and ancillary equipment are generally available through the respective manufacturers. Skills may be required in several areas including mechanical and hydraulic systems, electronics and instrumentation, computers and software, thermal management, and environmental control.

• In addition, it is necessary to keep abreast of the latest developments in fatigue behavior and fatigue life prediction technologies. Short courses are offered by a variety of educational institutions.

B. Overall Control of Materials to be Tested

• A record keeping system should be set up to keep track of all of the materials being tested. Information on each might include:

- Commercial name or designation
- Nominal (and actual) chemical composition
- Commercial source and dates of production and acquisition
- Product form (billet, plate, sheet, bar, etc.)
- Method of production (casting, forging, rolling, heat treatment, etc.)
- AMS, ASM, ASTM, or other specifications
- X-rays and or NDE results
- Representative micrographs and documentation of anisotropy of material stock
- Proper storage of material stock to avoid any possible contamination
- Reference to mechanical and pertinent physical, thermal & electrical properties
- Tensile test properties (elastic modulus, Poisson's ratio yield and ultimate strength, ductility as % reduction of area and % elongation)
- Clear designation of material stock (stamped ID, color coding, etc.)

C. Overall Control of Specimens

• A record keeping system should be set up to track all specimens made of the above materials. Specimen information might include:

- Diagram of specimen location and orientation relative to material stock
- Specimen drawing(s), dimensions, and specifications for machining
- Specimen final preparation (heat treatment, surface treatment, etc.)
- Specimen dimensions and means of measurement
- Specimen and material & individual ID scheme (stamped alphanumeric in visible area near both ends and visible once installed in machine)
- Accessible yet protective specimen storage to prevent damage prior to test
- Document thermocouple attachment techniques & calibration (temp gradients)

- Care exercised in gripping specimens in testing machine
- Orientation of specimen in grips in fatigue machine
- Care to not damage fracture surface prior to machine auto-shut down
- Care exercised in removing fatigued specimens from testing machine
- Accessible storage system for tested specimens (don't store with fracture surfaces of mating pieces touching)
- Maintain records of metallographic mounts taken from broken specimens

D. Laboratory Documentation of Set Ups, Procedures, Calibrations, and Maintenance

• Maintain continuous laboratory documentation books for recording particulars of each new set up and each new program. Books should be kept along with fatigued specimens and raw data records for as long as is practical (then a little longer!). Resurrecting old data is far less costly than having to generate new, and is invaluable if untested material specimens are no longer available at a much later date. Data books should be signed and dated by the test engineer(s) and technician(s).

• Design of experiments (DoE) and statistical interpretation of results are covered elsewhere in Handbook (Sections ___ and ___).

E. Conducting a Fatigue Test

• Maintain a check list to go over prior to the start of each new test.

- Always predict the cyclic and clock lifetime of each specimen prior to testing.
- All pertinent test information (fatigue machine #, material, specimen ID#, type of test, temperature, frequency, hold periods, control parameter(s), parameters to be recorded, equipment being used, test engineer, extensometer and load cell ranges of scales employed, ranges of analog recorders, strip chart speeds, computer control programs and data processors utilized, date, time, and any other unique test information) is entered onto any data sheets, paper recorders, computerized data taking and manipulating systems.

- An analog X-Y recorder for load cell and extensometer output (stress and strain) is highly recommended even though results may also be recorded electronically. In case of a mishap, the X-Y recording provides a better vision of what might have gone wrong and how to correct it than do individual load or extensometer signals as a function of time.

- Ensure each piece of equipment is turned on and functioning properly (for example, pens of recorders are ready to write, timers and cycle counters are working, etc.).

- Ensure safety limits are set to prevent overload of specimen and damage of equipment in case of an accident.

- Before actually starting a test, trace a low-amplitude stress-strain hysteresis loop on the X-Y recorder as a check that the recorder is functioning and to check that the modulus of elasticity is close to its expected value. If not, one or more bits of information may be erroneous (load or extensometer scales, X-Y recorder scales, specimen dimensions, etc.).

- Decide, up front, how to abort a test that is not following the expected response (abrupt shut down, gradual shut down, etc.). During the early stages of a test, be prepared to switch scales of recorders or signal conditioners to better record response signals. For example, large amounts of cyclic strain hardening under strain control may require a coarser load scale be switched to in order to avoid missing measurement of off-scale signals. Don't switch ranges of the control signal during the test.

- As a test progresses, make note of any changes in specimen response (cyclic strain hardening, softening, relaxation of initial mean stresses under strain control, any strain ratchetting occurring under load control, any changes in specimen).

- Pay particularly close attention to the progression of failure of the test specimen, making notes of anything out of the ordinary.

- After specimen failure and the machine has been stopped, make note of and record the orientation (relative to the specimen and its mounting in the grips and machine) of the initiation location(s) of cracking.

- Shut down and re-zero all equipment that will not be needed immediately for the next test.

- Record observations of the fracture surface (single or multiple cracks, multiple planes of cracking, secondary cracking, angular orientation of cracks to specimen axis).

- Ascertain cyclic lifetimes (and hence half-life values) at various points along the process of cracking and final fracture using criteria contained in the text of this Section.

- Reduce and tabulate the fatigue characterization data (half-life values of total, elastic, and inelastic strain ranges, stress range or amplitude, mean stress, etc.), and compare observed lives with lives predicted prior to testing.

- Add each fatigue data point to the evolving fatigue curve to maintain a current view of the extent of the fatigue curve. This knowledge may dictate the conditions to be imposed on the next fatigue test.

Table 1 Applicable ASTM Standards [3] for baseline fatigue testing

Designation	Vol.	Title	Description
Fatigue			
E466-96	3.01	Conducting Force Controlled Constant Amplitude Axial Fatigue Tests of Metallic Materials	Load controlled fatigue. No measurement of strain.
E467-90	3.01	Verification of Constant Amplitude Dynamic Loads on Displacements in an Axial Load Fatigue Testing System	Calibration of dynamic loads under HCF.
E468-90	3.01	Presentation of Constant Amplitude Fatigue Test Results for Metallic Materials	Reporting of load controlled fatigue data.
E606-92	3.01	Strain-Controlled Fatigue Testing	Fatigue testing using strain measurement.
E739-91	3.01	Statistical Analysis of Linear or Linearized Stress-Life (S-N) and Strain-Life (ε-N) Fatigue Data	Statistical analysis of fatigue life curves.
E1049-85	3.01	Cycle Counting in Fatigue Analysis	Cycle counting procedures for spectrum loads.
E1823-96	3.01	Terminology Relating to Fatigue and Fracture Testing	Definitions used in fatigue testing.
B593-85	2.01	Bending Fatigue Testing for Copper-Alloy Spring Materials	Cantilever bend-testing methods.
Equipment			
E4-98	3.01	Force Verification of Testing Machines	Calibration of load cells for test frames.
E8-98	3.01	Tension Testing of Metallic Materials	Lists specimen and grip designs.
E21-92	3.01	Elevated Temperature Tension Tests of	Guidance for elevated temperature testing.

		Metallic Materials	
E74-95	3.01	Calibration of Force-Measuring Instruments for Verifying the Force Indication of Testing Machines	Calibration of force standards.
E83-96	3.01	Verification and Classification of Extensometers	Calibration and classes of extensometers.
E1012-97	3.01	Verification of Specimen Alignment under Tensile Loading	Load frame alignment and measurement of bending strains.
E1237-93	3.01	Installing Bonded Resistance Strain Gages	Installation of strain gages.
E1319-89	3.01	High-Temperature Strain Measurement	Use of high temperature strain gages.
E1856-97	3.01	Evaluating Computerized Data Acquisition Systems Used to Acquire Data from Universal Testing Machines	Use and accuracy of computerized data acquisition systems.
B557	2.02	Tension Testing of Wrought and Cast Aluminum- and Magnesium Alloy Products	Lists specimen and grip designs.

Other Fatigue Standards

(Available in the USA through Global Engineering Documents, Clayton, MO.)

1) ISO/DIS 12106, 1998, Metallic Materials – Fatigue Testing – Axial Strain-controlled Method
2) ISO 1099, 1975, Metals – Axial Load Fatigue Testing
3) ISO 1143, 1975, Rotating Bar Bending Fatigue Testing
4) ISO 1352, 1977, Steel - Torsional Stress Fatigue Testing
5) JIS Z 2279, 1992, Method of High Temperature Low Cycle Fatigue Testing for Metallic Materials. (Japanese Industrial Standard)
6) DIN 51228, 1993, Fatigue Testing Machines – General Requirements. (German Industry Standards
7) DIN 50113, 1982, Testing of Metals - Rotating Bending Fatigue Test

Table 2 Pre-test information guidelines for baseline fatigue tests (including studies of pre-existing effects on fatigue)

- **Alloy designation and description:**
  Heat number and composition; forming processes; degree of anisotropy; heat-treatment and environmental pre-exposure conditions; final machining parameters; photomicrographs; hardness, tensile properties

- **Specimen configuration:**
  Drawing and specifications; orientation of axis to product form; accurately measured specimen dimensions (including notch description) and area of cross-section (diameter and area for direct stress mode of loading); surface finish and method of preparation; final heat-treatment; individual specimen ID No.; description of any coatings including any processing affecting the surface layer (pre-oxidation, pre-fretting or galling, wear, erosion, corrosion, carburizing, nitriding, anodizing, shot peening, laser-shock peening, burnishing, and other means of introducing residual stresses, magnitude and sign of residual stresses, etc.; thickness; orientation of gripped specimen to testing machine

- **Testing Machine:**
  Designation of machine; type of grips; dates of last alignment and calibration of load cell; types of heating and environmental control; type of extensometer and date of last calibration

- **Test Engineer and Operator:**
  Names and date of set up/start of test

- **Testing mode, control details, and test conditions:**
  Model of control (strain, load, deflection or other); cyclic frequency and waveform including description of mean and alternating components; test temperature and means of measurement and control; relative humidity and nature of environment; Starting date and time; error detector limits for shut down; estimate of test duration and basis for estimate

Table 3 In-test and post-test information guidelines for baseline fatigue tests (including studies of pre-existing effects on fatigue)

- **Cyclically varying parameters:**
  Value of fixed test control parameters (stress, strain, displacement, etc.); continuous recording of variations of maximum, minimum, amplitude, range and mean values of stress and strain as a function of applied cycles; cyclic variation of load range variation and ratio of tensile to compressive peak loads to help define failure life and half-life; continuous or periodic recording of variations of stress-strain hysteresis loops

- **Lifetime information:**
  Cyclic failure lives based on various cyclic failure criteria; failure life (cycles and corresponding time) for criterion adopted; half-life cycles; total, inelastic, and elastic strain ranges at half-life; maximum, minimum, stress amplitude, stress range, mean stress, and mean stress ratio at half-life; degree of cyclic hardening/softening from first cycle to half-life (or cycles at stabilization of stress-strain response); description of fracture surface including initiation site(s); location of fracture relative to extensometer probes

- **Deviations from original test plans:**
  Details of stress and strain history immediately prior to controlled or uncontrolled shutdowns prior to test completion

- **Data analysis from multiple specimens:**
  Cyclic stress-strain curve and equation constants at half-life (or cycles at stabilization), fatigue curves and equation constants, i.e., the fatigue properties

Table 4 - Significant Variables Affecting Fatigue Resistance

BULK PROPERTY EFFECTS
- Degree of cold working/annealing
- Heat treatment
- Anisotropy (forming, directional solidification, single crystal)
- Alloy composition
- Nuclear radiation

SURFACE RELATED EFFECTS
- Mechanical surface finish (as-cast, forged, machined, ground, etc.)
- Residual stresses
    - -- Mechanically induced (shot peening, burnishing, laser shock peening (LSP), machining, grinding
    - -- Thermally assisted (rapid surface solidification, welding, electro-discharge machining, carburizing, nitriding, etc.)
- Environment (oxidation, sulfidation, corrosion, ion transport, hydrogen embrittlement)
- Cavitation
- Fretting & Galling
- Wear & Erosion
- Coatings (plating, anodizing, ion implantation, oxidation protective, thermal barriers)

GEOMETRIC EFFECTS
- Notches
- Edges & thin sections
- Size effects & highly stressed volume

ACTIVE LOADING RELATED EFFECTS
- Actively imposed mean stresses and strains
- Multiaxiality of stress and strain (proportional and non-proportional)
- Cumulative damage (variable levels and types of loading)
- Temperature of testing (from cryogenic to high)
- Creep-fatigue interaction (low frequency, low strain rate, stress hold times, strain hold, and tensile versus compressive hold times)
- Thermal fatigue, TMF (continuous temperature-strain cycling and bithermal cycling)

Table 5 In-test and post-test information guidelines for creep-fatigue and thermomechanical fatigue

- **Cyclically varying parameters:**

  Value of fixed test control parameters (stress, strain, temperature, temperature and straining rates, hold times, phasing relation between temperature and strain, as applicable); continuous recording of variations of maximum, minimum, amplitude, range and mean values of stress, strain and temperature as a function of applied cycles (or sufficient information for calculation of these parameters); cyclic variation of load range and ratio of tensile to compressive peak loads (under strain control), and cyclic variation of strain range and ratio of maximum to minimum strain peaks (under load control) to help define failure life and hence half-life; continuous or periodic recording of variations of stress-strain hysteresis loops and stress versus time and strain versus time; plus any parameter deemed necessary for evaluation of a particular creep-fatigue or TMF model (for example, for Strainrange Partitioning, the amounts of tensile and compressive creep and plastic strains)

- **Lifetime information:**

  Cyclic failure lives based on various cyclic failure criteria; failure life (cycles and corresponding time) for criterion adopted; half-life cycles; total, inelastic (partitioned strain ranges and method of partitioning if using Strainrange Partitioning), and elastic strain ranges at half-life; maximum, minimum, stress amplitude, stress range, mean stress, and mean stress ratio at half-life; degree of cyclic hardening/softening from first cycle to half-life (or cycles at stabilization of stress-strain response); description of fracture surface including initiation site(s); degree of transgranular and intergranular cracking; location of fracture relative to extensometer probes

- **Deviations from original test plans:**

  Details of stress and strain history and temperature immediately prior to controlled or uncontrolled shutdowns prior to test completion

- **Data analysis from multiple specimens:**

  Cyclic stress-strain curve and how it varies with strain rate, frequency, cycle time, hold time, and temperature; and equation constants at half-life (or cycles at stabilization), i.e., the cyclic flow properties; fatigue curves, creep-fatigue curves, and TMF fatigue curves expressed in terms of inelastic strain range, total strain range, and elastic strain range versus cyclic life; equation constants and how they vary with temperature and some measure of testing time, i.e., the cyclic failure properties

XI. REFERENCES

1. L. D. Roth, Ultrasonic Fatigue Testing, Metals Handbook Ninth Edition, Vol. 8, Mechanical Testing, 1989, p 240-258

2. W. J. Putnam and J. W. Harsch, "Rise of Temperature" Method of Determining Endurance Limit. In, An Investigation of the Fatigue of Metals by H. F. Moore and J. B. Kommers. Engineering Experiment Station Bulletin No. 124, University of Illinois, Urbana-Champaign, October, 1921, p 119-127.

3. ASTM Standards Pertaining to Various Aspects of Fatigue Testing. American Society for Testing and Materials, West Conshohocken, PA

4. *Strain Gage Based Transducers, Their Design and Construction,* Measurements Group, Inc., Raleigh, North Carolina, 1988

5. M. F. Day and G. F. Harrison, Design and Calibration of Extensometers and Transducers, *Measurement of High Temperature Mechanical Properties*, M. S. Loveday et al, Eds., National Physical Laboratory, London, 1982, p 225-240

6. G. B. Thomas, Axial Extensometry for Ridged Specimens in *Techniques for High Temperature Fatigue Testing*, G. Sumner and V. B. Livesey, Eds., Elsevier Applied Science Publishers, New York, 1985, p 45-56

7. *Strain Gage Users' Handbook*, R. L. Hannah and S .E. Reed, Eds., Elsevier Applied Science, New York, 1992

8. J-F. Lei and W. D. Williams, PdCr Based High Temperature Static Strain Gage, AIAA 2nd International National Aerospace Planes Conference Publication, AIAA-90-5236, 1990

9. J-F. Lei, M. G. Castelli, D. Androjna, C. Blue, R. Blue and R. Y. Lin, Comparison Testings Between Two High-Temperature Strain Measurement Systems, *Experimental Mechanics*, Vol 36 (No. 4), 1996, p 430-435

10. E. G. Ellison, Thermal-Mechanical Strain Cycling and Testing at Higher Temperatures, *Measurement of High Temperature Mechanical Properties*, M. S. Loveday et al., Eds., National Physical Laboratory, London, 1982, p 204-224

11. E. G. Ellison and R. D. Lohr, The Extensometer-Specimen Interface in *Techniques for High Temperature Fatigue Testing*, G. Sumner and V. B. Livesey, Eds., Elsevier Applied Science Publishers, New York, 1985, p 1-28

12. Creep, Stress-Rupture, and Stress-Relaxation Testing, Vol 8, Mechanical Testing in *Metals Handbook, 9th Edition*, 1985, p 313

13. J. Z. Gyekenyesi and P. A. Bartolotta, "An Evaluation of Strain Measuring Devices for Ceramic Composites," NASA TM 105337, National Aeronautics and Space Administration, November, 1991

14. R. Hales and D. J. Walters, Measurement of Strain in High Temperature Fatigue in *Measurement of High Temperature Mechanical Properties*, M. S. Loveday et al. Eds., National Physical Laboratory, London, 1982, p 241-254

15. *Manual of Low Cycle Fatigue Testing, ASTM STP 465*, R. M. Wetzel and L. F. Coffin, Eds., American Society for Testing and Materials, 1969

16. M. G. Castelli and J. R. Ellis, Improved Techniques for Thermomechanical Testing in Support of Deformation Modeling, *Thermomechanical Fatigue Behavior of Materials, ASTM STP 1186*, H. Sehitoglu, Ed., American Society for Testing and Materials, 1993, p 195-211

17. S. S. Manson, G. R. Halford, and M. H. Hirschberg, "Creep-Fatigue Analysis by Strain-Range Partitioning," Symposium on Design for Elevated Temperature Environment, American Society of Mechanical Engineers, 1971, p 12-28

18. K. D. Sheffler and G. S. Doble, "Influence of Creep Damage on the Low-Cycle Thermal-Mechanical Fatigue Behavior of Two Tantalum Base Alloys," NASA CR-121001, National Aeronautics and Space Administration, 1972

19. M. H. Hirschberg, D. A. Spera, and S. J. Klima, "Cyclic Creep and Fatigue of TD-NiCr (Thoria-Dispersion-Strengthened Nickel-Chromium), TD-Ni, and NiCr Sheet at 1200°C," NASA TN D-6649, National Aeronautics and Space Administration, 1972

20. P. R. Breakwell, J. R. Boxall and G. A. Webster, Specimen Manufacture, *Measurement of High Temperature Mechanical Properties,* M. S. Loveday et al. Eds., National Physical Laboratory, London, 1982, p 322-340

21. E. T. Camponeschi, Jr., Compression of Composite Materials: A Review, *Composite Materials: Fatigue and Fracture (Third Volume), ASTM STP 1110*, T. K. O'Brien, Ed., American Society for Testing and Materials, 1991, p 550-578

22. F. A. Kandil and B. F. Dyson, Influence of Load Misalignment During Fatigue Testing I and II, *Fatigue and Fracture of Engineering Materials and Structures*, Vol 16 (No. 5), 1993, p 509-537

23. J. Bressers, "Axiality of Loading," *Measurement of High Temperature Mechanical Properties,* M. S. Loveday et al., Eds., National Physical Laboratory, London, 1982, p 278-295

24. A Code of Practice for the Measurement of Misalignment Induced Bending in Uniaxially Loaded Tension-Compression Test Pieces, J. Bressers, Ed., ISBN 92-826-9681-2, 1995

25. F. A. Kandil, "Measurement of Bending in Uniaxial Low Cycle Fatigue Testing," National Physical Laboratory, Teddington, England, 1998

26. A. K. Schmieder, Measuring the Apparatus Contribution to Bending in Tension Specimens, *Elevated Temperature Testing Problem Areas, ASTM STP 488,* American Society for Testing and Materials, 1971, p 15-42

27. A. A. Braun, A Historical Overview and Discussion of Computer-Aided Materials Testing, *Automation in Fatigue and Fracture: Testing and Analysis, ASTM STP 1231*, C. Amzallag, Ed., American Society for Testing and Materials, 1994, p 5-17

28. S. Dharmavasan, D. R. Broome, M. C. Lugg, and W. D. Dover, FLAPS- A Fatigue Laboratory Applications Package, *Proceedings, 4th International Conference on Engineering Software*, Adey, R. A., Ed., Springer-Verlag, London, 1985, p 8.53-8.64

29. A. A. Braun, The Development of a Digital Control System Architecture for Materials Testing Applications in *Proceedings, 17th International Symposium for Testing and Failure Analysis*, American Society for Metals International, Metals Park, OH, 1991, p 437-444

30. S. Dharmavasan, and S. M. C. Peers, General Purpose Software for Fatigue Testing, *Automation in Fatigue and Fracture: Testing and Analysis, ASTM STP 1231*, C. Amzallag, Ed., American Society for Testing and Materials, 1994, p 18-35

31. M. A. McGaw, and P. J. Bonacuse, Automation Software for a Materials Testing Laboratory in *Proceedings: Turbine Engine Hot Section Technology (HOST), NASA CP-2444,* National Aeronautics and Space Administration, 1986, p 399-406

32. M. A. McGaw, and P. J. Bonacuse, Automation Software for a Materials Testing Laboratory, *Applications of Automation Technology to Fatigue and Fracture Testing, ASTM STP 1092*, A. A. Braun et al., Eds., American Society for Testing and Materials, 1990, p 211-231

33. M. A. McGaw, and P. A. Bartolotta, The NASA Lewis Research Center High Temperature Fatigue and Structures Laboratory, *Proceedings, Fourth Annual Hostile Environments and High Temperature Conference*, Society for Experimental Mechanics, 1987, p 12-29

34. M. A. McGaw, Materials Testing Software, LEW-16160, COSMIC, Athens, GA, 1995

35. J. Christiansen, R. L. T. Oehmke, and E. A. Schwarzkopf, Materials Characterization Using Calculated Control, *Applications of Automation Technology to Fatigue and Fracture Testing, ASTM STP 1303*, A. A. Braun and L. N. Gilbertson, Eds., American Society for Testing and Materials, 1995, p 131-146

36. S. S. Manson, Fatigue – A Complex Subject, *Experimental Mechanics*, Vol. 5, No. 7, 1965, p 193-226

37. J. Morrow, Cyclic Plastic Strain Energy and Fatigue of Metals, *Internal Friction, Damping, and Cyclic Plasticity, ASTM STP 378*, American Society for Testing and Materials, Philadelphia, July, 1965, p 45-84

38. J. F. Newell, A Note of Appreciation for the MUS, *Material durability/Life Prediction Modeling: Materials for the 21st Century, PVP-Vol. 290*, S. Y. Zamrik and G. R. Halford, Eds., American Society of Mechanical Engineers, 1994, p 57-58

39 R. W. Landgraf, The Resistance of Metals to Cyclic Deformation, *Achievement of High Fatigue Resistance in Metals and Alloys, ASTM STP 467*,American Society for Testing and Materials, 1970, p 3-36.

40 Parameters for Estimating Fatigue Life, ASM Handbook, Vol. 19, Fatigue and Fracture. S. R. Lampman, Ed., ASM International, Materials Park, OH, 1996, p 963-979

41. S. S. Manson, Predictive Analysis of Metal Fatigue in the High Cyclic Life Range, *Methods for Predicting Material Life in Fatigue*, W. J. Ostergren and J. R. Whitehead, Eds., American Society of Mechanical Engineers, New York, 1979, p 145-183

42. *Characterization of Low Cycle High Temperature Fatigue by the Strainrange Partitioning Method*, AGARD Conference Proceedings No. 243, NATO, 1978

43. J. B. Conway, R. H. Stentz, and J. T. Berling, *Fatigue, Tensile, and Relaxation Behavior of Stainless Steels*, United States Atomic Energy Commission, Oak Ridge, TN, January, 1975, p 11

44. O. H. Basquin, The Exponential Law of Endurance Tests, *Proceedings, American Society for Testing and Materials*, Vol. 10, Part II, 1910, p 625-630

45. L. F. Coffin, Jr., Thermal stress Fatigue, *Product Engineering*, June 1957

46. B. F. Langer, Design of Pressure Vessels for Low Cycle Fatigue, *Journal of Basic Engineering, Transactions of the ASME*, Vol. 84, No. 4, December, 1962, p 389

47. S. S. Manson, discussion of ASME paper 61-WA-199 by J. F. Tavernelli and L. F. Coffin, Jr., Journal of Basic Engineering, Transactions of the ASME, Vol. 85, No. 4, December 1962, p 537-541.

48. D. F. Socie, N. E. Dowling, and P. Kurath, Fatigue Life Estimation of Notched Members. *Fracture Mechanics: Fifteenth Symposium*, ASTM STP 833, R. J. Sanford, Ed., American Society for Testing and Materials, Philadelphia, 1984, p 284-299

49. S. M. Tipton and D. V. Nelson, Developments in Life prediction of Notched Components Experiencing Multiaxial Fatigue, *Material Durability/Life Prediction Modeling - Materials for the 21st Century, PVP-Vol. 290*, S. Y. Zamrik and G. R. Halford, Eds., American Society of Mechanical Engineers, New York, 1994, p 35-48

50. H. Neuber, Theory of Stress Concentration for Shear strained Prismatical Bodies with Arbitrary Nonlinear Stress-Strain Law, *Journal of Applied Mechanics*, Vol 28, 1961, p 544-550

51. G. Glinka, Energy Density Approach to Calculation of Inelastic Stress-Strain near Notches and Cracks, Engineering Fracture mechanics, Vol 22, 1985, p 485-508

52. W. Z. Gerber, Bestimmung der Zulossigne Sannugen in Eisen Construction, *Bayer. Arch. Ing. Ver.*, Vol 6, 1974, p 101 (in German)

53. J. B. Conway and L. H. Sjodahl, Analysis and Representation of Fatigue Data, ASM International, Materials Park, OH, 1991, p 145-178

54. G. R. Halford and A. J. Nachtigall, The Strainrange Partitioning Behavior of an Advanced Gas Turbine Disk Alloy, AF2-1DA, *Journal of Aircraft*, Vol 17, 1980, p 598-604

55. M. Doner, K. R. Bain, and J. H. Adams, "Evaluation of Methods for Treatment of Mean Stress Effects on Low-cycle Fatigue," Journal of Engineering for Power, ASME, Vol. 104, 1982, pp. 403-411

56. The Rainflow Method in Fatigue, Y. Murakami, Ed., Butterworth Heinemann Ltd., Oxford, 1992

57. M. R. Mitchell, Fundamentals of Modern Fatigue Analysis for Design, Fatigue and Fracture, Vol 19, ASM Handbook, American Society for Metals International, Materials Park, OH, 1996, p 227-249.

58. S. S. Manson and G. R. Halford, Re-Examination of Cumulative Fatigue Damage Analysis -- An Engineering Perspective, *Engineering Fracture Mechanics*, Vol 25, 1986, p 539-571

59. G. R. Halford, Cumulative Fatigue Damage Modeling - Crack Nucleation and Early Growth, *International Journal of Fatigue*, Vol 19, Supplement, No. 1, 1997, p S253-S260

60. M. A. Miner, Cumulative Damage in Fatigue, *Journal of Applied Mechanics*, Vol 12, No. 3, September, 1945 (*Transactions of The American Society of Mechanical Engineers*, Vol 67, 1945), p A159-A164

61. P. T. Bizon, D. J. Thoma, and G. R. Halford, Interaction of High Cycle and Low Cycle Fatigue of Haynes 188 at 1400 F, *Structural Integrity and Durability of Reusable Space Propulsion Systems*, NASA CP-2381, 1985, p 129-138

62. S. Kalluri and P. J. Bonacuse, Cumulative Axial and Torsional Fatigue: An Investigation of Load-Type Sequencing Effects, Symposium on Multiaxial Fatigue and Deformation: Testing and Prediction, ASTM STP 1387, S. Kalluri and P. J. Bonacuse, Eds., American Society for Testing and Materials, West Conshohocken, PA, 2000 (*in press*)

63. R. M. Curran and B. M. Wundt, Continuation of a Study of Low-Cycle Fatigue and Creep Interaction in Steels at Elevated Temperatures, 1976 ASME-MPC Symposium on Creep-Fatigue Interaction, MPC-3, American Society of Mechanical Engineers, New York, 1976, p 203-282

64. S. S. Manson, Critical Review of Predictive Methods for Treatment of Time-Dependent Metal Fatigue at High Temperatures, *Pressure Vessels and Piping: Design Technology - 1982 - A Decade of Progress*, American Society of Mechanical Engineers, New York, 1982, p 203-225

65. D. A. Miller, R. H. Priest, and E. G. Ellison, A Review of Material Response and Life Prediction Techniques under Fatigue-Creep Loading Conditions, *High Temperature Materials and Processes*, Vol 6, 1984, p 155-194

66. V. M. Radhakrishnan, An Assessment of Time Dependent Fatigue Life, *SAMPE Quarterly*, 1983, p 45-50

67. G. R. Halford, Evolution of Creep-Fatigue Life Prediction Models, *Creep-Fatigue Interaction at High Temperature, AD-Vol. 21*, G. K. Haritos and O. O. Ochoa, Eds., American Society of Mechanical Engineers, New York, 1991, p 43-57

68. G. R. Halford, Creep-Fatigue Interaction, *ASM Specialty Handbook Series: Heat Resistant Materials*, ASM International, Materials Park, OH, 1997, p 499-517

69. Anon, *Code Case N-47-23*, American Society of Mechanical Engineers, New York, 1986.

70. S. S. Manson, G. R. Halford, and M. H. Hirschberg, Creep-Fatigue Analysis by Strain-Range Partitioning, *Symposium on Design for Elevated Temperature Environment*, American Society of Mechanical Engineers, New York, 1971, p 12-28

71. J. F. Saltsman and G. R. Halford, An Update on the Total Strain Version of SRP, *Low Cycle Fatigue —Directions for the Future*, ASTM STP 942, H. D. Solomon, G. R. Halford, L. R. Kaisand, and B. N. Leis, Eds., American Society for Testing and Materials, Philadelphia, 1988, p 329-341

72. J-L. Chaboche, Continuous Damage Mechanics: A Tool to Describe Phenomena before Crack Initiation. *Nuclear Engineering Design*, Vol 64, 1981, p 233-247

73. C. E. Jaske, H. Mindlin, J. S. Perrin, Combined Low-Cycle Fatigue and Stress Relaxation Behavior of Alloy 800 and Type 304 Stainless steel at Elevated Temperatures, *Fatigue at Elevated Temperature, ASTM STP 520*, American Society for Testing and Materials, 1973, p 365-376

74. S. S. Manson, The Challenge to Unify Treatment of High Temperature Fatigue — A Partisan Proposal Based on Strainrange Partitioning, *Fatigue at Elevated Temperature, ASTM STP 520*, American Society for Testing and Materials, 1973, p 744-782

75. Anon, Proposed Standard Test Method for Strain Controlled Thermomechanical Fatigue Testing, *Draft Working Document* prepared by the ASTM Thermomechanical Fatigue Task Group, E08.05.07, American Society for Testing and Materials, West Conshohocken, PA, 1999

76. G. R. Halford, Low-Cycle Thermal Fatigue, Chapter 6. *Thermal Stresses II*, R. B. Hetnarski, ed., Elsevier Science Publishers B. V., Amsterdam, 1987, p 329-428

77. H. Sehitoglu, Thermal and Thermomechanical Fatigue of Structural Alloys. *Fatigue and Fracture*, Vol 19, *ASM Handbook*, 1996, p. 527-556. see also *Heat-Resistant Materials, ASM Specialty Handbook*, J. R, Davis, ed., ASM International, 1997, p. 454-485

78. K. D. Sheffler, Vacuum Thermal-Mechanical Fatigue Testing of Two Iron-Base High Temperature Alloys, *Thermal Fatigue Resistance of Materials and Components, ASTM STP 612*, D. A. Spera and D. F. Mowbray, Eds., American Society for Testing and Materials, Philadelphia, 1976, p 214-226

79. C. E. Jaske, Thermal-Mechanical, Low-Cycle Fatigue of AISI 1010 Steel, *Thermal Fatigue Resistance of Materials and Components, ASTM STP 612*, D. A. Spera and D. F. Mowbray, Eds., American Society for Testing and Materials, Philadelphia, 1976, p 170-198

80. R. Neu and H. Sehitoglu, Thermo-Mechanical Fatigue Oxidation, Creep, Part I: Experiments, *Metallurgical Transactions A*, Vol 20A, 1989, p 1755-1767

81. R. Neu and H. Sehitoglu, Thermo-Mechanical Fatigue Oxidation, Creep, Part II: Life Prediction, *Metallurgical Transactions A*, Vol 20A, 1989, p 1769-1783

82. J. F. Saltsman and G. R. Halford, Life Prediction of Thermomechanical Fatigue Using The Total Strain Version of Strainrange Partitioning (SRP)---A Proposal, NASA TP-2779, February 1988

83. G. R. Halford, M. A. McGaw, R. C. Bill, and P. D. Fanti, Bithermal Fatigue: A Link Between Isothermal and Thermomechanical Fatigue, *Low Cycle Fatigue, ASTM STP 942*, H. D. Solomon, G. R. Halford, L. R. Kaisand, and B. N. Leis, Eds., American Society for Testing and Materials, Philadelphia, 1988, p 625-637

84. D. N. Robinson and R. W. Swindeman, Unified Creep-plasticity Constitutive Equations for 2-1/4Cr-1Mo Steel at Elevated Temperature, ORNL/TM-8444, 1982.

85. G.-Y. Lui, M. B. Behling, and G. R. Halford, Bithermal Low-Cycle Fatigue Evaluation of Automotive Exhaust System Alloy SS409Submitted, November 1999 for publication in the *Journal of Fatigue and Fracture of Engineering Material and Structures*.

XII. FIGURE CAPTIONS

Fig. 1 Modern servohydraulic axial fatigue testing machine
(a) basic load train ***{halford3.ppt}***
(b) hydraulic actuator, servo-valve, and displacement sensor (LVDT) ***{halford3.ppt}***

Fig. 2 Schematics of various fatigue machines employed over the years
(a) rotating eccentric crank and lever machine for axial (direct stress) loading
(b) four-point loading R. R. Moore rotating beam machine
(c) cantilever loading rotating beam machine
(d) cantilever plane-bending machine
(e) forced vibration, rotating eccentric mass machine
(f) closed-loop resonant machine
(g) Ultrasonic (20 KHz) machine with mean load capability

Fig. 3 Ancillary equipment installed on an axial servohydraulic fatigue machine
(a) general view ***{halford3.ppt}***
(b) spool, conventional servo-valve ***(to be supplied by MTS}***
(c) spool, high-frequency servo-valve ***(to be supplied by MTS}***

Fig. 4 Schematic of typical hydraulic wedge grip

Fig. 5 Grip insert design used for axial fatigue testing
(a) three-piece collet grip for cylindrical specimens
(b) V-grips for rounds for use in wedge grip body
(c) wedges for flat specimens
(d) universal open-front holders
(e) adapters for special samples (screws, bolts, studs, etc.) for use with open-front holders
(f) holders for threaded samples
(g) snubber-type wire grips for flexible wire or cable

Fig. 6 Adjustable work coil fixture for direct induction heating

Fig. 7 Environmental chamber for fatigue testing

Fig. 8 Nomenclature for a typical test specimen
Ends of round specimens may have smooth shanks, button-heads, or threads
Smooth shanks should be long enough to accommodate some type of wedge grip
Rectangular specimens are generally made with smooth shanks, but may be shouldered to contain a hole for a pin bearing

Fig. 9 Typical fatigue test specimens

Fig. 10 Typical round and flat fatigue test specimen configurations
(a) hourglass specimen with continuous radius between grip ends
(b) round specimen with tangentially blended fillets between test section and grip ends
(c) flat specimen with tangentially blended fillets between test section and grip ends
(d) flat specimen with continuous radius between the grip ends

Fig. 11 Alignment fixture for minimizing bending strains

Fig. 12 Typical closed-loop servocontroller block diagram **[35]**

Fig. 13 Typical supervisory (outer loop) calculated variable controller block **[35]**

Fig. 14 Representation of the cyclic strain resistance of idealized alloys (strong, tough, ductile), after Landgraf **[39]**
(a) fatigue curves
(b) stress-strain hysteresis loops

Fig. 15 Cyclic load response during strain controlled low-cycle fatigue test of annealed AISI 304 stainless steel in air at 816 °C, total strain range = 3.26%, 0.056 Hz **[43]**
(a) cyclic load response for defining cyclic life to crack initiation
(b) cyclic load range and ratio of tensile to compressive peak load versus applied cycles

Fig. 16 Typical S-N diagrams for various alloys subjected to completely reversed loading at ambient temperature

Fig. 17 Typical strain-life fatigue curve showing elastic and plastic components

Fig. 18 Schematic axial fatigue curve illustrating the effect of tensile mean stress, after Conway and Sjodahl **[53]**

Fig. 19 Effect of tensile mean stresses on axial fatigue resistance of 2024-T3 aluminum alloy at room temperature, after Conway and Sjodahl **[53]**

Fig. 20 Schematic illustration of cyclic mean strain cycling effects on low-cycle fatigue resistance. Mean stresses relax to zero at large strain ranges, but remain at low strain ranges, thus reducing life

Fig. 21 Non-steady fatigue loading, after **[56]**
(a) random appearing original loading pattern
(b) loading pattern reconstructed by rainflow method of cycle counting

Fig. 22 Examples of Classic Loading Order Effect in Two Load Level Tests of British Aluminum Alloy D. T. D. 683 **[58]**

Fig. 23 Schematic hysteresis loops encountered in isothermal creep-fatigue testing
(a) pure fatigue, no creep
(b) tensile stress hold, strain limited
(c) compressive stress hold, strain limited
(d) tensile and compressive stress hold, strain limited
(e) tensile strain hold (stress relaxation)
(f) compressive strain hold (stress relaxation)
(g) tensile and compressive strain hold (stress relaxation)
(h) slow tensile straining rate
(i) slow compressive straining rate
(j) slow tensile and compressive straining rate

Fig. 24 Creep-fatigue interaction effects on isothermal cyclic life of AISI type 304 stainless steel tested in air at 650 °C, normal straining rate of 4×10^{-3} s^{-1}, after **[66]**

Fig. 25. Predictability of creep-fatigue lives for tensile strain hold time cycles for Incoloy 800 and AISI type 304 stainless steel at elevated temperatures **[72]**, data from **[71]**

Fig. 26. Basic TMF strain cycles

Fig. 27. Comparison of isothermal and TMF fatigue resistance of A-286 precipitation-hardening stainless steel **[77]**, data from **[78]**

Fig. 28. Comparison of isothermal and TMF fatigue resistance of AISI 1010 carbon steel **[77]**, data from **[79]**

Fig. 29. Schematic bithermal hysteresis loop (out-of-phase)

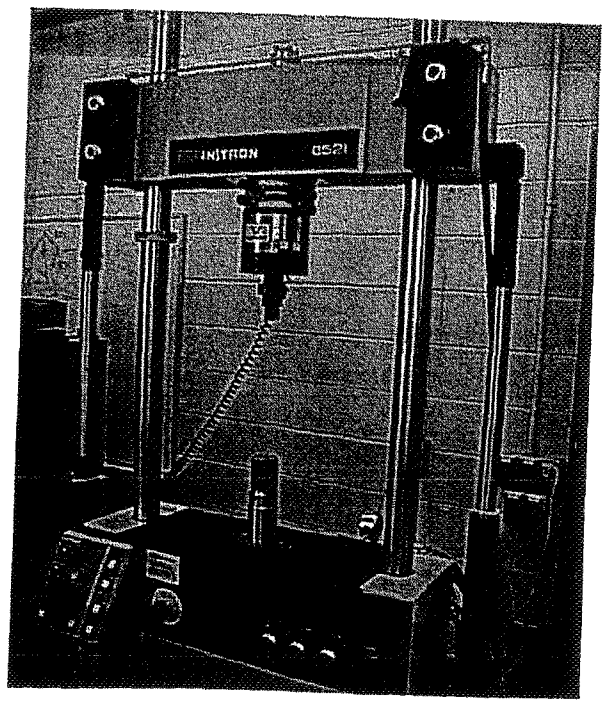

(a) basic load train *{NASA-Glenn digital photo}* *{halford3.ppt}*

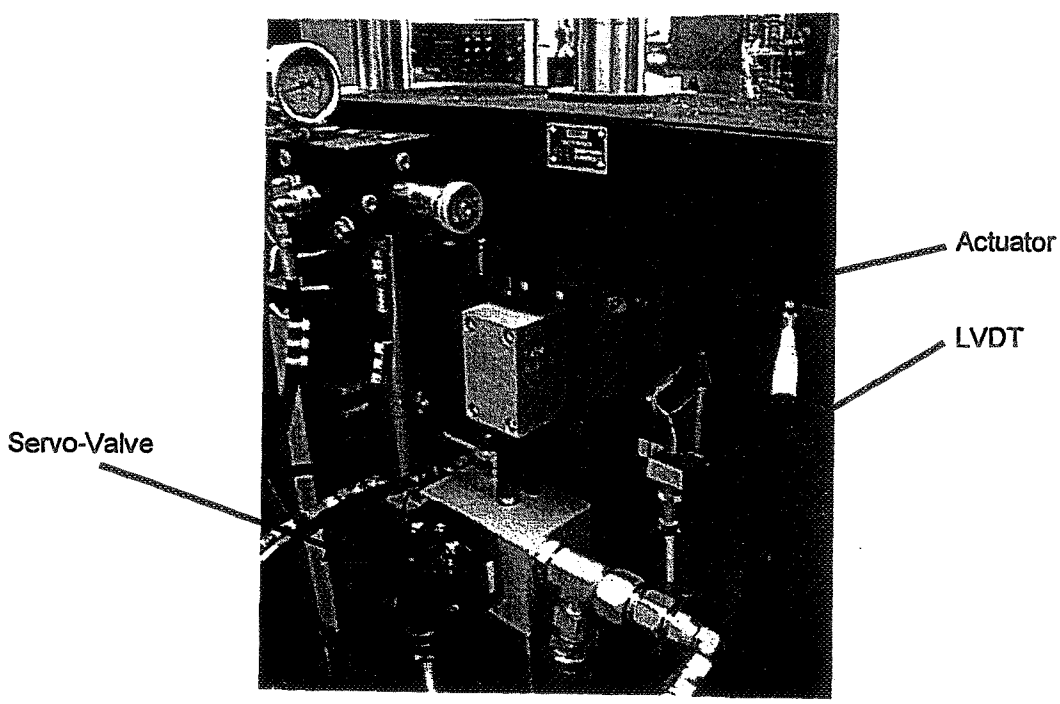

(b) hydraulic actuator, servo-valve, and displacement sensor (LVDT)
{NASA-Glenn digital photo} *{halford3.ppt}*

Fig. 1 Modern servohydraulic axial fatigue testing machine

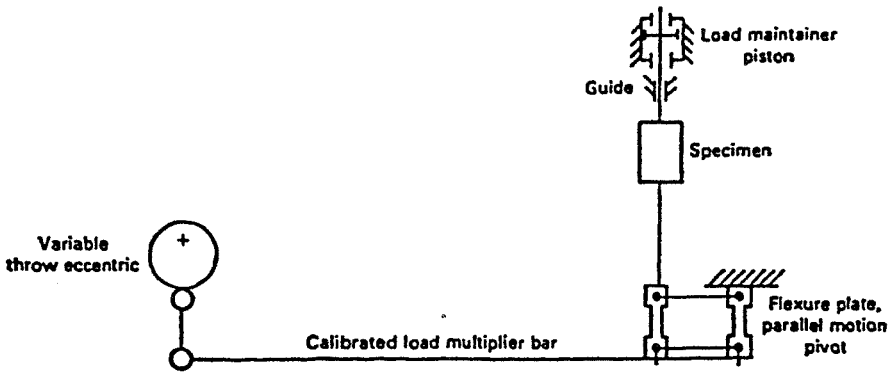

(a) rotating eccentric crank and lever machine for axial (direct stress) loading *{ASM Metals Handbook Ninth Edition, V8, Mech. Testing, Fig. 5, p 370}*

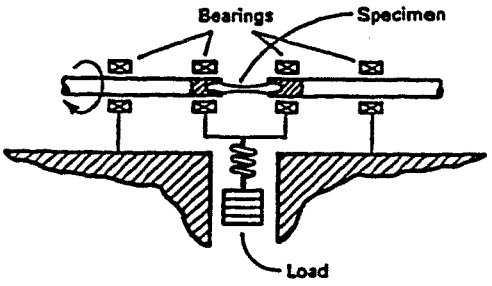

(b) four-point loading R. R. Moore rotating beam machine *{ditto, Fig. 6(a). p 370}*

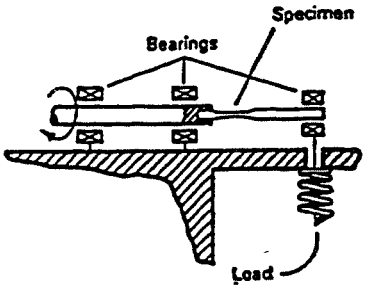

(c) cantilever loading rotating beam machine *{ditto, Fig. 6(b). p 370}*

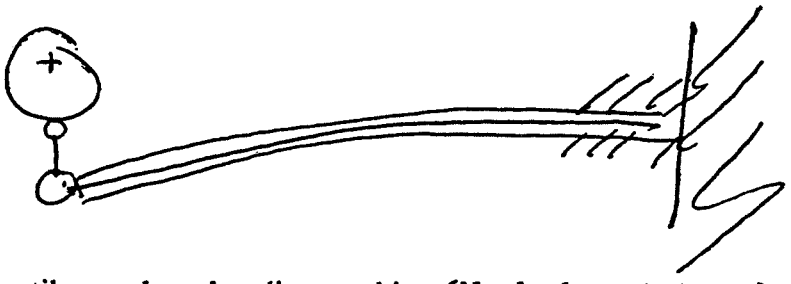

(d) cantilever plane-bending machine *{Need schematic figure}*

Fig. 2 Schematics of various fatigue machines employed over the years (continued)

(1) Stationary frame; large top provides ample work space. (2) Reciprocating platen. (3) Rotating eccentric mass is source of dynamic force, which is varied by screwing threaded rod in or out. (4) Thread screw locks threaded rod in position. (5) Scale reads in pounds of vibratory force. (6) Flexure plates absorb horizontal centrifugal force so that only vertical force is transmitted to platen. (7) Synchronous motor drives eccentric mass at constant 1800 cycles/min. (8) Springs provide seismic mounting so that no vibration is transmitted to or from surroundings. (9) Dial indicates preload. (10) Compensator springs absorb all inertia forces produced by reciprocating masses, preventing transmission to the specimen. (11) Plate holds one end of compensator springs firmly to stationary frame. (12) Preload mechanism

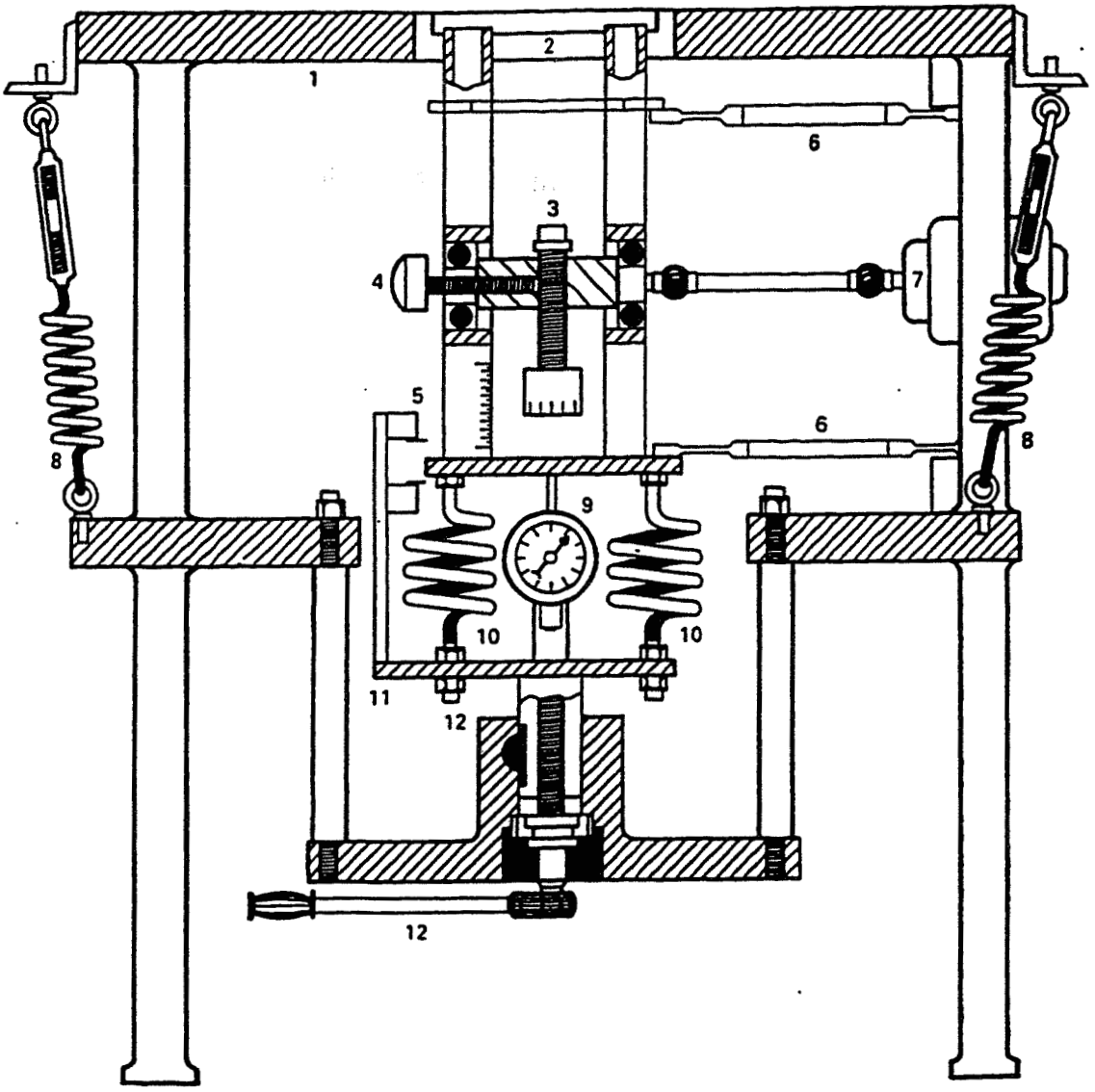

(e) forced vibration, rotating eccentric mass machine *{ditto, Fig. 27, p 392}*

Fig. 2 Schematics of various fatigue machines employed over the years (continued)

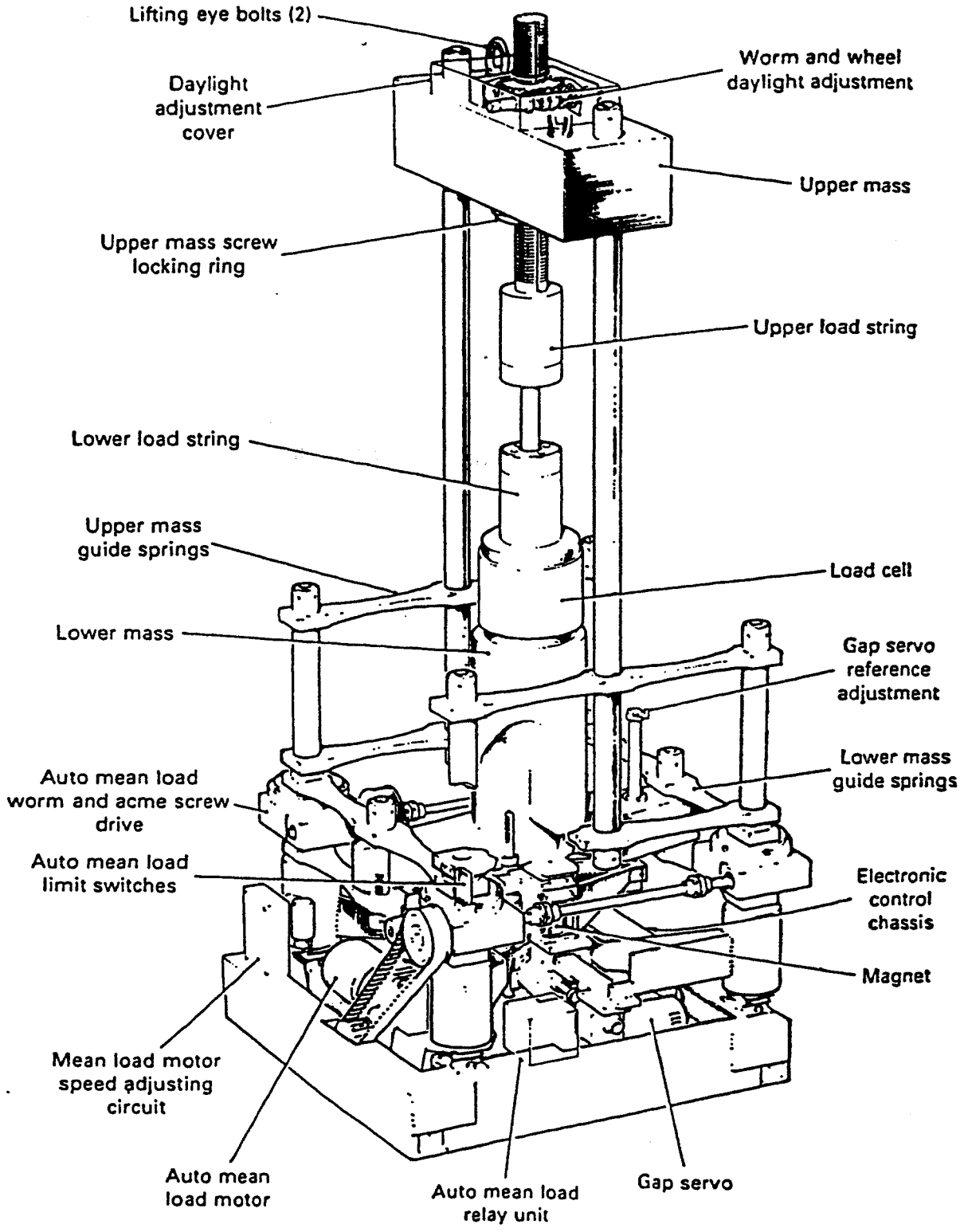

(f) closed-loop resonant machine *{ditto, Fig. 30, p 393}*

Fig. 2 Schematics of various fatigue machines employed over the years *(continued)*

1, Converter; 2, booster horn; 3, connecting horn; 4, specimen; 5, capacitance gage; 6, cooling ring; 7, four air inlets; 8, venturi air cooler; 9, air supply; 10, upper and lower support plates; 11, hydraulic pistons; 12, window; 13, infrared camera

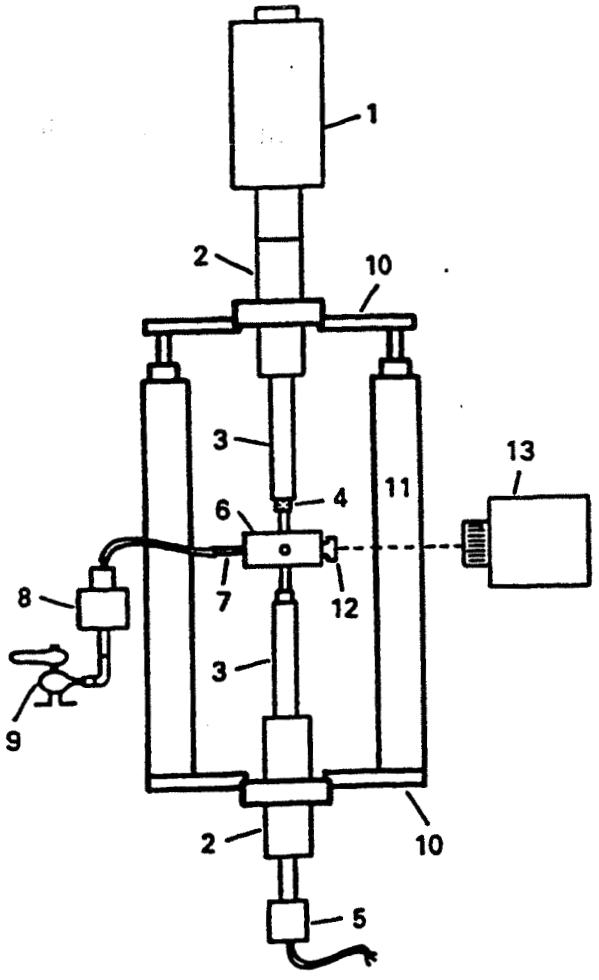

(g) Ultrasonic (20 KHz) machine with mean load capability *{ ditto, Fig. 11, p 248}*

Fig. 2 Schematics of various fatigue machines employed over the years (concluded)

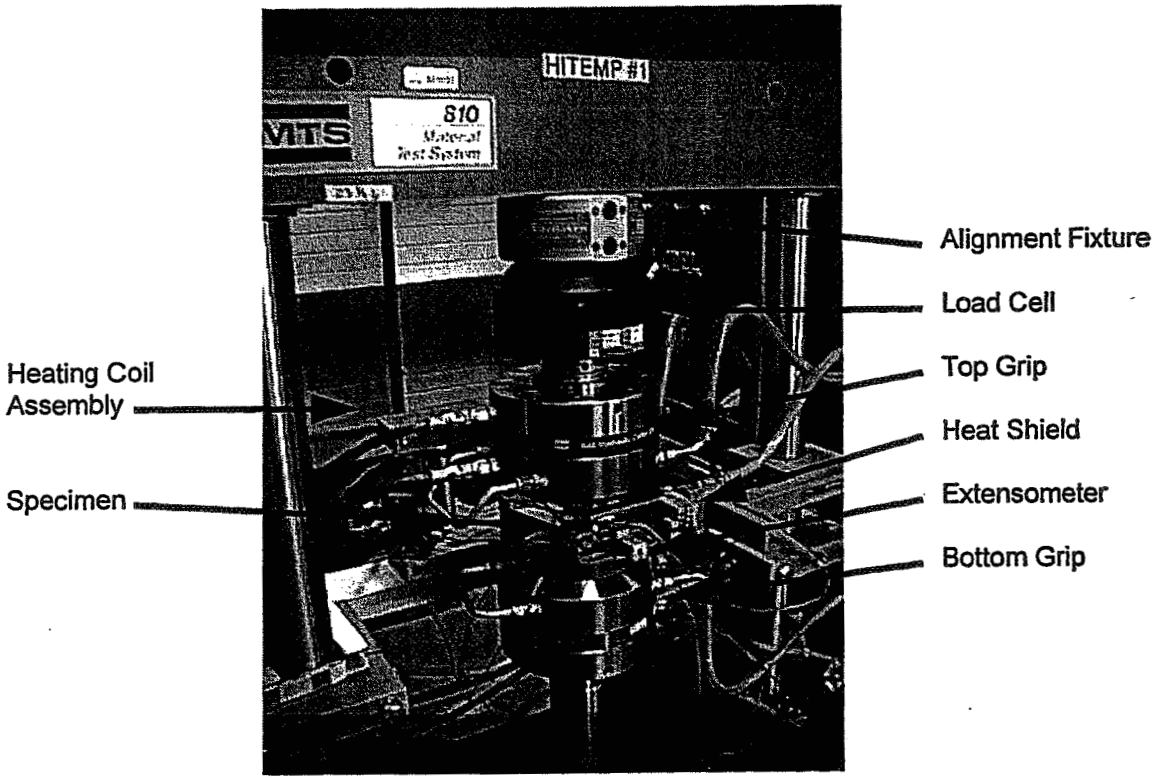

(a) General view *{halford3.ppt}*

Fig. 3 Ancillary equipment installed on an axial servohydraulic fatigue machine *(continued)*

(b) Spool, Conventional Servo-valve *{to be supplied by MTS or Instron}*

Fig. 3 Ancillary equipment installed on an axial servohydraulic fatigue machine *(continued)*

(c) Spool, High-frequency Servo-valve *{to be supplied by MTS or Instron}*

Fig. 3 Ancillary equipment installed on an axial servohydraulic fatigue machine *(concluded)*

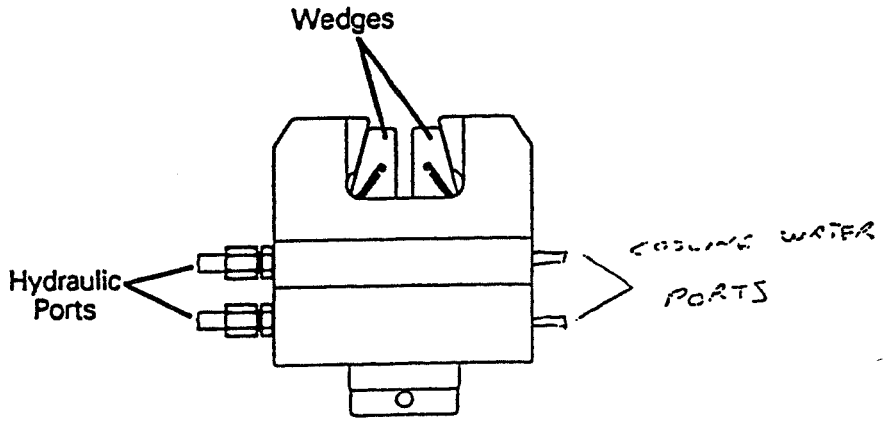

Fig. 4 Schematic of typical hydraulic wedge grip *{ASM - Tensile Testing, Patricia Han, Ed., 1992, Fig. 12, p. 42}*

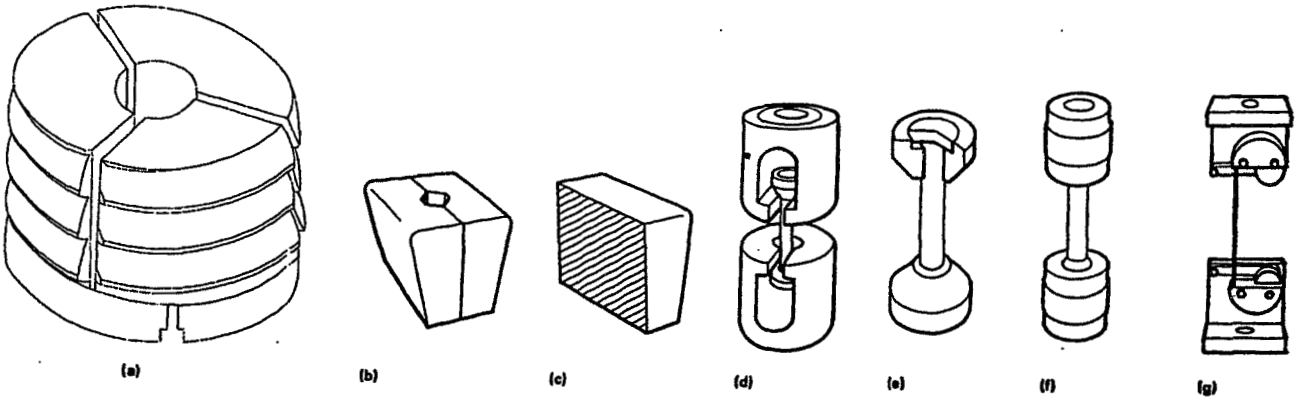

(a) three-piece collet grip for cylindrical specimens *{collet fig.doc}*
(b) V-grips for rounds for use in wedge grip body
(c) wedges for flat specimens
(d) universal open-front holders
(e) adapters for special samples (screws, bolts, studs, etc.) for use with open-front holders
(f) holders for threaded samples
(g) snubber-type wire grips for flexible wire or cable

Fig. 5 Grip insert design used for axial fatigue testing
{Adapted - ASM Hdbk, V8, Mech. Test., Fig. 4, p. 369}

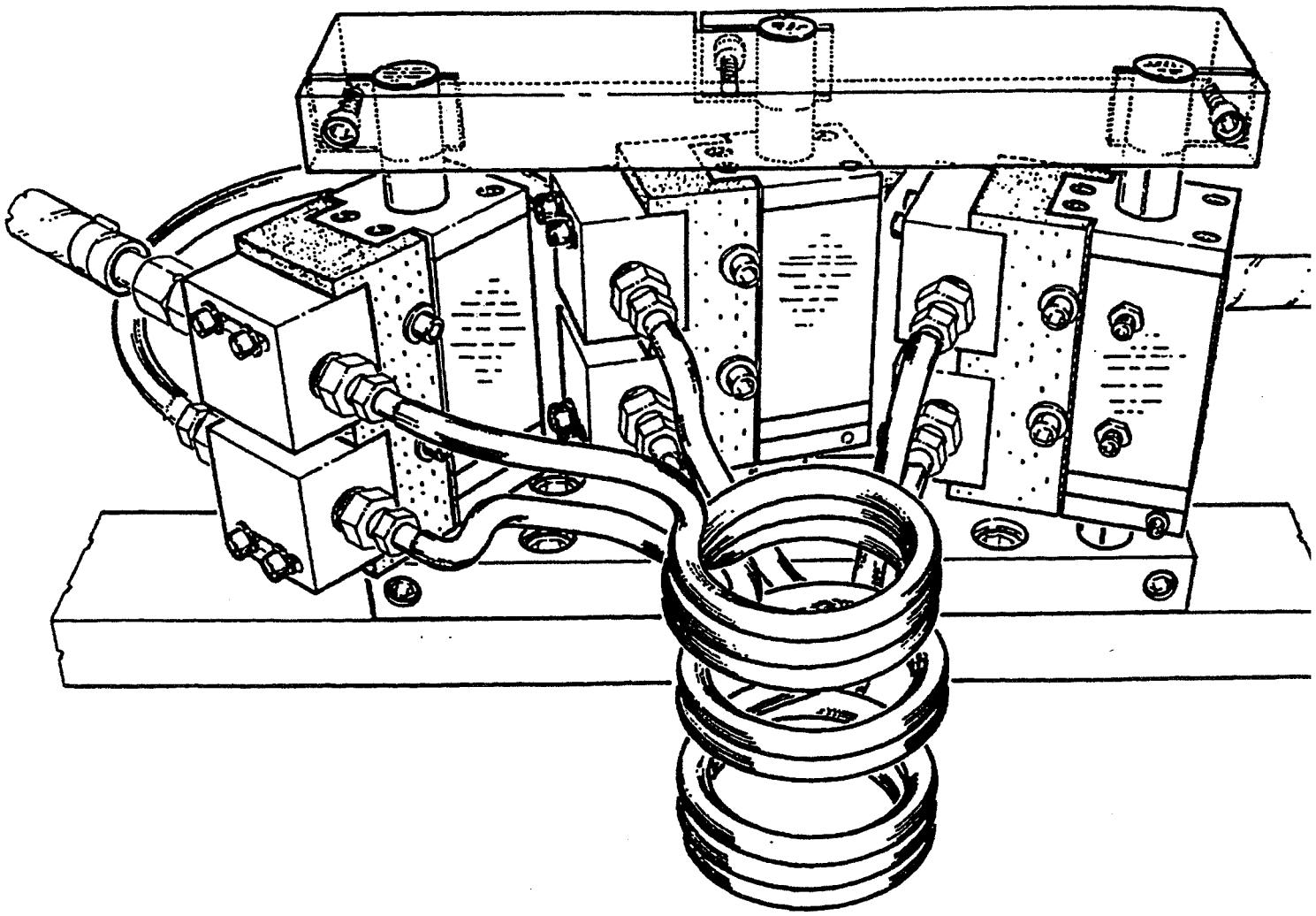

Fig. 6 Adjustable work coil fixture for direct induction heating *{NASA-Glenn drawing CD-99-31558}*

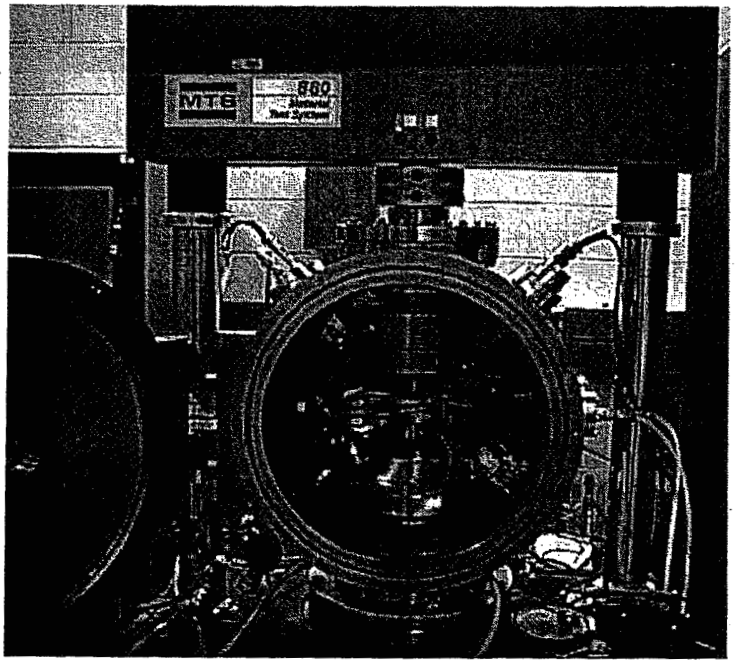

Fig. 7 Environmental chamber for fatigue testing *{halford3.ppt}*

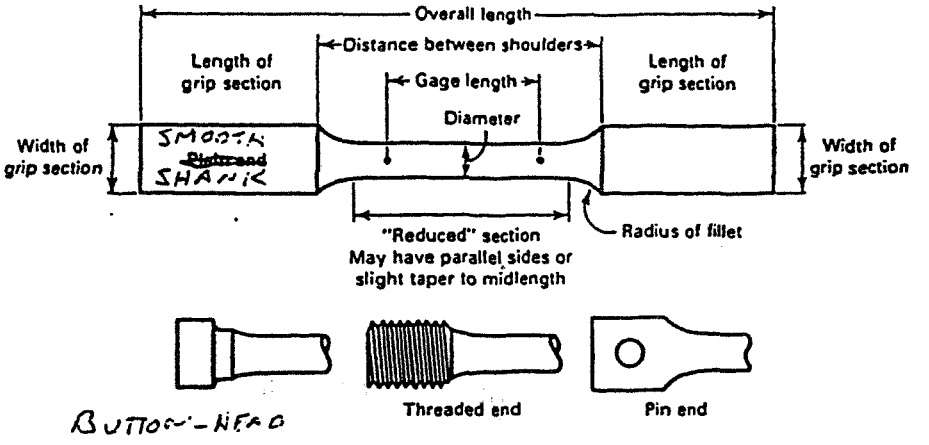

Fig. 8 Nomenclature for a typical test specimen. The ends of round specimens may have smooth shanks, button-heads, or threads. Smooth shanks should be long enough to accommodate some type of wedge grip. Rectangular specimens are generally made with smooth shanks, but may be shouldered to contain a hole for a pin bearing.

{Adapted - ASM Hdbk, V8, Mech. Test., Fig. 1, p. 29}

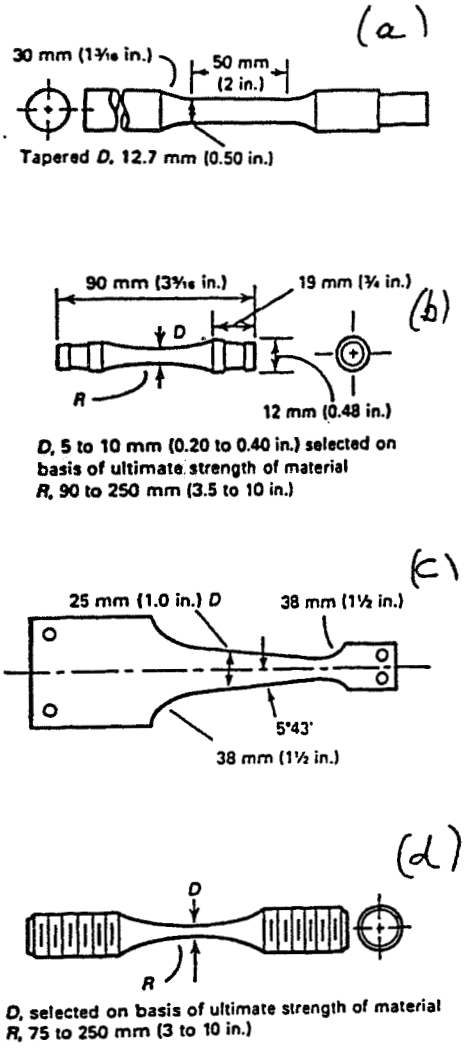

Fig. 9 Typical fatigue test specimens *{Adapted - ASM Hdbk, V8, Mech. Test., Fig. 8, p. 371}*

Fig. 10 Typical round and flat fatigue test specimen configurations *{Adapted - ASM Hdbk, V8, Mech. Test., Fig. 9, p. 372}*

(a) Hourglass specimen with continuous radius between the grip ends. (b) Round specimen with tangentially blended fillets between the test section and the grip ends. (c) Flat specimen with tangentially blended fillets between the test section and the grip ends. (d) Flat specimen with continuous radius between the grip ends.

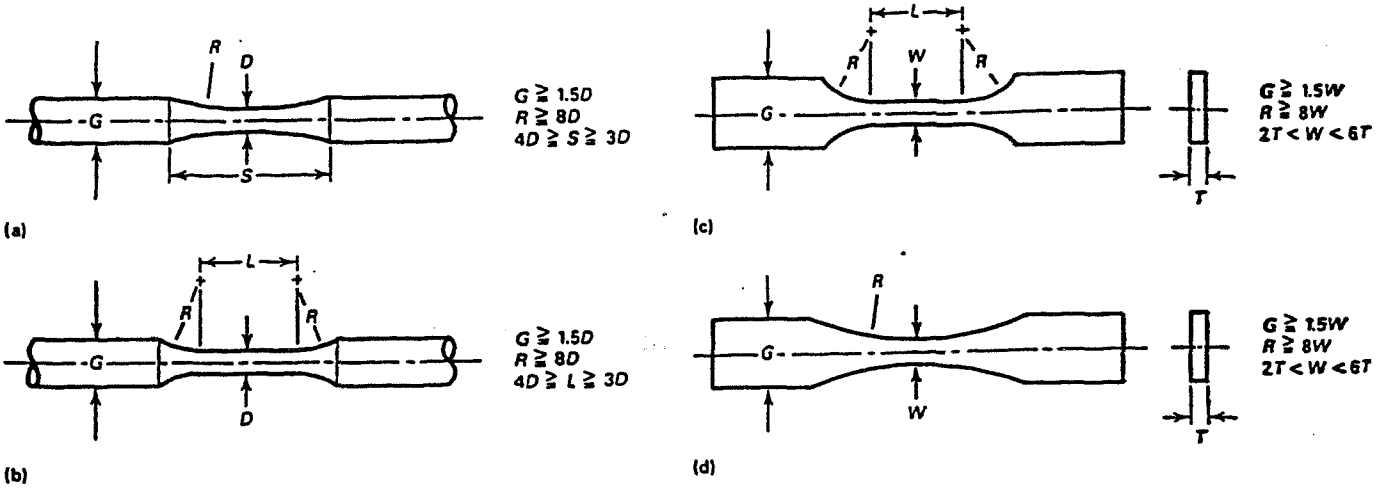

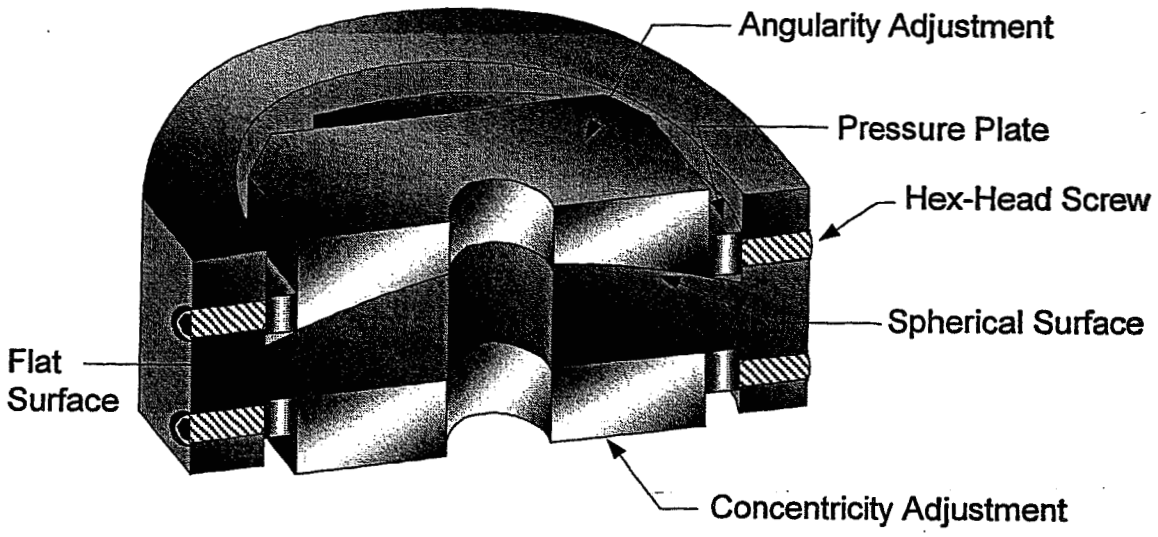

Fig. 11 Alignment fixture for minimizing bending strains *{alignd.ppt}*

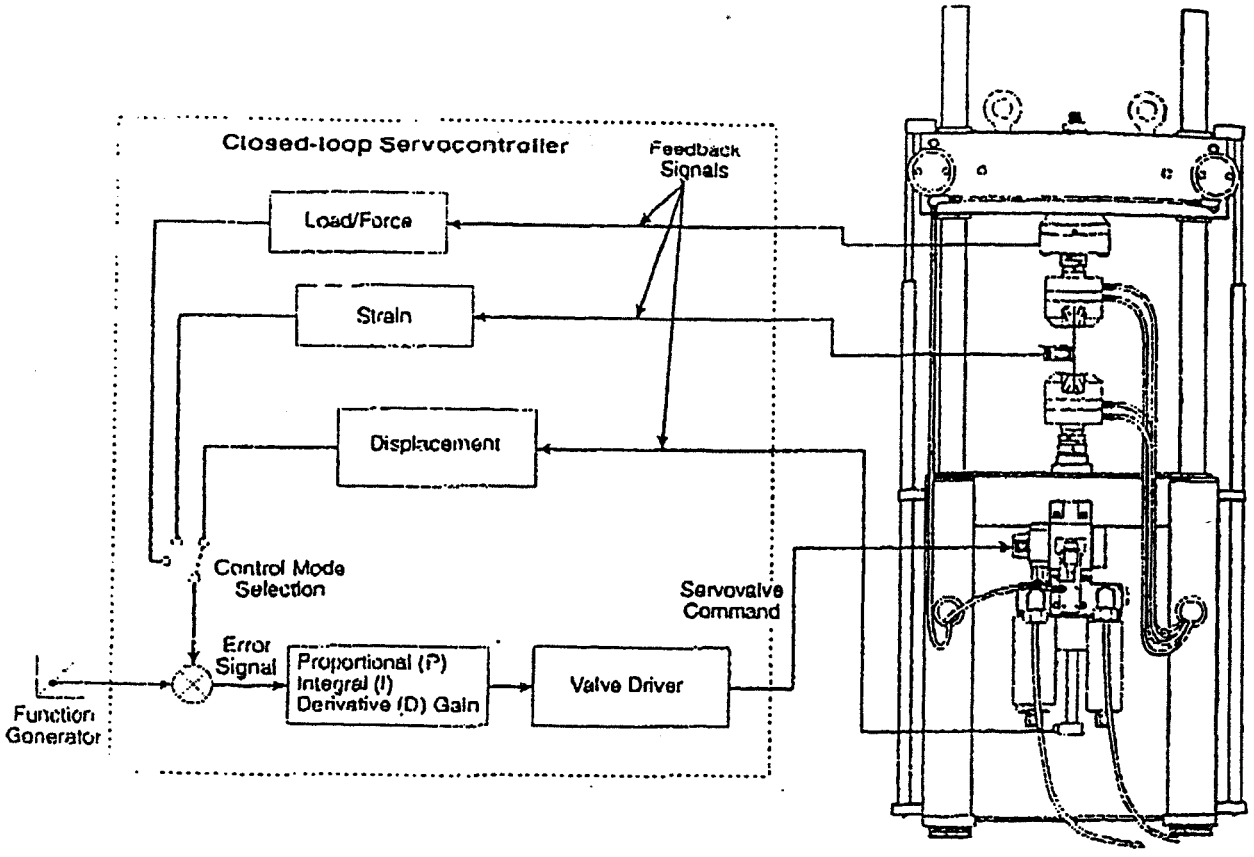

Fig. 12 Typical closed-loop servocontroller block diagram **[Ref. 35]**
{STP 1303, 1995, Fig. 2, p. 132}

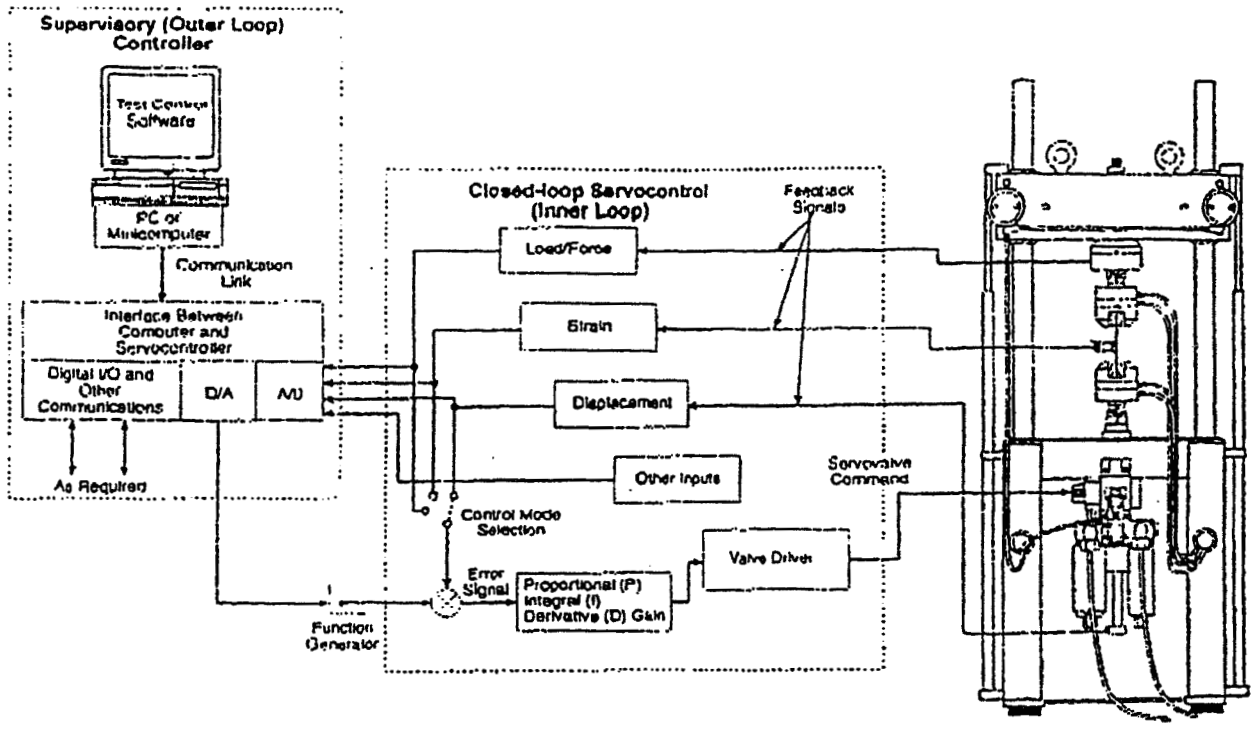

Fig. 13 Typical supervisory (outer loop) calculated variable controller block **[35]** ***{STP 1303, 1995, Fig. 2, p. 133}***

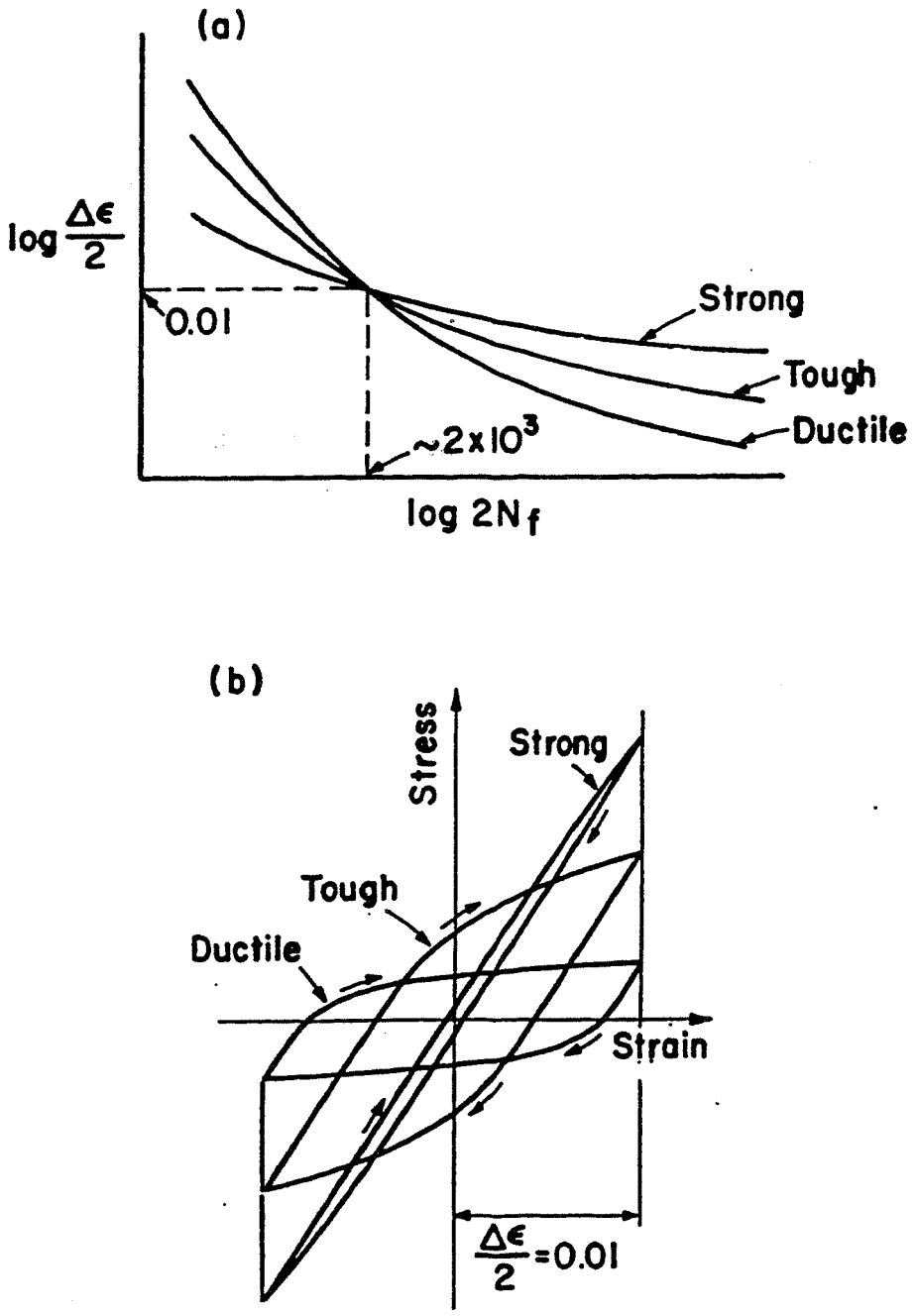

Fig. 14 Representation of the cyclic strain resistance of idealized alloys (strong, tough, ductile), *After Landgraf [Ref. 39]*

(a) fatigue curves

(b) stress-strain hysteresis loops

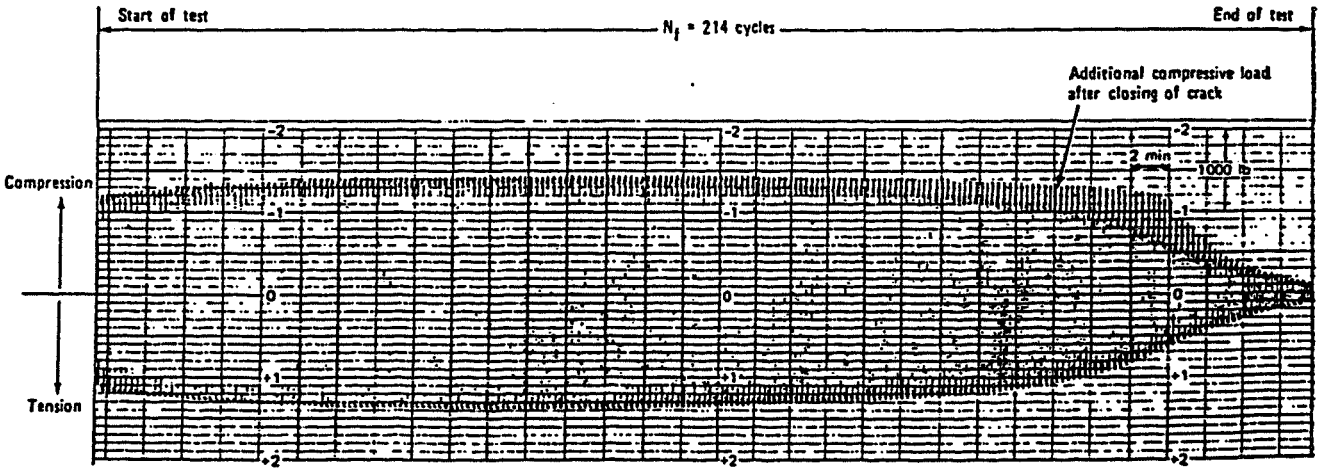

(a) cyclic load response for defining cyclic life to crack initiation

Fig. 15 Cyclic load response during strain controlled low-cycle fatigue test of annealed AISI 304 stainless steel in air at 816 °C, total strain range = 3.26%, 0.056 Hz (continued) [43]

(b) cyclic load range and ratio of tensile to compressive peak load versus applied cycles

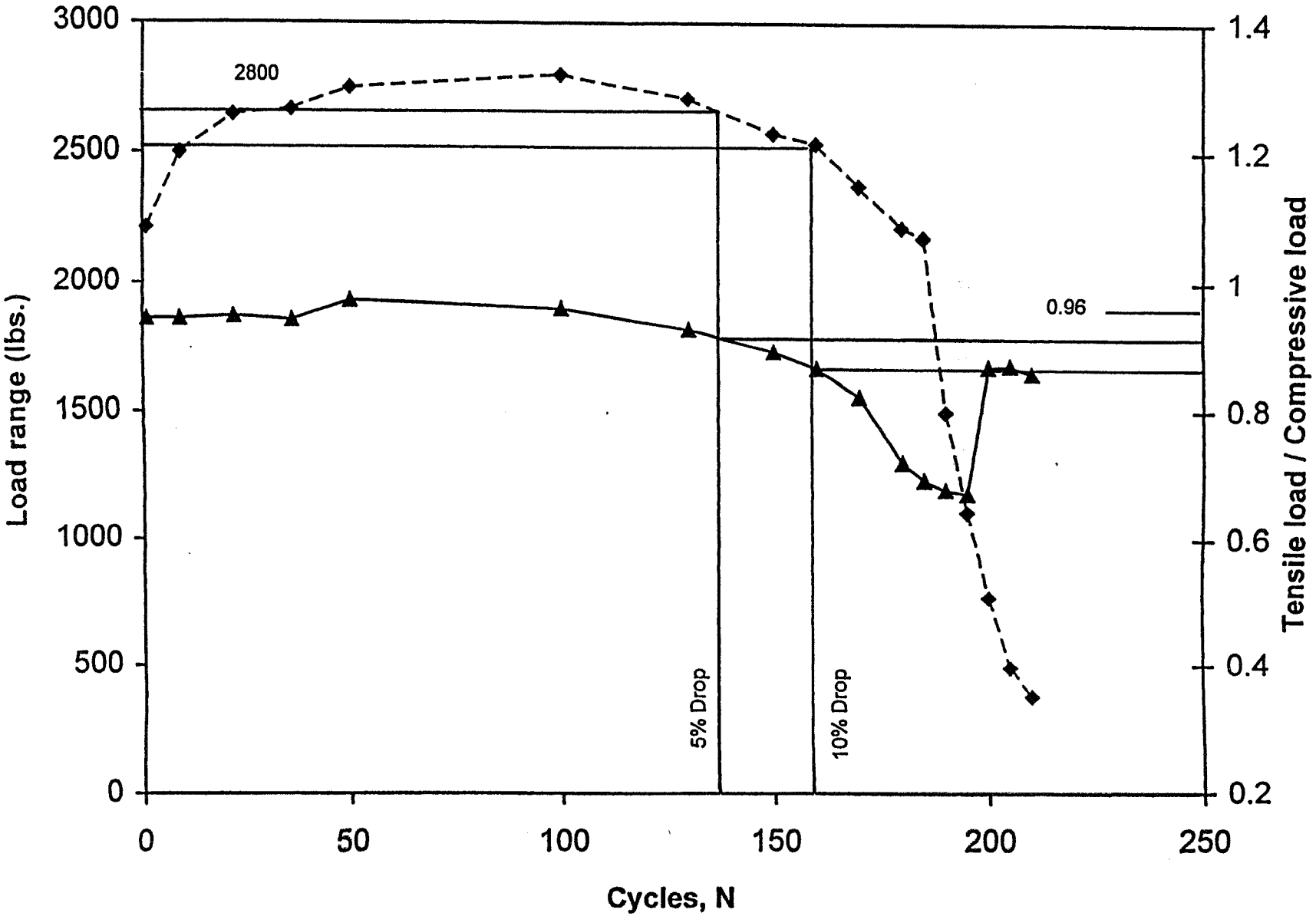

Fig. 15 Cyclic load response during strain controlled low-cycle fatigue test of annealed AISI 304 stainless steel in air at 816 °C, total strain range = 3.26%, 0.056 Hz (concluded) [43]

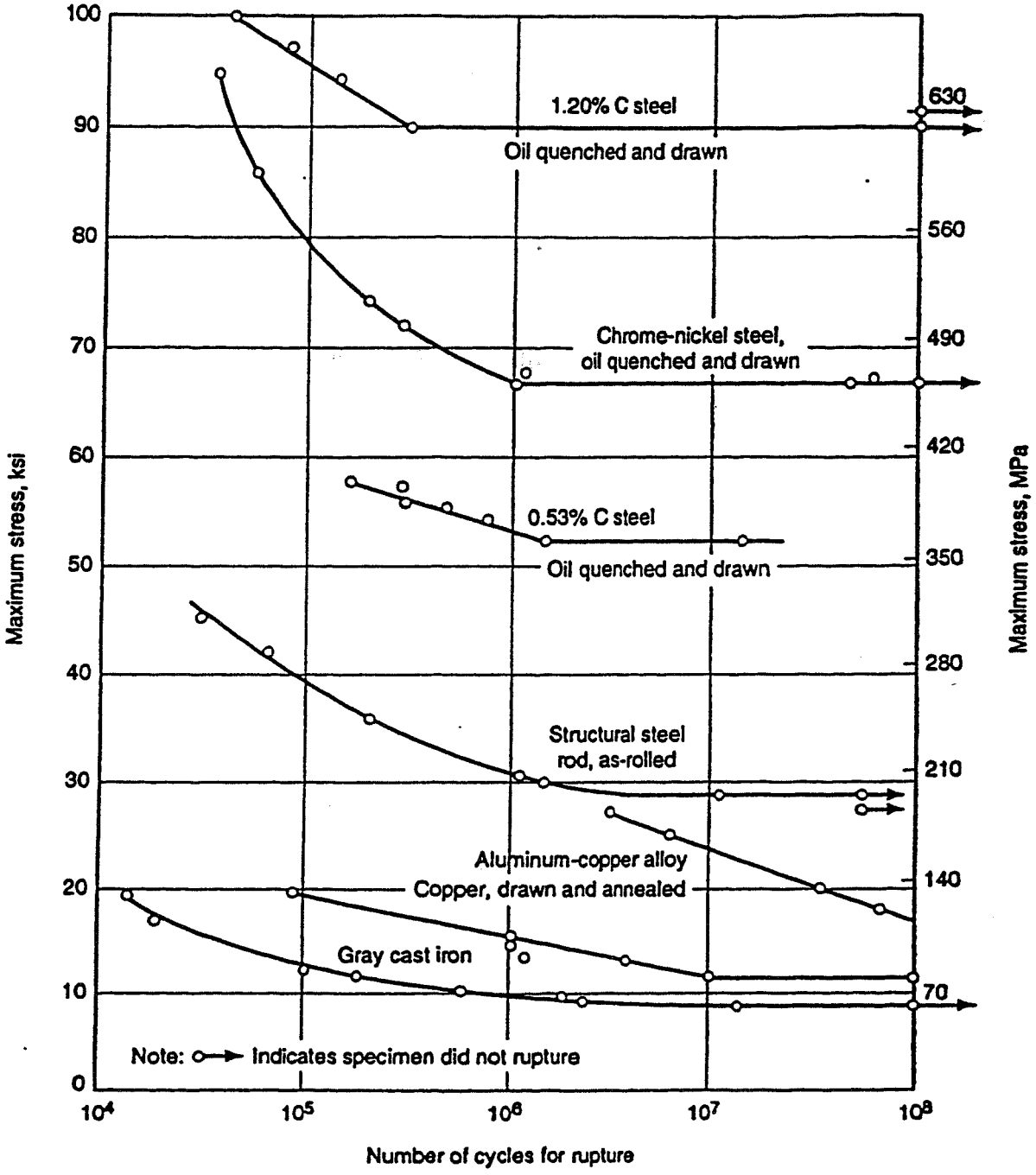

Fig. 16 Typical S-N diagrams for various alloys subjected to completely reversed loading at ambient temperature

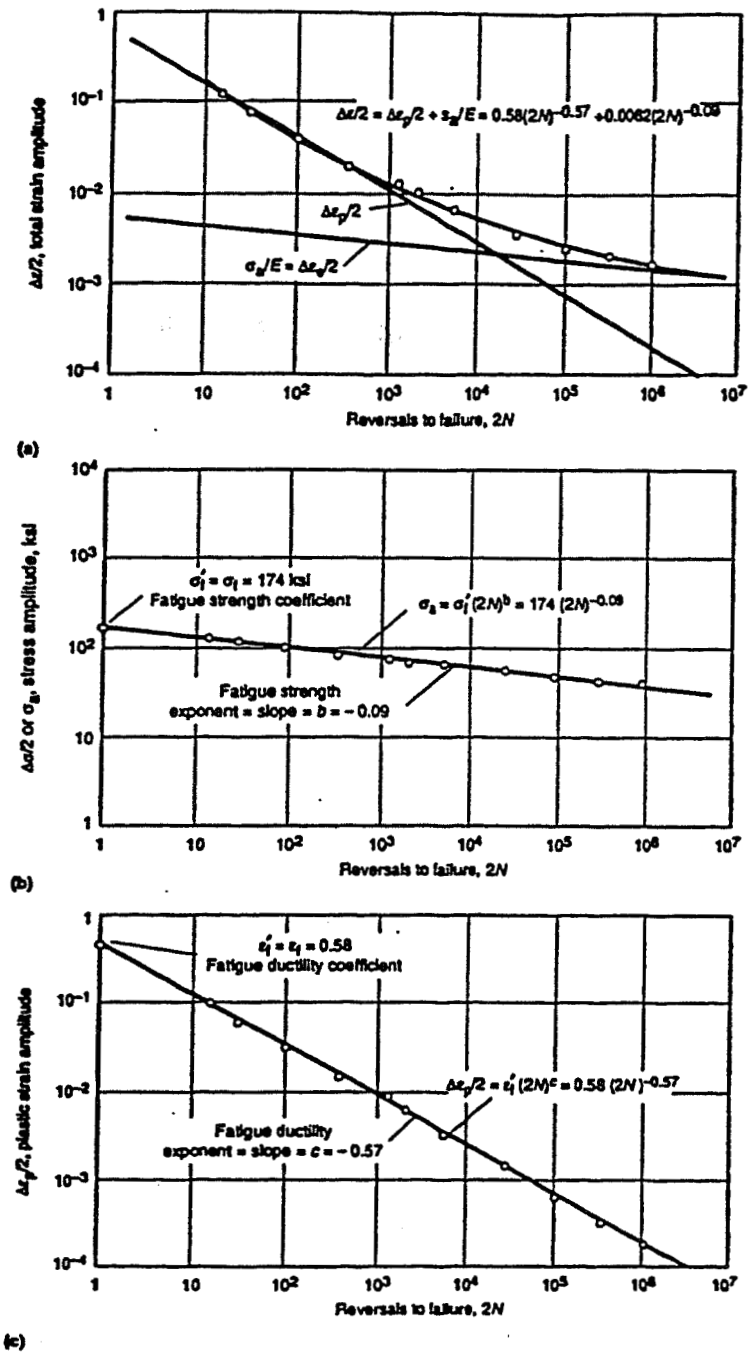

Fig. 17 Typical strain-life fatigue curve showing elastic and plastic components

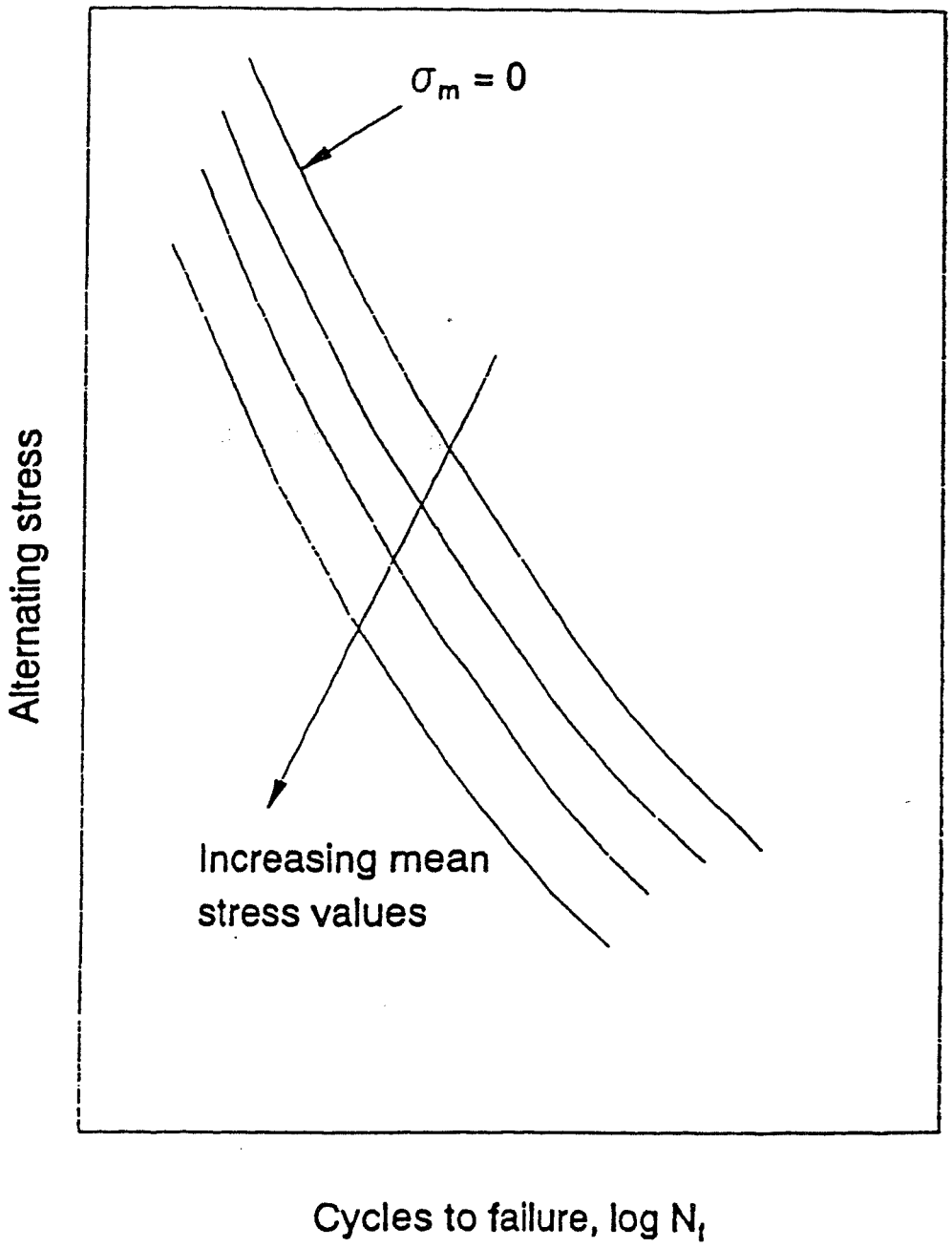

Fig. 18 Schematic axial fatigue curve illustrating the effect of tensile mean stress. After Conway and Sjodahl [53]

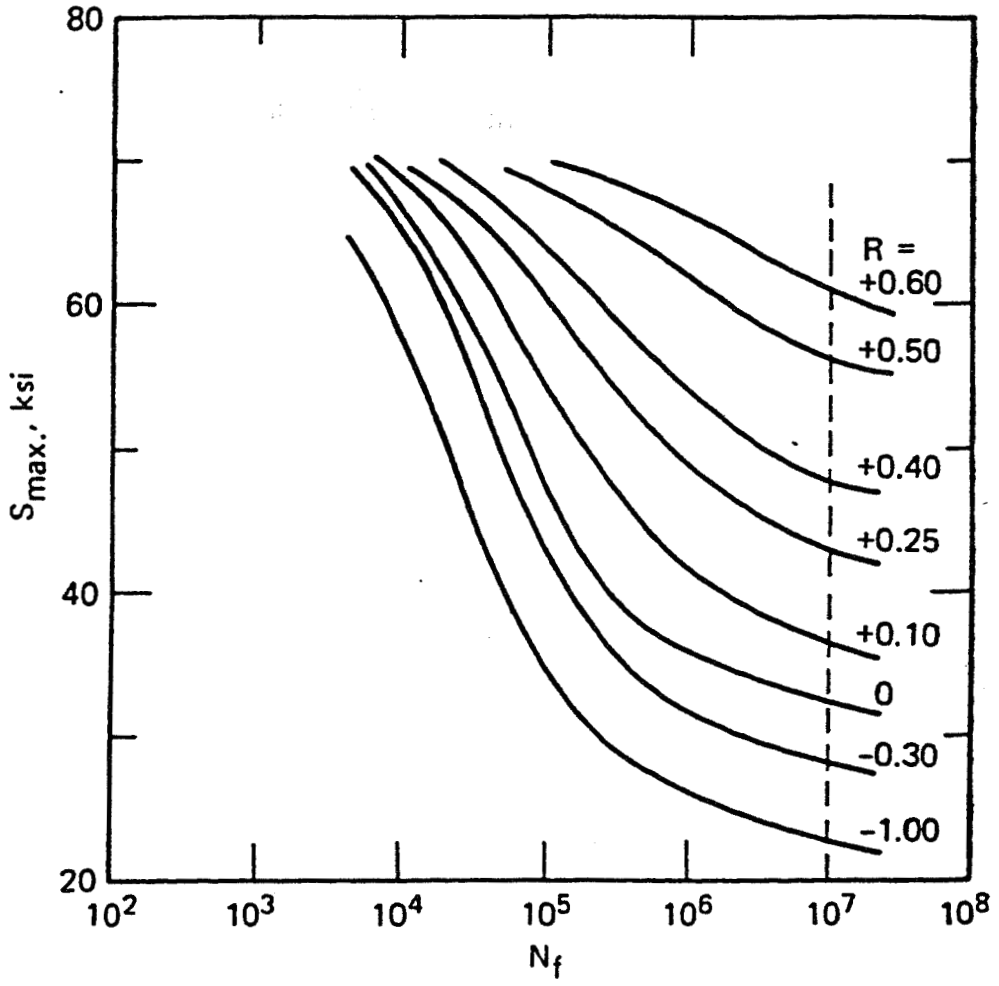

Fig. 19 Effect of tensile mean stresses on axial fatigue resistance of 2024-T3 aluminum alloy at room temperature. After Conway and Sjodahl [54]

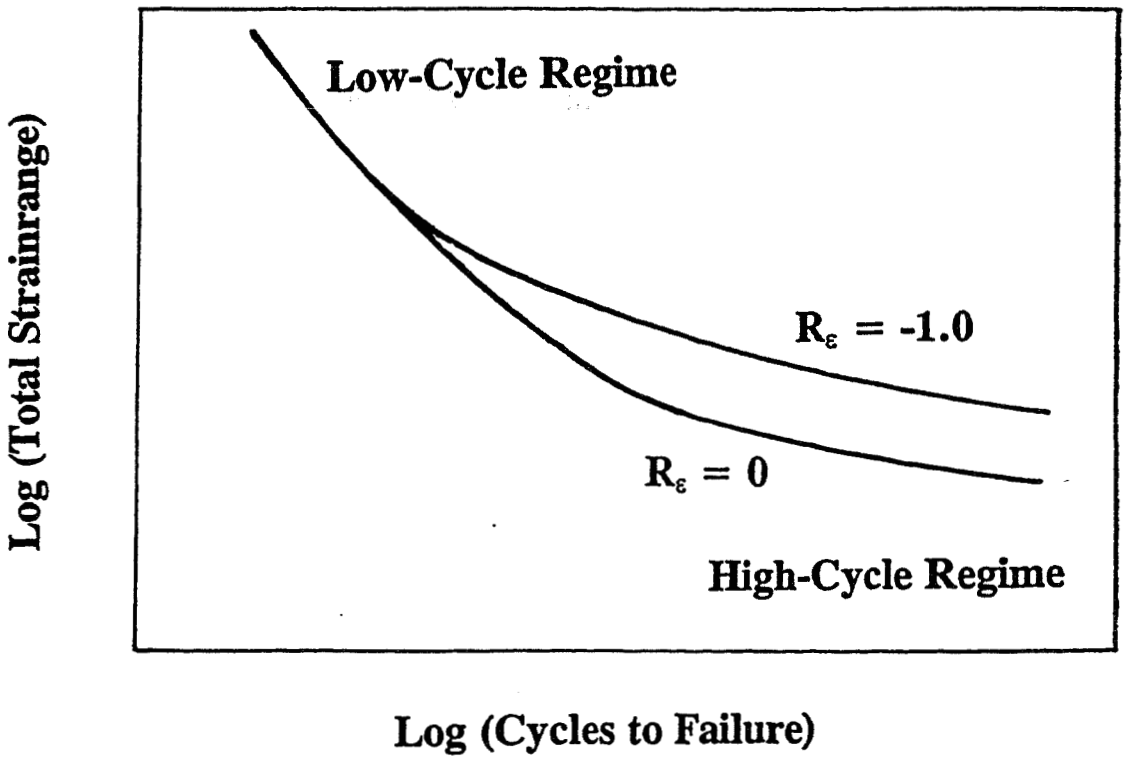

Fig. 20 Schematic illustration of cyclic mean strain cycling effects on low-cycle fatigue resistance. Mean stresses relax to zero at large strain ranges, but remain at low strain ranges, thus reducing life.

{NASA GLENN SKETCH}

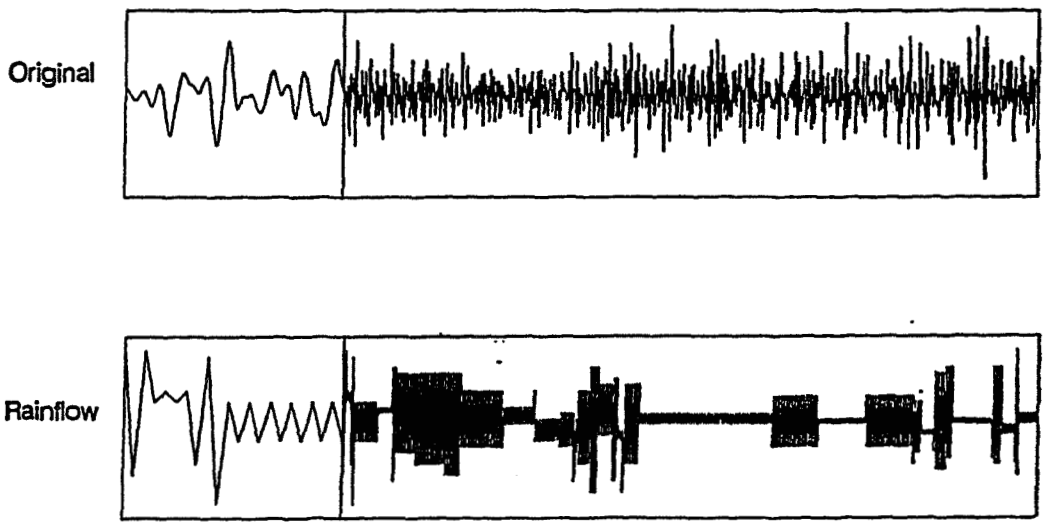

Fig. 21 Non-Steady Fatigue Loading, after [56]
(a) random appearing original loading pattern
(b) loading pattern reconstructed by rainflow method of cycle counting

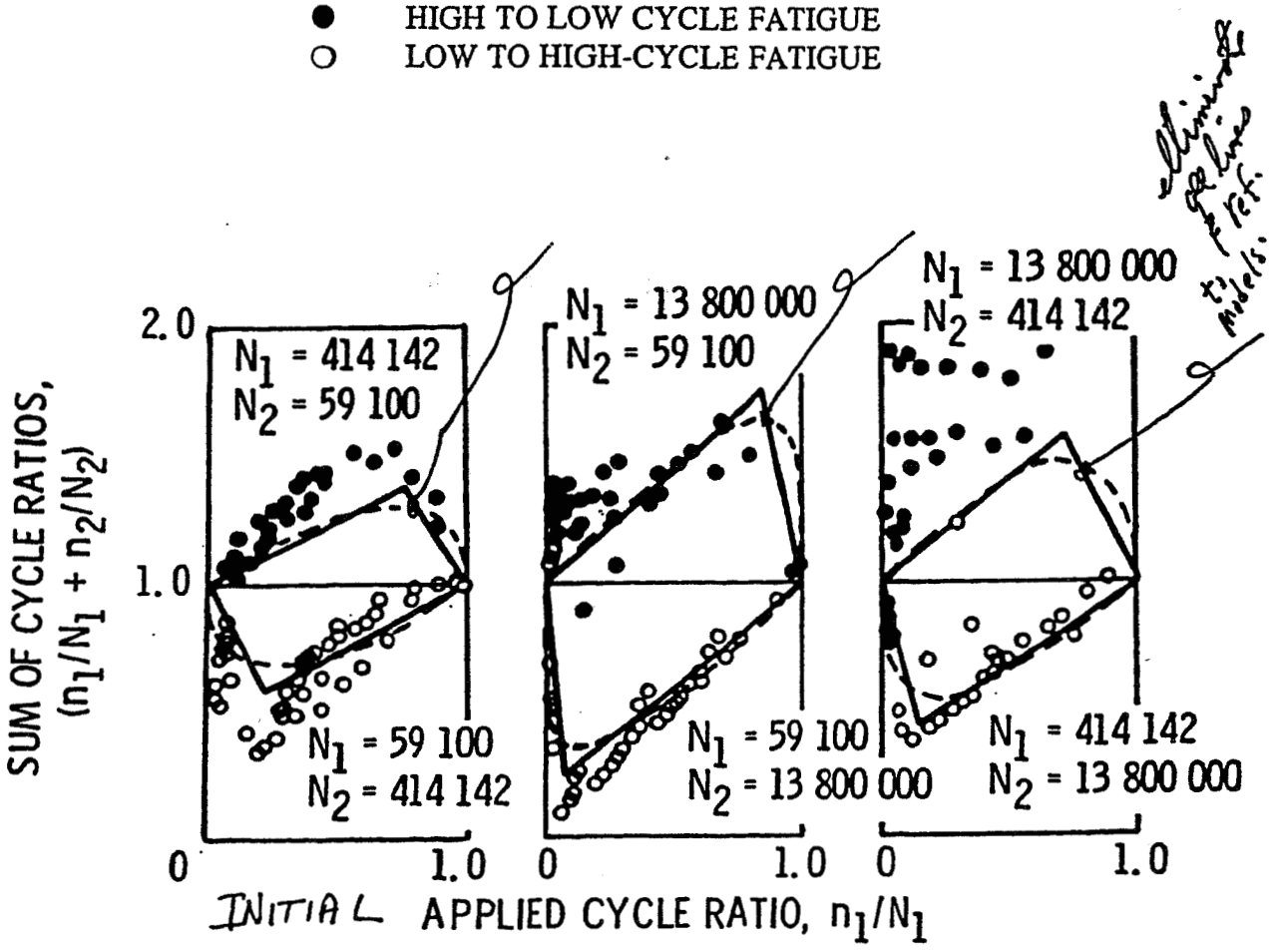

Fig. 22 Examples of classic loading order effect in two load level tests of British aluminum alloy D. T. D. 683 [58]

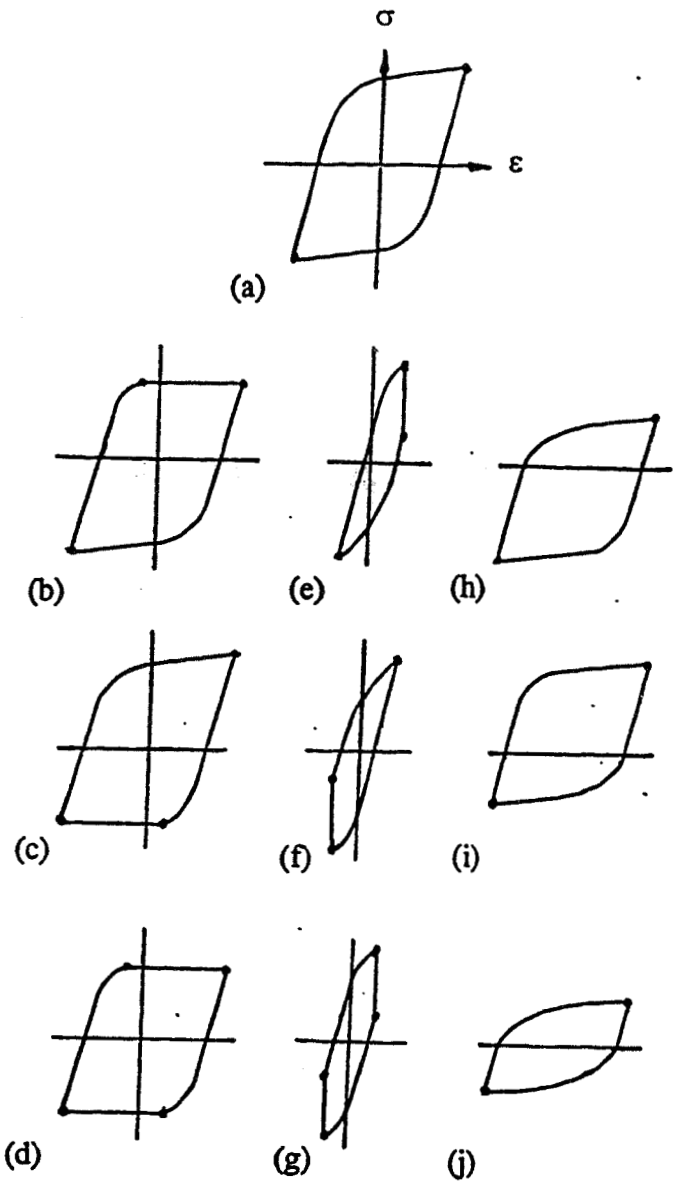

Fig. 23 Schematic hysteresis loops encountered in isothermal creep-fatigue testing
(a) pure fatigue, no creep
(b) tensile stress hold, strain limited
(c) compressive stress hold, strain limited
(d) tensile and compressive stress hold, strain limited
(e) tensile strain hold (stress relaxation)
(f) compressive strain hold (stress relaxation)
(g) tensile and compressive strain hold (stress relaxation)
(h) slow tensile straining rate
(i) slow compressive straining rate
(j) slow tensile and compressive straining rate

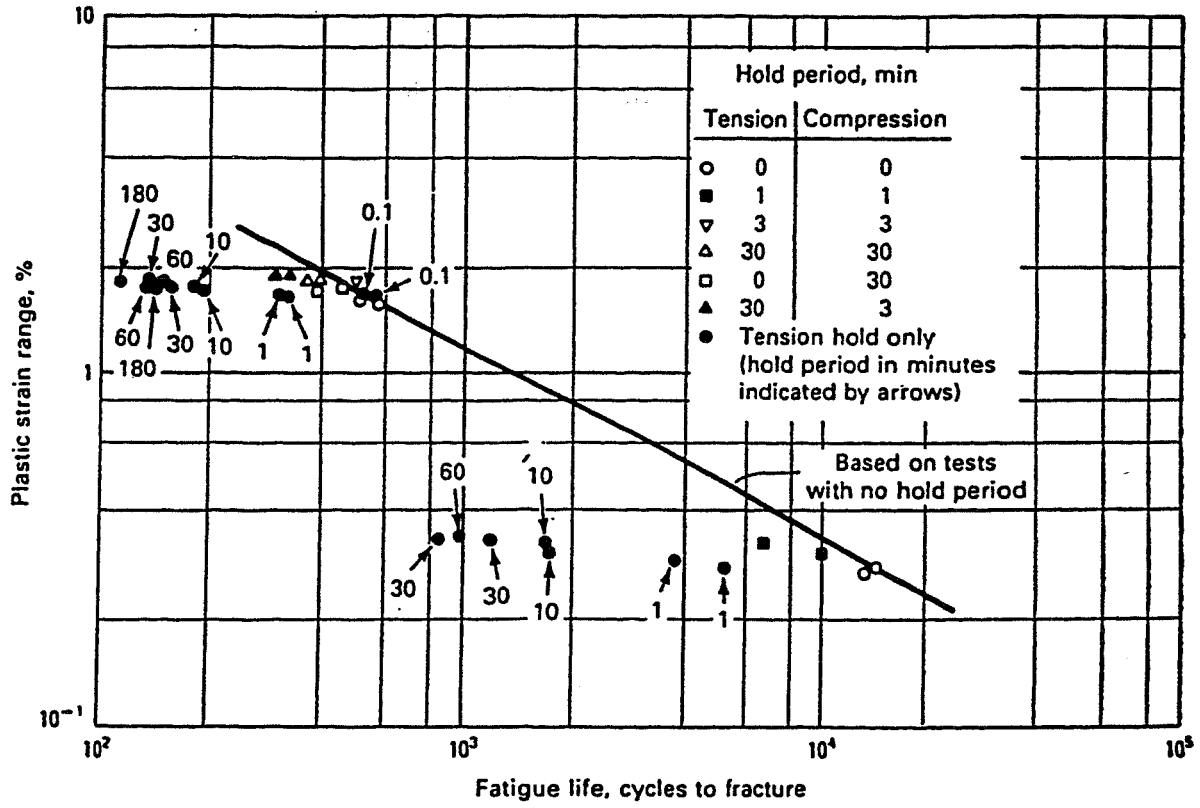

Fig. 24 Creep-fatigue interaction effects on isothermal cyclic life of AISI type 304 stainless steel tested in air at 650 °C, normal straining rate of 4 x 10^{-3} s^{-1}, after [66]

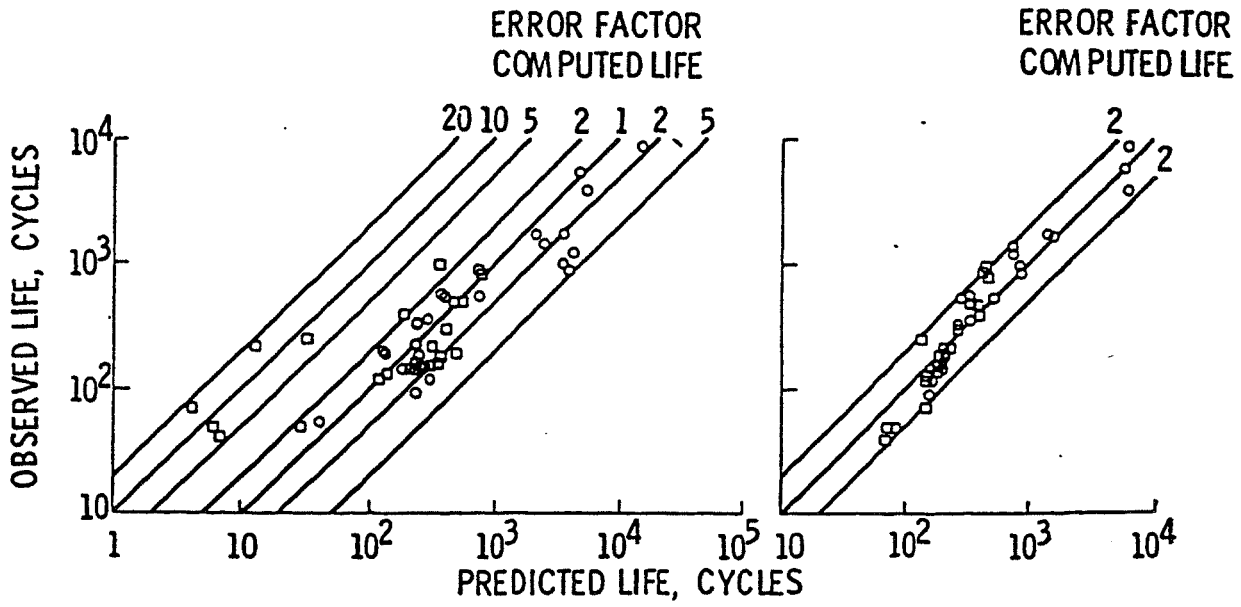

(a) USING PREDICTED TIME- AND CYCLE-FRACTIONS.

(b) USING STRAINRANGE PARTITIONING.

Fig. 25. Predictability of creep-fatigue lives for tensile strain hold time cycles for Incoloy 800 and AISI type 304 stainless steel at elevated temperatures [72], data from [71]

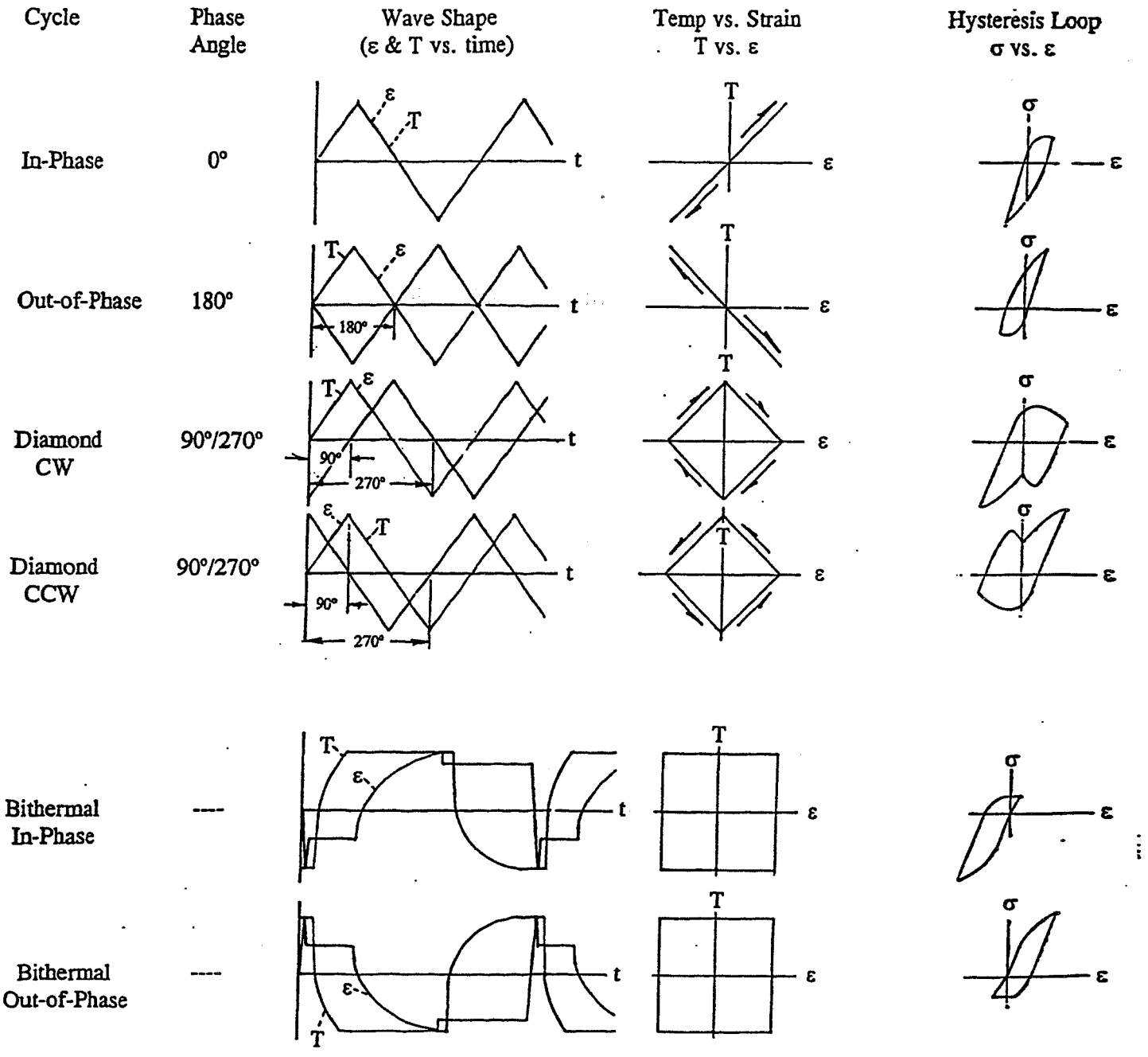

Fig. 26. Basic TMF strain cycles

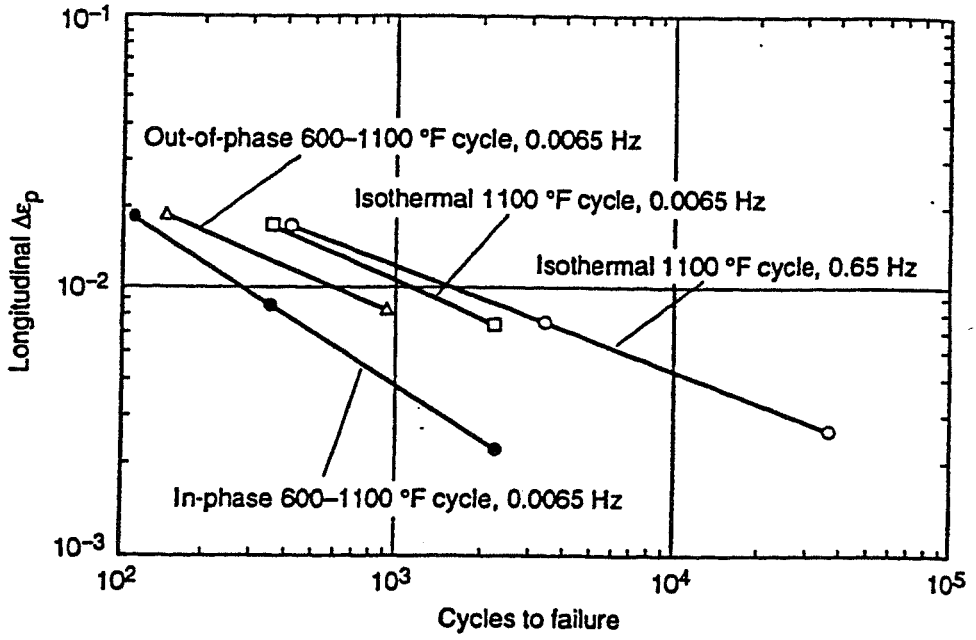

Fig. 27. Comparison of isothermal and TMF fatigue resistance of A-286 precipitation-hardening stainless steel [77], data from [78]

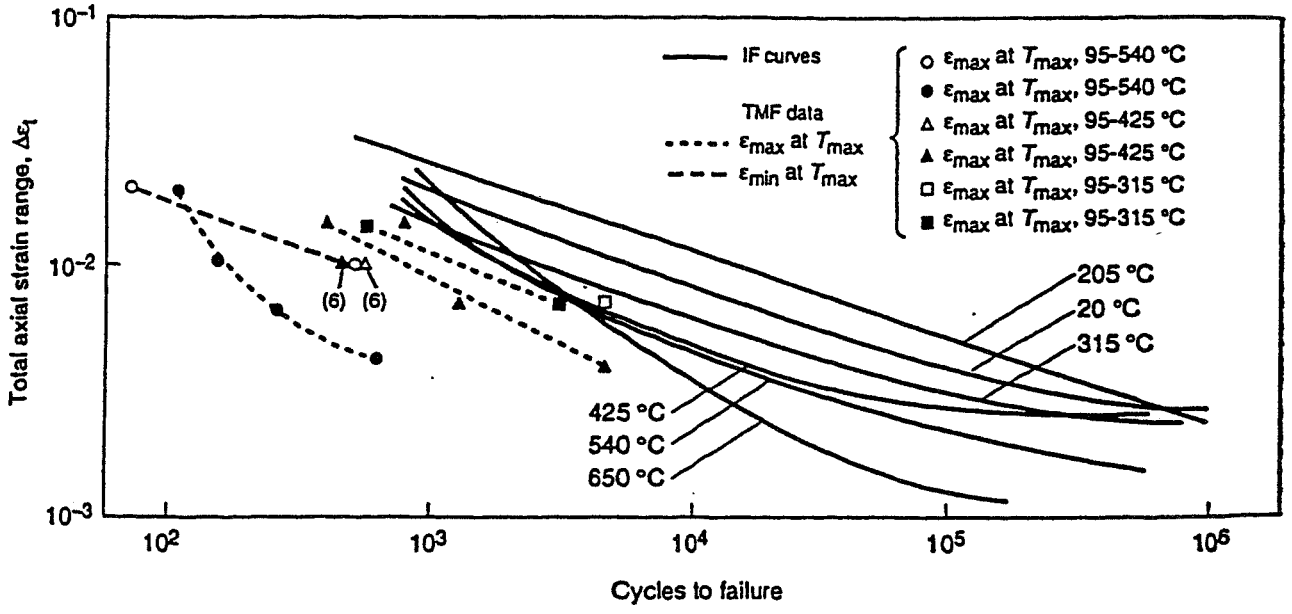

Fig. 28. Comparison of isothermal and TMF fatigue resistance of AISI 1010 carbon steel [77], data from [79]

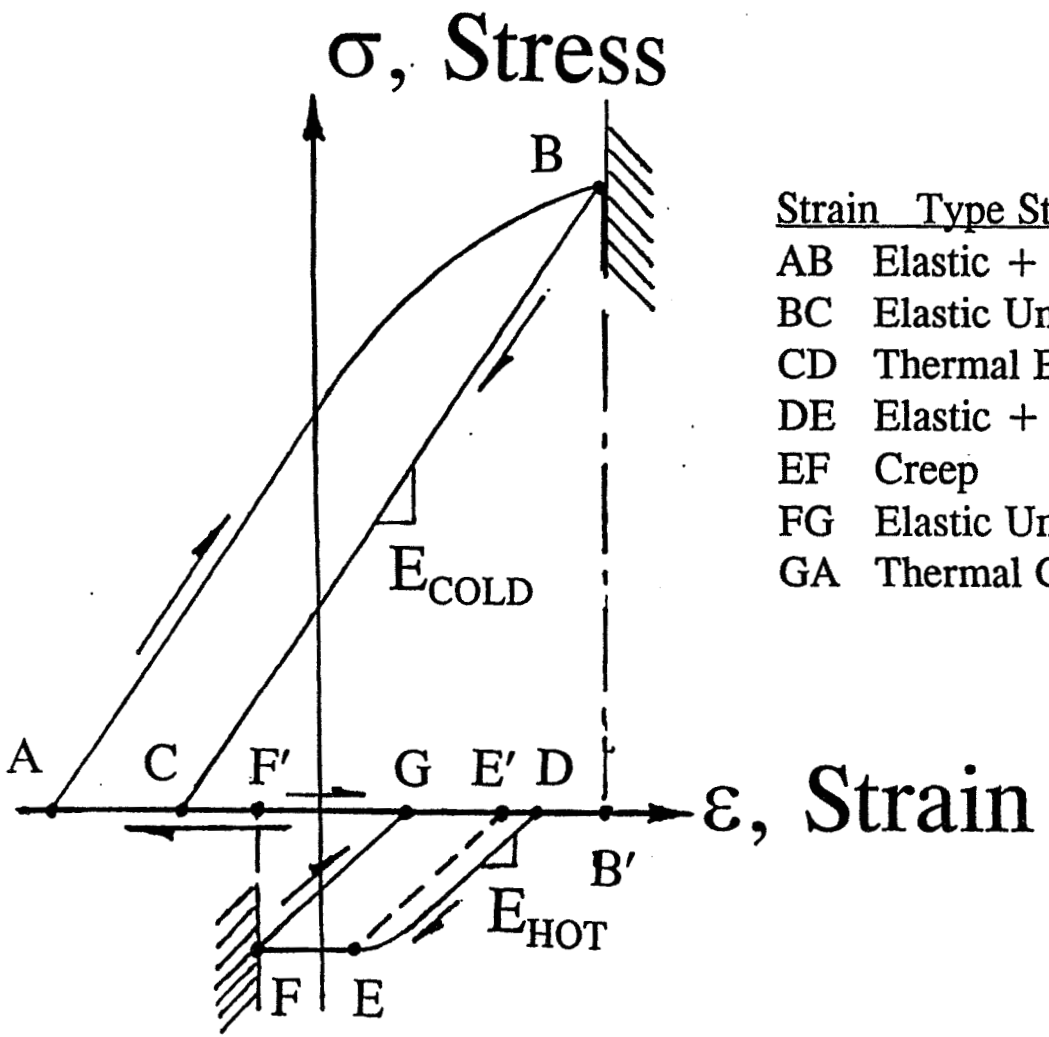

Strain	Type Strain	Temp	Action
AB	Elastic + Plastic	Low	Rapid Straining
BC	Elastic Unloading	Low	Rapid Straining
CD	Thermal Expansion	Low-High	Zero Stress
DE	Elastic + Plastic	High	Rapid Straining
EF	Creep	High	Constant Stress
FG	Elastic Unloading	High	Rapid Straining
GA	Thermal Contraction	High-Low	Zero Stress

Fig. 29 Example bithermal hysteresis loop showing thermal expansion